UNIVERSITAT POLITÈCNICA DE VALÈNCIA

UNIVERSITAT
POLITÈCNICA
DE VALÈNCIA

DEPARTMENT OF CONSTRUCTION ENGINEERING AND CIVIL

ENGINEERING PROJECTS

EFFICIENT DESIGN OF POST-TENSIONED CONCRETE BOX-GIRDER ROAD BRIDGES BASED ON SUSTAINABLE MULTI-OBJECTIVE CRITERIA

Thesis submitted by

Tatiana García Segura

Advisors:

Dr. Victor Yepes Piqueras

Valencia (Spain), September 2016

Acknowledgements

Firstly, I would like to express my appreciation to my advisor Dr. Víctor Yepes for guiding me during the doctoral period and giving me the precise advises. I extend my thanks to the other professors of our research group, especially to Dr. Julián Alcalá and Dr. Jose Vicente Martí. Thank you for your invaluable aid in helping me whenever I need it.

I also wish to acknowledge the economic support of the Spanish Ministry of Economy and Competitiveness, formerly called Spanish Ministry of Science and Innovation. This thesis has been possible thanks to the FPI fellowship and the financially support of HORSOST (Research Project BIA2011-23602) and BRIDLIFE (Research Project BIA2014-56574-R). I cannot forget to thanks *Cátedra* CEMEX and AEIPRO. Their prizes gave me a boost.

My special gratitude to Dr. Dan M. Frangopol, for inviting me to join his research group at Lehigh University during part of my doctoral period. It was an honor for me to learn and collaborate with one of the world's biggest expert in life-cycle performance maintenance of structures under uncertainty. Likewise, I would like to thank my colleagues from that period for their kind welcome and support.

I also wish to thank my colleagues from Universitat Politècnica de València: Paula, Clara, Yasna, Paqui, Rober, Vicent, Vicente, Javi and Aitor. After these years, we are not only colleagues, but rather we have become good friends. Finally and most importantly, I would like to give a big thank you to my family and friends for their continuous support and understanding. To my parents, for always relying on me. I have no doubt my father would be proud of me. To Javi, thank you for your positive attitude and for being my companion in good and bad times. To my friends from Castellón, for giving me the valuable advises and encouragements. Finally, to my future son, for being part of myself during this final and hard time.

Abstract

Bridges, as an important component of infrastructure, are expected to meet all the requirements for a modern society. Traditionally, the primary aim in bridge design has been to achieve the lowest cost while guaranteeing the structural efficiency. However, concerns regarding building a more sustainable future have change the priorities of society. Ecological and durable structures are increasingly demanded. Under these premises, heuristic optimization methods provide an effective alternative to structural designs based on experience. The emergence of new materials, structural designs and sustainable criteria motivate the need to create a methodology for the automatic and accurate design of a real post-tensioned concrete bridge that considers all these aspects. For the first time, this thesis studies the efficient design of post-tensioned concrete box-girder road bridges from a sustainable point of view. This research integrates environmental, safety and durability criteria into the optimum design of the bridge. The methodology proposed provides multiple trade-off solutions that hardly increase the cost and achieve improved safety and durability. Likewise, this approach quantifies the sustainable criteria in economic terms, and evaluates the effect of these criteria on the best values of the variables.

In this context, a multi-objective optimization is formulated to provide multiple trade-off and high-performing solutions that balance economic, ecologic and societal goals. An optimization design program selects the best geometry, concrete type, reinforcement and post-tensioning steel that meet the objectives selected. A three-span continuous box-girder road bridge located in a coastal region is selected

for a case study. This approach provides vital knowledge about this type of bridge in the sustainable context. The life-cycle perspective has been included through a lifetime performance evaluation that models the bridge deterioration process due to chloride-induced corrosion. The economic, environmental and societal impacts of maintenance actions required to extend the service life are examined. Therefore, the proposed goals for an efficient design have been switch from initial stage to life-cycle consideration.

Faced with the large computational time of multi-objective optimization and finite-element analysis, artificial neural networks (ANNs) are integrated in the proposed methodology. ANNs are trained to predict the structural response based on the design variables, without the need to analyze the bridge response. The multi-objective optimization problem results in a set of trade-off solutions characterized by the presence of conflicting objectives. The final selection of preferred solutions is simplified by a decision-making technique. A rational technique converts a verbal pairwise comparison between criteria with a degree of uncertainty into numerical values that guarantee the consistency of judgments. This thesis gives a guide for the sustainable design of concrete structures. The use of the proposed approach leads to designs with lower life-cycle cost and emissions compared to general design approaches. Both bridge safety and durability can be improved with a little cost increment by choosing the correct design variables. In addition, this methodology is applicable to any type of structure and material.

Resumen

Los puentes, como parte importante de una infraestructura, se espera que reúnan todos los requisitos de una sociedad moderna. Tradicionalmente, el objetivo principal en el diseño de puentes ha sido lograr el menor coste mientras se garantiza la eficiencia estructural. Sin embargo, la preocupación por construir un futuro más sostenible ha provocado un cambio en las prioridades de la sociedad. Estructuras más ecológicas y duraderas son cada vez más demandadas. Bajo estas premisas, los métodos de optimización heurística proporcionan una alternativa eficaz a los diseños estructurales basados en la experiencia. La aparición de nuevos materiales, diseños estructurales y criterios sostenibles motivan la necesidad de crear una metodología para el diseño automático y preciso de un puente real de hormigón postesado que considere todos estos aspectos. Por primera vez, esta tesis estudia el diseño eficiente de puentes de hormigón postesado con sección en cajón desde un punto de vista sostenible. Esta investigación integra criterios ambientales, de seguridad estructural y durabilidad en el diseño óptimo del puente. La metodología propuesta proporciona múltiples soluciones que apenas encarecen el coste y mejoran la seguridad y durabilidad. Al mismo tiempo, se cuantifica el enfoque sostenible en términos económicos, y se evalúa el efecto que tienen dichos criterios en el valor óptimo de las variables.

En este contexto, se formula una optimización multiobjetivo que proporciona soluciones eficientes y de compromiso entre los criterios económicos, ecológicos y sociales. Un programa de optimización del diseño selecciona la mejor combinación de geometría, tipo de hormigón, armadura y postesado que cumpla con los objetivos seleccionados. Se ha escogido como caso de estudio un puente continuo en cajón de tres vanos situado en la costa. Este método proporciona un mayor conocimiento

sobre esta tipología de puentes desde un punto de vista sostenible. Se ha estudiado el ciclo de vida a través de la evaluación del deterioro estructural del puente debido al ataque por cloruros. Se examina el impacto económico, ambiental y social que produce el mantenimiento necesario para extender la vida útil del puente. Por lo tanto, los objetivos propuestos para un diseño eficiente han sido trasladados desde la etapa inicial hasta la consideración del ciclo de vida.

Para solucionar el problema del elevado tiempo de cálculo debido a la optimización multiobjetivo y el análisis por elementos finitos, se han integrado redes neuronales en la metodología propuesta. Las redes neuronales son entrenadas para predecir la respuesta estructural a partir de las variables de diseño, sin la necesidad de analizar el puente. El problema de optimización multiobjetivo se traduce en un conjunto de soluciones de compromiso que representan objetivos contrapuestos. La selección final de las soluciones preferidas se simplifica mediante una técnica de toma de decisiones. Una técnica estructurada convierte los juicios basados en comparaciones por pares de elementos con un grado de incertidumbre en valores numéricos que garantizan la consistencia de dichos juicios. Esta tesis proporciona una guía que extiende y mejora las recomendaciones sobre el diseño de estructuras de hormigón dentro del contexto de desarrollo sostenible. El uso de la metodología propuesta lleva a diseños con menor coste y emisiones del ciclo de vida, comparado con diseños que siguen metodologías generales. Los resultados demuestran que mediante una correcta elección del valor de las variables se puede mejorar la seguridad y durabilidad del puente con un pequeño incremento del coste. Además, esta metodología es aplicable a cualquier tipo de estructura y material.

Resum

Els ponts, com a part important d'una infraestructura, s'espera que reunisquen tots els requisits d'una societat moderna. Tradicionalment, l'objectiu principal en el disseny de ponts ha sigut aconseguir el menor cost mentres es garantix l'eficiència estructural. No obstant això, la preocupació per construir un futur més sostenible ha provocat un canvi en les prioritats de la societat. Estructures més ecològiques i durables són cada vegada més demandades. Davall estes premisses, els mètodes d'optimització heurística proporcionen una alternativa eficaç als dissenys estructurals basats en l'experiència. L'aparició de nous materials, dissenys estructurals i criteris sostenibles motiven la necessitat de crear una metodologia per al disseny automàtic i precís d'un pont real de formigó posttesat que considere tots estos aspectos. Per primera vegada, esta tesi estudia el disseny eficient de ponts de formigó posttesat amb secció en calaix des d'un punt de vista sostenible. Esta investigació integra criteris ambientals, de seguretat estructural i durabilitat en el disseny òptim del pont. La metodologia proposada proporciona múltiples solucions que a penes encarixen el cost i milloren la seguretat i durabilitat. Al mateix temps, es quantifica l'enfocament sostenible en termes econòmics, i s'avalua l'efecte que tenen els dits criteris en el valor òptim de les variables.

En este context, es formula una optimització multiobjetivo que proporciona solucions eficients i de compromís entre els criteris econòmics, ecològics i socials. Un programa d'optimització del disseny selecciona la millor geometria, tipus de formigó, armadura i posttesat que complisquen amb els objectius seleccionats. S'ha triat com a cas d'estudi un pont continu en calaix de tres vans situat en la costa. Este mètode proporciona un major coneixement sobre esta tipologia de ponts des d'un punt de vista sostenible. S'ha estudiat el cicle de vida a través de l'avaluació del

deteriorament estructural del pont a causa de l'atac per clorurs. S'examina l'impacte econòmic, ambiental i social que produïx el manteniment necessari per a estendre la vida útil del pont. Per tant, els objectius proposats per a un disseny eficient han sigut traslladats des de l'etapa inicial fins a la consideració del cicle de vida.

Per a solucionar el problema de l'elevat temps de càlcul degut a l'optimització multiobjetivo i l'anàlisi per elements finits, s'han integrat xarxes neuronals en la metodologia proposada. Les xarxes neuronals són entrenades per a predir la resposta estructural a partir de les variables de disseny, sense la necessitat d'analitzar el pont. El problema d'optimització multiobjetivo es traduïx en un conjunt de solucions de compromís que representen objectius contraposats. La selecció final de les solucions preferides se simplifica per mitjà d'una tècnica de presa de decisions. Una tècnica estructurada convertix els juís basats en comparacions per parells d'elements amb un grau d'incertesa en valors numèrics que garantixen la consistència dels dits juís. Esta tesi proporciona una guia que estén i millora les recomanacions sobre el disseny d'estructures de formigó dins del context de desenrotllament sostenible. L'ús de la metodologia proposada porta a dissenys amb menor cost i emissions del cicle de vida, comparat amb dissenys que seguixen metodologies generals. Els resultats demostren que per mitjà d'una correcta elecció del valor de les variables es pot millorar la seguretat i durabilitat del pont amb un xicotet increment del cost. A més, esta metodologia és aplicable a qualsevol tipus d'estructura i material.

Table of contents

List of figures

List of Tables

Chapter 1
Introduction

1.1. Background

Traditional methods for bridge design require a trial-and-error procedure to obtain an acceptable design. While the geometry is defined *a priori* based on the designer's experience, the remaining variables are determined based on the code's limit states. On this regard, the final design does not guarantee to be optimal. Optimization methods provide an effective alternative to structural designs based on experience. Metaheuristic or stochastic algorithms are used as an effective alternative to optimize the design. These algorithms are characterized by their combination of rules and randomness to effectively search large discrete variable spaces and find an optimal solution. Besides, this technique explores all possible combinations, and therefore it prevents designers from falling into a usual design rules.

Box-girder bridges have a number of advantages from the resistance perspective, as well as due to the low dead load. That is why this is one of the most common type of continuous bridges. However, the design rules do not always take into account the evolving objectives and priorities of society. Brundtland report (WCED, 1987) proposes a long-term vision to maintain the resources, which will be necessary for the future needs. Sustainable development requires a triple vision that balances economic development and environmental and social needs. Therefore, concerns regarding building a more sustainable future require us to consider aspects like environmental impact, durability, and safety level, among others. This has led to the development of low-carbon materials, the search for new designs that reduce the environmental impact, the maintenance planning to extend the service life of civil

structures and the evaluation of the structure life-cycle to see its impact as a whole.

There needed to be a renewed design methodology that considers all sustainable criteria, allows for the implementation of new materials, and simultaneously, carries out a precise structural analysis. Multi-objective optimization finds multiple trade-off solutions that are optimal with regard to the objectives considered. This tool has been used to optimize the initial design and the maintenance actions. Nevertheless, there is a tendency to consider both goals separately. On one hand, the structure is designed for a safety and service live target. On the other hand, the maintenance is optimized from a particular design. As maintenance depends on the safety and condition state, the initial design should consider the life-cycle aspects that also minimize the future maintenance. Therefore, it is important to consider durability in order to design for longevity and reduced long-term impacts.

Multi-objective optimization (MOO) of structures requires a large computational time due to the existence of many decision variables and objective functions, and the evaluation procedure like the use of the finite-element method. The use of approximate models, like artificial neural network (ANN), can reduce the exact function evaluations. ANN learns from training examples and then, this method predicts a response or output from new input parameters. In this sense, ANN can predict the structural behavior from multiple bridge designs. Thus, ANN is integrated in the multi-objective optimization process to reduce the high computational cost needed to analyze a real bridge.

MOO leads to a range of optimal solutions, which are considered equally good. The decision-making process takes places *a posteriori*. Experts chose one solution according to their preferences. Decision-making techniques provide a rational procedure to the decisions based on certain information, experience and judgment. However, the definition of a scale to a specific criterion is subject to uncertainty. On this basis, this research suggests a methodology to introduce the decision-maker's preferences in a multi-criteria decision-making process in which there are uncertainties associated to the criteria comparison.

1.2. Aims and contributions

This thesis proposes a methodology for the automated design of a full-scale post-tensioned concrete box-girder bridge by finite-element analysis that takes into account sustainable criteria and provides multiple trade-offs and high-performing solutions. Besides, an integrated multi-objective harmony search with artificial neural networks is proposed to reduce the high computation time required for the finite-element analysis and the increment in conflicting objectives. Finally, this thesis presents AHP-VIKOR under uncertainty method to introduce the decision-maker's preferences and select preferred solutions.

The objective of this methodology is:

- Discover useful knowledge regarding how each criterion affects the bridge

design.

- Determine if cost optimization is a good approach to reduce the material consumption or requires an additional consideration.
- Study the increment in cost when designing according to sustainable criteria.
- Obtain the best values of the variables to improve each sustainable criteria.
- Evaluate the main limit states that affect the design.
- Analyze the relationship between the criteria. For example, check if the relationship between cost and CO_2 changes according to the safety requirements.
- Determine if high-strength concrete reduces the short-term cost, long-term cost or both.
- Analyze the criteria to consider in the initial design optimization that reduce the future maintenance.
- Establish design criteria that improve safety, guarantee longevity, and reduce long-term impacts.
- Study the optimal maintenance plan that minimizes the economic, environmental and societal impacts.
- Check the efficiency of the proposed method to reduce the high computation time.
- Determine the preferred solutions and obtain relevant knowledge of this process.

This thesis, therefore, contributes to a better understanding of post-tensioned concrete box-girder bridges in the sustainable context. The results provide trade-off solutions that reduce the cost and emissions and achieve improved safety and durability. The findings from the research illustrate the best values of geometry, concrete type, reinforcement and post-tensioning steel to meet the objectives selected. Besides, a lifetime performance evaluation allows designs with longer corrosion initiation time or improved safety level to be compared according to the life-cycle perspective. Consequently, the benefits of designing with different objectives, i.e. the lowest initial emissions, the longest corrosion initiation time, or the maximum safety, is highlighted.

1.3. Research methodology

The process followed to carry out this thesis can be divided in 4 stages (see Figure 1.1). Firstly, the state-of the-art is reviewed to know the outcomes obtained in this field and the research gaps that need further investigation. This includes the benefits and problems of box-girder bridges, the heuristic optimization techniques, the applications to structural optimization, the objectives to achieve a sustainable development, the techniques and criteria used to analyze the sustainability of structures, the aspects that are considered in multi-objective optimizations and the decision-making techniques.

Secondly, six studies are conducted with the objective of learning about the aspects

that should be considered for the following study, which is the main body of the thesis. The materials, criteria, life-cycle evaluation, heuristic algorithms, and decision-making techniques are analyzed to achieve an efficient design based on sustainability. These studies have been published in scientific journals and they are listed in Annex I. The findings are used as basis for the following research that focuses on the efficient design of post-tensioned concrete box-girder road bridges subjected to sustainable criteria.

A three-span continuous box-girder road bridge located in a coastal region is analyzed. For this case study, a multi-objective optimization is applied by simultaneously minimizing the cost and CO_2 emissions, and maximizing the overall safety factor. This approach provides a range of possibilities for the bridge design. A second study integrates the corrosion initiation time as objective. In this instance, the durability is transformed from a constraint to an objective. This gives the opportunity to explore new designs without limiting the design by predefined constraints on durability measures. A third study evaluates the deterioration process and the consequent reduction in structural safety from those trade-off solutions. The optimum maintenance plan that satisfies the reliability target during a life-span with the minimum economic, environmental and societal impacts is investigated.

Finally, the issues detected during the development of the methodology have led to propose several complementary tools. A meta-model for reducing the computational cost is suggested. ANN are integrated in a multi-objective optimization to predict the structural response without the need to analyze the bridge response. In addition, a decision-making technique is proposed to select preferred designs from the results of the multi-objective optimization. This method allows the decision-makers to introduce easily their preferences, and simultaneously, analyze the characteristics of the solutions.

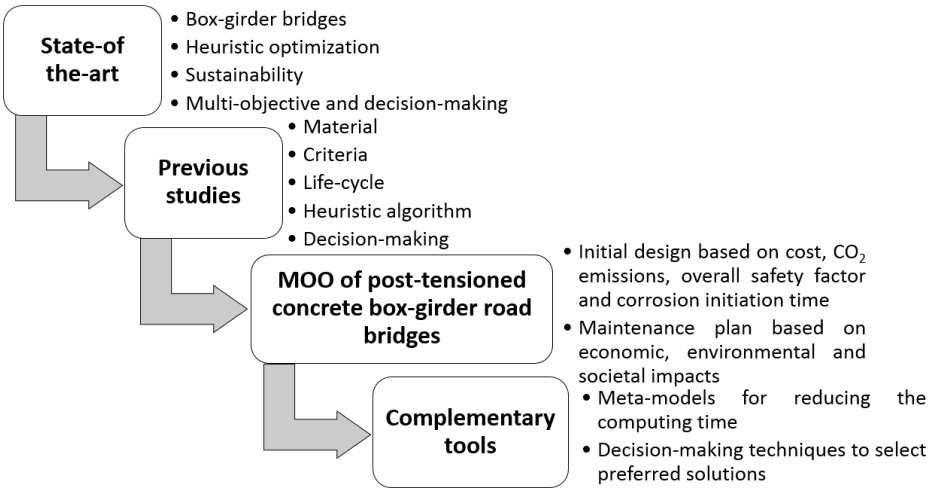

Figure 1.1. Research structure

1.4. Dissertation structure

The dissertation presents the research into 11 chapters.

Chapter 1 describes the background research, the aims and contributions of this thesis and the research methodology.

Chapter 2 reviews the state-of-the-art related to this thesis, which covers aspects of box-girder bridges, heuristic optimization, sustainable development, multi-objective optimization and decision-making.

Chapter 3 summarizes the main results of six previous studies. These studies examine the life-cycle greenhouse gas emissions of blended cement concrete including carbonation and durability (García-Segura et al., 2014a), the optimization of concrete I-beams through a new hybrid glowworm swarm algorithm and the use of self-compacting concrete (García-Segura et al., 2014c), the cost and CO_2 emission optimization of precast–prestressed concrete U-beam road bridges (Yepes et al., 2015b), the design of precast-prestressed concrete U-beam road bridges based on embodied energy (Martí et al., 2016), the hybrid harmony search for sustainable design of post-tensioned concrete box-girder pedestrian bridges (García-Segura et al., 2015), and a cognitive approach to analyze and reduce multi-objective optimization problems (Yepes et al., 2015a).

Chapter 4 describes the optimization problem. The parameters, variables and heuristic algorithm used for the present dissertation are explained in this chapter.

Chapter 5 explains in detail the objective functions considered, both for the initial design and for the maintenance optimization.

Chapter 6 gives the details of the structural analysis and limit state verification. Besides, the computer support tool with its corresponding modulus are expounded.

Chapter 7 presents a study that carries out a multi-objective optimization of cost, CO_2 emissions, and safety.

In view of the results obtained in the previous study, **Chapter 8** presents a work that conducts a multi-objective optimization of cost, safety and corrosion time by integrating artificial neural networks in the multi-objective optimization.

Chapter 9 presents a study that starts from the results of previous chapter and carries out a maintenance lifetime optimization.

Chapter 10 describes a decision-making process that selects preferred solutions based on AHP-VIKOR under uncertainty method.

Finally, **Chapter 11** resumes the main conclusions drawn from this thesis and suggests future research lines.

Chapter 2
State-of the-art

2.1. Box-girder bridges

The Sclayn Bridge over the river Maas was the first continuous prestressed box-girder bridge. The bridge was built by Magnel in 1948. It has two spans of 62.7 m. The box-girder cross-section can be found in beam, arc, portal frame, cable-stayed and suspensions bridges. The number of continuous bridges of this type has increased recently (Ates, 2011) due to its resistance against positive and negative bending moments, as well as torsional stresses. Besides, another important feature is the low dead load. Regarding the construction methods, concrete box-girders are usually cast in situ, or precast in segments and then erected and prestressed (Sennah & Kennedy, 2002).

Researchers have explored new ways to promote knowledge and achieve a proper design. Firstly, they focused on the structural behavior (Chang & Gang, 1990; Ishac & Smith, 1985; Luo et al., 2002; Mentrasti, 1991; Razaqpur & Li, 1991; Shushkewich, 1988) for the better understanding of the complex problem. Most of them focused on analyzing shear-lag and distortion. Later, Ates (2011) studied the behavior of a continuous box-girder bridge during the construction stage, including time dependent effects. Moon et al. (2005) also focused on construction stage. These researchers studied the cracks that occurred in the bottom slab of a precast segmental bridge. They concluded that the cracks resulting from the excessive deformation during temporary post-tensioning while joining the segments.

Other authors carried out research regarding the effect of durability conditions on the strength conditions. Liu et al. (2009) proposed a structural health baseline to detect damage, develop monitoring techniques, and evaluate the bridge condition.

Guo et al. (2010) carried out a time-dependent reliability assessment to study creep, shrinkage, and corrosion of a composite prestressed concrete box-girder bridge exposed to a chloride environment. Lee et al. (2010) proposed a construction project life-cycle management system that integrates design and construction of concrete box-girder bridges. Fernandes et al. (2012) used magnetic methods to detect corrosion in prestressing strands of precast prestressed concrete box-beam bridges. Saad-Eldeen et al. (2013) tested the ultimate bending moment on corroded box-girders. The results were used to propose an equivalent tangent modulus that takes into account the total reduction of the cross-sectional area due to corrosion degradation.

On the other hand, there are some guidelines for the geometry and amount of material (Fomento, 2000; Schlaich, 1982). However, relatively little research has attempted to address the efficient design. Efficiency, in terms of maximum safety with minimum investment, is a common target in structural design. The great number of variables that can take a wide range of values makes it impossible to be addressed without artificial intelligence. In addition to this, the environmental concern, the importance of durability and the novel material development may modify the bridge design. Optimization methods provide an effective alternative to designs based on experience (García-Segura et al., 2014b). Thus, this technique has been used to study structural systems.

2.2. Heuristic optimization

The design of structures has always been based on the previous experience of the design engineer. The over-all structural design is determined according to the topographical and traffic conditions. From there, the cross-section dimensions, the concrete grade, and the general set-up of the reinforcement are usually defined based on the professional experience and the design criteria recommendations. Next, the last variables are adjusted after checking the serviceability and ultimate limit states. A trial-and-error process is used to reduce the materials consumption and consequently the cost. Contrarily, metaheuristic methods follow an intelligent process of selecting a design, carrying out structural analysis, constrain checking, and redesign in which the design variables are modified for the purpose of optimizing the objective function.

Cohn & Dinovitzer (1994) presented the state-of-the-practice in structural optimization and tried to address the gap between theoretical aspects and practical problems of structural optimization. Sarma & Adeli (1998) provided a review of nonheuristic structural concrete optimization studies. Later, Hare et al. (2013) reviewed the heuristic algorithms employed in structural optimization. These methods differ from the exact methods based on sequential techniques of mathematical programming in that they can be used in complex and realistic structural optimization problems of discrete variables. Besides, mathematical programming optimizers require the calculation of gradients of the constraints, and heuristic optimization techniques incorporate the constraints of the design code in a

straightforward manner (Lagaros et al., 2006).

Metaheuristic or stochastic algorithms base the search on a combination of certain governing rules and randomness to effectively search large discrete variable spaces and find an optimal solution. Genetic Algorithms (GAs) are population-search procedures inspired by the process of natural evolution (Holland, 1975). GAs create better-adapted individuals through genetic crossover and mutation. The crossover technique creates the new generation combining the characteristics of the two selected solutions. The new generation will have the characteristics of the two previous solutions. The probability of selecting each individual is usually proportional to its aptitude, according to Coello (1994). Therefore, the population is selected in an elitist way. The mutation operator randomly changes some characteristics of the new solution. Memetic Algorithm (MA) (Moscato, 1989) was later introduced to combine a population-based global search and a local search metaheuristic. Each individual of a population is improved through a local search with the objective of improving the genes for the parents to obtain better results in the following generations.

Swarm intelligence is also a population-search procedure. However, this type of heuristics is based on neighbor interactions. It imitates the collective behavior of some agents, which follow a global pattern. Besides, they learn from the interaction between the individuals. Swarm algorithms differ in philosophy from genetic algorithms because they use cooperation rather than competition (Dutta et al., 2011). Among the biologically-artificial intelligence, Ant Colony Optimization (ACO), Particle Swarm Optimization (PSO), Artificial Bee Colony (ABC), Glowworm Swarm Optimization (GSO), and Tabu Search (TS), can be outlined. ACO (Colorni et al. , 1991) based the strategy on the ant behavior leaving pheromone trails to find the food. PSO (Kennedy & Eberhart, 1995) simulates a simplified social system. ABC (Karaboga & Basturk, 2008) imitates the food forage behavior of honeybees. GSO (Krishnanand & Ghose, 2009) mimics a glowworm movement towards a neighbor that glows brighter. TS (Glover, 1989, 1990) is characterized by the use of artificial memory to record information about recent search moves and forbid certain moves.

Group search algorithms have the advantage of broad search ability, strong robustness, and parallel search. However, the accuracy of the solutions is sometimes affected. To improve the performance, these algorithms are combining with local search operators, to speed up the local search. The main objective of the hybridization is to exploit the complementary character of different optimization strategies. Luo & Zhang (2011) stated that the hybrid algorithm had faster convergence, higher accuracy and was more effective for solving constrained engineering optimization problems. Blum et al. (2011) provided a survey on the hybridization of metaheuristics with other techniques for combinatorial optimization problems.

Simulated Annealing (SA) was suggested by Kirkpatrick et al. (1983). SA is a popular local search algorithm in structural optimization. This algorithm is based on the physical phenomenon of annealing process. SA has a jumping property since the

algorithm admits working solutions of lower quality. This characteristic avoids that the algorithm could get trapped into local optimum and ensures a good convergence. Threshold Accepting (TA), described by Dueck & Scheuer (1990), also admits working solutions of lower quality. Nevertheless, while the acceptance of TA is deterministic the acceptance of SA is probabilistic. GA was hybridized with SA to design prestressed concrete precast road bridges (Martí et al., 2013; Martí et al., 2016) and reinforced concrete (RC) I-beams (Yepes et al., 2015a). Other authors improved the algorithm efficiency by proposing a hybrid PSO (Shieh et al., 2011; Valdez et al., 2011; Wang et al., 2013) and ACO (Behnamian et al., 2009; Chen et al., 2012).

Qu et al. (2011) stated the low convergence rate of GSO and Zhang et al. (2010) outlined that some shortcomings exist for searching the global optimum solution. SA was hybridized with GSO (García-Segura et al., 2014c; Yepes et al., 2015b) to combine the broad search ability of GSO and the effectiveness to find a global optimum of SA. García-Segura et al. (2014c) pointed out that a hybrid glowworm swarm optimization algorithm (SAGSO) obtained considerably better results in regard to quality and computing time. SAGSO outperformed GSO in terms of efficiency, accuracy and convergence rate. However, a good calibration is required to guarantee high quality solutions with a short computing time.

Harmony search (HS) was described by Geem et al. (2001) based on jazz improvisations of new combinations of notes. The notes, instruments and best harmony represent, respectively, the values, the variables and the global optimum. Alberdi & Khandelwal (2015) compared ACO, GA, HS, PSO, SA, and TS for the design optimization of steel frames. After testing the structures through five benchmarks steel frames, the best results were obtained in the design-driven HS. The algorithm proved its efficiency in optimization problems with large and poorly organized variable spaces. HS has been used to optimize rectangular reinforced concrete columns (de Medeiros & Kripka, 2014), composite floor system (Kaveh & Shakouri Mahmud Abadi, 2010) and reinforced concrete plane frames (Akin & Saka, 2015). Alia & Mandava (2011) provided an overview of the variants of HS hybridization. García-Segura et al. (2015) used a hybrid harmony search algorithm, which combines harmony search and threshold accepting, to find sustainable optimal designs of post-tensioned concrete box-girder pedestrian bridges.

Applications of Optimization in Structural Design

Bridge optimization captured engineer's attention from the 70's decade, including reinforcing slab bridges (Barr et al., 1989), precast prestressed concrete girders (Aguilar et al., 1973; Lounis & Cohn, 1993; Rabbat & Russell, 1982), steel girders (Wills, 1973), and cast-in-place prestressed concrete box-girders (Bond, 1975; Yu et al., 1986). Since the appearance of the artificial intelligence, greater emphasis has been placed on using heuristic optimization techniques to optimize structures. Srinivas & Ramanjaneyulu (2007) used artificial neural networks and genetic algorithms to optimize the cost of a T-girder bridge deck system. A global optimization called evolutionary operation (EVOP) was proposed by Rana et al.

(2013) to minimize the cost of a two span continuous prestressed concrete I-girder bridge structure. A hybrid simulated annealing algorithm (Martí et al., 2013) was implemented to find the most economical solutions of precast-prestressed concrete U-beam road bridges. The use of steel fiber reinforcement in the same type of bridge was later studied by memetic algorithms with variable-depth neighborhood search (Martí et al., 2015). Genetic algorithms were proposed to optimize hybrid fiber reinforced polymeric decks and cable-stayed bridges have been optimized using (Cai & Aref, 2015).

Likewise, there are other types of structures that have been optimized by heuristic algorithms, such as precast concrete floors (de Albuquerque et al., 2012), steel reinforced concrete columns (Park et al., 2013), reinforced concrete columns (Nigdeli et al., 2015; Park et al., 2013), cold-formed steel channel columns optimization with simulated annealing method (Kripka & Chamberlain Pravia, 2013), steel space frames (Degertekin et al., 2008), reinforced concrete frames (Camp & Huq, 2013), reinforced concrete building frames (Paya-Zaforteza et al., 2010), reinforced concrete I-beams (García-Segura et al., 2014c; Yepes et al., 2015a), reinforced concrete bridge frames (Perea et al., 2008), tall piers for railway bridge viaducts (Martínez et al., 2011; Martínez-Martín et al., 2013), retaining walls (Gandomi et al., 2015; Pei & Xia, 2012; Yepes et al., 2008, 2012), reinforced concrete footings (Camp & Assadollahi, 2013; Camp & Huq, 2013) and road vaults (Carbonell et al., 2011).

2.3. Aim of sustainability development

The World Commission on Environment and Development (WCED) proposed on "Our Common Future", the long-term vision to maintain the resources necessary to provide future needs (Butlin, 1989). They aimed the sustainable development through a balance between the economic, environmental and social pillars. This term is commonly called "the triple bottom line" of sustainability (Elkington, 1998). From then on, sustainability challenges have been translated to the construction field in different lines of research.

Construction is one of the main sectors generating greenhouse gases (Liu et al., 2013). This industry consumes over 40% of all raw stone, gravel, and sand, 25% of all raw timber, 16% of the water and 40% of energy used annually in the world (Lippiatt, 1999). In 2001, Spain had the highest consumption rate of concrete in Europe. The construction industry produced 1.76 m^3 of concrete per capita per year (ECO-SERVE, 2004). The manufacture of Portland cement generates large amounts of CO_2 given the high-energy demands during manufacture and limestone calcination. This represents the largest contribution to the total emissions from concrete construction and 5% of the world's embodied greenhouse gas (GHG) (Worrell et al., 2001). In 2007, clinker production reached around 55 million tons in Spain. However, this number was reduced to 16.7 million tons in 2012 as a consequence of the financial crisis (Oficemen, 2012).

Guidelines for green concrete structures (fib, 2012) gives a guide to reduce the

environmental impact of concrete structures. Specifically, this guide provides inspiration and tools to work towards that objective. Firstly, the life-cycle phases form cradle to grave are considered. The correct choice of raw materials, like supplementary cementitious materials is one of the keys to reduce the environmental impact. Other directions focuses on the use of more environmental friendly processes in concrete production and transportation. This guide also talks about optimizing structures based on environmental indicators and performance. Finally, it concludes that structures should be optimized comparing different alternatives and taking into account environmental indicators, specially embodied CO_2 since it is the main parameter that accounts the environmental impact. Besides, fib (2012) stated that significant reductions in CO_2 emissions can be achieved if the life-cycle of a structure is considered previous construction.

In this line, research related to sustainability in the field of construction is conducted. Researches focus on: providing a guidance to select structural materials based on economic, environmental and constructability indicators (Zhong & Wu, 2015), using recycled concrete and steel (Collins, 2010; Yellishetty et al., 2011), employing novel materials like low-carbon cements and clinker substitutes (García-Segura et al., 2014a; Gartner, 2004), evaluating the life-cycle emissions of concrete structures (Barandica et al., 2013; Tae et al., 2011), reducing the CO_2 emissions of construction activities (Börjesson & Gustavsson, 2000; González & García Navarro, 2006; Wong et al., 2013), optimizing the production process of cement (Castañón et al., 2015), estimating the embodied energy of construction projects (Wang & Shen, 2013; Wang et al., 2012) and identifying the best maintenance planning (Liu & Frangopol, 2005; Yang et al., 2006), among others.

2.3.1. *Life-cycle perspective*

Bridges are designed to provide service during many years. The life-cycle perspective requires the consideration of the process of design, construction, operation and demolition as a whole. In this regard, the investment decision should take into account the deterioration process of the bridge and the corresponding maintenance to keep the structure in good conditions. Sarma & Adeli (1998) provided a review on cost optimization of concrete structures and pointed out that additional research needs to be done on life-cycle cost optimization instead of its initial cost of construction only. Frangopol & Kim (2011) also claimed the importance of extending the service life of civil structures due to the large number of civil structures that started to show significant signs of deterioration. In order to extend the service life of deteriorating structures, maintenance actions can be applied to delay the damage propagation or reduce the degree of damage (Kim et al., 2013). Frangopol & Soliman (2016) outlined the effective planning maintenance actions to achieve the maximum possible life-cycle benefits under budget constraints.

The maintenance of corroded components represents the greater part of the life-cycle costs of long-span coastal bridges (Cheung et al., 2009). Kendall et al. (2008) considered an integrated life-cycle assessment and life-cycle cost analysis model to

compare alternative bridge designs from a sustainability perspective. Lee et al. (2006) evaluated the bridge reliability when corrosion and heavy truck traffic affect the structure. They proposed a realistic life-cycle cost methodology, which included the initial cost, expected life-cycle maintenance cost and expected life-cycle rehabilitation costs, fatality and injury losses, road user costs, and indirect socio-economic losses.

Neves & Frangopol (2005) stated that the safety assessment is an essential performance measure, since condition state is not accurate to evaluate the safety and serviceability of a bridge. Liu & Frangopol (2005) studied the best life-cycle maintenance planning by a multi-objective optimization of the lifetime condition, safety level and life-cycle maintenance cost. Chiu & Lin (2014) formulated the optimization of maintenance strategies by minimizing LCCs (economy), failure probability of the building (safety), spalling probability of concrete cover (serviceability) and maintenance times while maximizing rationality. These performance and economic objectives have been extended to the environmental and societal aspects of maintenance actions (Dong et al., 2013).

2.3.2. *Life-cycle Assessment*

Life-cycle Assessment (LCA) is a complete measure of sustainability that evaluates the inputs-outputs as well as the potential environmental impacts of a product system throughout its life-cycle. Four phases are distinguished in a LCA: the goal and scope definition phase, the inventory analysis phase, the impact assessment phase, and the interpretation phase (International Organization for Standardization, 2006). The LCA covers all the stages of a product's life from cradle-to-grave, that is, from obtaining the raw materials and processing them, to demolition and recycling. Life-Cycle Inventory (LCI) study is considered in the construction industry when only the inventory analysis and interpretation phases are implemented.

Sustainability in the construction industry is possible to be optimized by applying a LCA (Ortiz-Rodriguez et al., 2009). LCA technique is used to obtain optimal solutions of reinforced concrete structures (Fraile-Garcia et al., 2016). The LCA model was also used to compare the energy and GHG from different pavement rehabilitation strategies (Wang et al., 2012). García-Segura et al. (2014a) compared the life-cycle greenhouse gas emissions of several columns using blended cement. Blended cements decrease the CO_2 emissions, but at the same time, there is a reduction in carbon capture and service life. Thus, the life-cycle study incorporates the CO_2 capture (carbonation) during the service life and after demolition. Similarly, Collins (2010) studied the carbonation of built and recycled concrete during its life-cycle and its influence on the carbon carbon footprint.

2.3.3. *CO_2 capture*

The emission assessment through the concrete life has commonly neglected the question of CO_2 concrete capture from the atmosphere during its service life and in its secondary life. The carbonation process is sometimes recognized as

recarbonation because the final product, calcium carbonate, is chemically the same as one of cement's primary raw ingredients. Concrete carbonation has been evaluated using three different models: theoretical models (Papadakis et al., 1991), experimental models (Jiang et al., 2000) and models based on the diffusion theory and practical testing (Houst & Wittmann, 2002).

Carbonation penetrates progressively during service life while capturing CO_2. The rate of ingress of the aggressive agents depends on the quality of the porosity, the permeability of the concrete cover and the wetting and drying conditions (Bertolini et al., 2004). The water-binder ratio is decisive, since this factor conditions the concrete porosity. The porosity, in turn, speed up carbonation. The carbonation rate increases when cement is replaced by waste materials, as blast furnace slag and fly ash, due to the reduced alkaline reserve produced by the pozzolanic reaction (Zornoza et al., 2009). The concentration of CO_2 in the surrounding air and the specific climatic conditions influence the carbonation. The carbonation rate is lower in concrete non-protected against rain, as the pores are partially blocked by the rain (Galán, 2011). In this line, humidity is one of the most influential factors in concrete carbonation (Galan et al., 2010). Other crucial factor is the concrete cover. The greater the depth of the embedded steel, the longer it takes for CO_2 to carbonate the steel protection.

Leber & Blakey (1956) estimated the effects of CO_2 on mortars and concrete, assuming that all absorbed CO_2 react with the lime to form calcium carbonate. Concrete carbonation captures CO_2 and compensates for the emissions from other stages of the life-cycle. The type of cement and the use of recycled concrete during the secondary life have an important influence over the quantity of the CO_2 capture (Collins, 2010). Flower & Sanjayan (2007) found that blast furnace slag and fly ash could reduce, respectively, the concrete CO_2 emissions by 22%, and between 13% to 15%. Collins (2010) considered a primary life of 100 years and a secondary life of 30 year. This author estimated that if carbon capture is ignored, emission rates might be overestimated by as much as 13-48%.

Pade & Guimaraes (2007), Collins (2010) and Dodoo et al. (2009) considered the predictive models of Fick's first law of diffusion to estimate CO_2 capture. According to that, CO_2 capture depends on the carbonation rate coefficient, the time, the quantity of Portland cement per cubic meter of concrete, the amount of CaO content in Portland cement CaO, the proportion of calcium oxide that can be carbonated and the exposed surface area. Pade & Guimaraes (2007) surveyed the amount of demolished concrete that is recycled for secondary use according to the country. They stated that the crushing of concrete after service life increases the amount of carbonation significantly thanks to the greater surface area. About two-thirds of the calcination emissions can be captured if the crushed concrete after demolition is exposed for 30 years (Dodoo et al., 2009). In fact, 70% of the CO_2 released in cement production would be recaptured by the hardened concrete within 100 years (Börjesson & Gustavsson, 2000).

The reinforced concrete durability can be substantially reduced by degradation

processes of environmental or functional origins (Angst et al., 2009; Guzmán et al., 2011). Consequently, the reduction in service life leads to greater balance of emissions per year. Besides, durability is also fundamental for good conceptual design, quality management in construction and a good maintenance plan. Thus, Aïtcin (2000) pointed out the importance of not just the cost of 1 m^3 of concrete but rather the cost of 1 MPa or 1 year of the life-cycle of a structure. Carbonation may help to reduce the total CO_2 emissions associated to concrete production. However, this phenomenon can completely dissolve the protective layer inducing corrosion.

García-Segura et al. (2014a) studied the life-cycle greenhouse gas emissions of concrete using blended cement. The paper evaluated carbonation during service life and after demolition, considering that the calcium oxide that did not carbonate during the use stage can be carbonated after demolition. They found that carbonation during use stage decreases the total emissions by 22% in concrete with Portland cement. Moreover, most importantly, the atmospheric exposure after recycling guarantee a complete carbonation and a huge reduction in CO_2 emissions.

2.3.4. *Emission minimization*

The traditional goal of structural optimization was the design of economic structures while satisfying the safety conditions. However, the growing concern for sustainability has led engineers to choose environmentally-friendly materials and cross-section dimension to minimize the impact and the consumption of natural resources. The emergence of optimization methods to minimize the structural weight (Felkner et al., 2013; Li et al., 2009) and the economic cost (Madhkhan et al., 2013; Martí et al., 2015; Martínez-Martín et al., 2013) has led to a reduction in material consumption. Therefore, the optimization of both objectives is a good approach to achieve efficient designs. In this context, some authors have taken one step further proposing environmental emissions minimization. In contrast to the studies that quantify the environmental effect once the design is completed, the emission optimization finds out the form and the materials involved in the structural design which minimize the environmental impact.

Paya-Zaforteza et al. (2009) and Yepes et al. (2012) compared optimization designs based on the CO_2-efficiency and the cost-design for RC building frames and walls. Park et al. (2013) optimized cost and embodied CO_2 of steel reinforced concrete columns in high-rise buildings. Camp & Assadollahi (2013, 2015) and Camp & Huq (2013) suggested an optimization technique for RC footings and frames that simultaneously considers the cost and CO_2 emissions at the structural design phase. Fernandez-Ceniceros et al. (2013) carried out a decision criterion of one-way floor slabs based on the CO_2 and the overall cost. The work of Yeo & Potra (2015) carried out a similar study for RC moment frames.

While these approaches have focus on optimal designs in terms of emissions, other environmental impact assessment indicators have been chosen. Medeiros & Kripka (2014) proposed CO_2, GWP, energy and *eco indicator* to achieve environmentally friendly rectangular RC column sections. CO_2 emission is measured in kg., the GWP denoted the kg of equivalent CO_2, the energy is quantified in MJ and the *eco*

indicator unit refers to one thousand of the annual environmental load of an average European inhabitant. The embodied energy has also been selected as an interesting objective for the optimization of buildings (Sattary & Thorpe, 2012; Yeo & Gabbai, 2011), slab systems (Miller et al., 2015) and deployable origami-inspired shelter (Quaglia et al., 2014).

Regarding reinforced concrete structures, simply-supported concrete I-beams using conventional vibrated concrete and self-compacting concrete (García-Segura et al., 2014c), and high-strength concrete (Yepes et al., 2015a) have been optimized to find the solutions with minimum CO_2 emissions. As for prestressed concrete (PC), precast-PC U-beam road bridges (Yepes et al., 2015b) and post-tensioned concrete box-girder pedestrian bridges (García-Segura et al., 2015) incorporated the environmental objective to be compared with economic designs. Later, Martí et al., (2016) compared the optimum results of precast-PC U-beam road bridges with the ones employing the embodied energy as an optimization criterion.

Findings indicate that, in some cases, optimal solutions in terms of monetary costs have quite satisfactory environmental results (de Medeiros & Kripka, 2014; Fraile-Garcia et al., 2016; García-Segura et al., 2015; Yepes et al., 2015b), while others find cost increments when CO_2 emission is optimized (Camp & Assadollahi, 2015; García-Segura et al., 2014c). The optimization of concrete I-beams using conventional vibrated concrete and self-compacting concrete (García-Segura et al., 2014c) concluded that, a beam with larger section, greater amount of concrete, less steel and conventional vibrated concrete with the lower strength grade is more effective to optimize the emissions. It is worth noting that the higher exposed surface area, the more CO_2 capture.

Regarding prestressed concrete, small differences between objectives are obtained due to the geometrical restrictions. García-Segura et al. (2015) found that the environmental goal also ensured economic solutions, given the emission-optimized results showed 1% less pollution and 2% more expense compared to cost-optimized results. The analysis of the main characteristics of García-Segura et al. (2015) revealed that solutions with greater depths, more strands and lower concrete strength were used when optimizing the emissions. Yepes et al. (2015b) also obtained that CO_2 emissions and cost were closely related. A euro reduction in cost results in savings of 1.75 kg in CO_2 emissions. Comparing the CO_2 and cost optimization solutions, the first ones exhibited larger volumes of concrete of lower concrete grade, and greater and lesser amounts of passive reinforcement in the beams and the slab, respectively. In the light of the results, it is worth noting that the environmental and economic costs of materials are not in any proportional relationship to one another. However, the range to which each criterion moves away from the structural efficiency, and the volume of the feasible space, determine the results.

2.4. Multi-objective and decision-making

Bridge design is characterized by the presence of conflicting objectives and the

selection between multiple alternatives. Quality, constructability, safety, environmental impact and cost are aspects that are usually considered in the planning and design of a bridge. Multi-objective optimization (MOO) technique results in a useful tool when several objectives want to be optimized. MOO provides a set of effective solutions. Koumousis & Arsenis (1998) introduced the use of multi-objective optimization to concrete structure design. Liao et al (2011) reviewed the studies that used metaheuristics for problems related to the life time of a construction or engineering project. Zavala et al. (2013) presented a survey of multi-objective metaheuristics applied to structural optimization.

Several studies used multi-objective optimization algorithms to compare environmental emission and cost efficiency designs applied to RC structures (García-Segura et al. 2014b; Martinez-Martin et al., 2012; Paya et al., 2008; Yepes et al., 2015a). Yepes et al. (2015a) incorporated the prediction of service life as a criterion in the design of a high-strength RC I-beam. Moreover, García-Segura et al (2014b) included the overall safety coefficient for the multi-objective optimization of the same structure. Martinez-Martin et al. (2012) considered that RC bridge piers should be studied according to the economic cost, the reinforcing steel congestion and the embedded CO_2 emissions. Paya et al. (2008) optimized RC building frames through the objectives of constructability, economic cost, environmental impact, and overall safety.

Despite designs must guarantee a certain level of durability, this criterion is more common for the management approach. The multi-objective optimization problem of deteriorating bridges was studied according to the lifetime condition, safety levels and life-cycle maintenance cost (Liu & Frangopol, 2005). Sabatino et al. (2015) sought optimal life-cycle maintenance actions that balance the utility associated with the total maintenance cost and the annual minimum utility associated with a sustainability performance indicator. Torres-Machi (2015) focused on sustainable pavement management. This paper considered economic, technical, and environmental aspects in decision-making.

Decision-making techniques provide a rational procedure to the decisions based on certain information, experience and judgment. These techniques can be classified in accordance with how the decision-maker articulates preferences. In an *a priori* process, the experts give the weight of the criteria at the initial stage. The *a posteriori* process does not require a previous articulation of preferences. Multi-objective optimization leads to a range of optimal solutions, which are considered equally good. In this case, the decision-making process takes places *a posteriori*. This approach allows relevant knowledge to be obtained from the multiple trade-off. The analysis of the best solutions according to each objective provides information of the relationship between objectives and solutions. The decision-maker has to choose among the wide range of solutions from the Pareto frontier. A review of multi-criteria decision making methods applied to construction is presented by Jato-Espino et al. (2014).

There are numerous multiple attribute decision-making techniques. Technique for Order of Preference by Similarity to Ideal Solution (TOPSIS), Multi-criteria

Optimization and Compromise Solution (VIKOR), Multi-Attribute Utility Theory (MAUT), Analytical Hierarchy Process (AHP), Analytical Network Process (ANP), Preference Ranking Organization Method for Enrichment Evaluations (PROMETHEE), Data Envelopment Analysis (DEA), Complex Proportional Assessment (COPRAS) and Quality Function Deployment (QFD) are widely used.

Abu Dabous & Alkass (2010) presented a hierarchy structure that captures the decision-making elements in bridge management based on multi-attribute utility theory (MAUT) and analytical hierarchy process (AHP). Sabatino et al. (2015) used multi-attribute utility theory to assess various aspects of structural sustainability considering risks associated with bridge failure and risk attitudes of decision makers. Ardeshir et al. (2014) used fuzzy AHP to select bridge construction site. Aghdaie et al. (2012) employed AHP and COPRAS to calculate the relative importance of criteria and rank alternatives of constructing locations for new footbridges. Balali et al. (2014) selected the material, construction technique, and structural system of bridges by PROMETHEE technique. Both VIKOR (Opricovic, 1998) and TOPSIS (Hwang & Yoon, 1981) are methods that select solutions based on the shortest distance to the ideal. VIKOR and TOPSIS were compared by Opricovic & Tzeng (2004), and these methods presented some differences in aggregation function and normalization effects.

Fuzzy technique (Zadeh, 1965) is a technique to represent uncertainty or vagueness in real life. Joshi et al. (2004) evaluated a set of criteria to select the most suitable foundation by a Fuzzy tool. AHP is combined with fuzzy (Jakiel & Fabianowski, 2015; Wang et al., 2001) to select among numerous structural types for a highway RC bridge and an offshore platform alternative. Dabous & Alkass (2010) stated that the relative importance between two elements is difficult to be defined by deterministic numbers due to the uncertainty in the behavior of the different elements under consideration.

Many methods have been proposed with the objective of reducing the Pareto set of solutions (Hancock & Mattson, 2013). The "knee method" (Rachmawati & Srinivasan, 2009) is *a posteriori* method that distinguishes the points for which an improvement in one objective results in a significant worsening of at least one other objective. Clustering methods focus on assembling solutions in groups and selecting representative solutions (Saha & Bandyopadhyay, 2009). Filtering methods eliminate Pareto solutions that offer little information to the designer (Mattson et al., 2004). Yepes et al. (2015a) proposed an *a posteriori* systematic procedure to filter the Pareto frontier, while simultaneously providing relevant knowledge derived from the resolution process. This technique simplifies the choice of the preferred solution. To this end, random AHP matrices are combined with distance minimization to select the closest solution to the ideal.

2.5. Conclusions

Box-girder bridges are one of the most used nowadays. In spite of the amount of research conducted regarding structural behavior, construction and durability,

relatively little research has attempted to address the efficient design. In addition to this, the environmental concern, the importance of durability and the novel material development may modify the bridge design. There is a need to develop a flexible methodology to study the efficient design of this type of bridges and consider sustainable criteria. **Metaheuristic** or stochastic algorithms follow an intelligent process, based on combination of certain governing rules and randomness, to find the optimum design variables that minimizes or maximizes the objective functions. This technique explores all possible combinations, and therefore it prevents designers from falling into a usual design rules.

The goal of maintaining the resources necessary to provide future needs and **reduce the world's greenhouse gas emissions** contrast with the carbon intensive construction industry. Several researches and guidelines pointed the importance of employing low-carbon materials, reducing CO_2 emissions of concrete structures through their life-cycle assessment, and optimizing structures based on environmental indicators. The **life-cycle perspective** requires the consideration of design, construction, use and demolition as a whole. It is in this regard that some authors used life-cycle assessment techniques to evaluate the environmental impacts throughout the life-cycle. Others authors claimed the importance of extending the service life and carried out studies related to durability improvement and maintenance applications.

The use of **multi-objective optimization** methods has increased during the recent years to find the best structural design according to conflicting objectives. However, the target objectives to cover the key aspects of sustainability are not straightforward. On one hand, studies that focus on **initial design** consider criteria like performance, constructability, economic and environmental metrics. On the other hand, other researches study the effective **maintenance** actions from a particular design. In the last case, safety and condition aspects are taken into account. The literature review shows the need for a well design bridge that minimizes the future maintenance.

Decision-making techniques provide a rational procedure to choose solutions. Bridge design is characterized by the presence of conflicting objectives and multiple alternatives. Multi-objective optimization requires *a posteriori* decision technique to select a preferred solution between the set of optimal solutions. There are numerous methods for a multiple attribute decision-making. Besides, these can be combined with tools to consider the uncertainty in the behavior of the different elements under consideration.

Chapter 3
Previous studies

3.1. Aim of the studies

These studies are conducted with the aim of obtaining relevant knowledge about the materials, criteria, life-cycle evaluation, heuristic algorithms, and decision-making techniques. Figure 3.1 summarizes the contribution of each study to these points. Findings are used to define the structure of the following problem, which focuses on the efficient design of post-tensioned concrete box-girder road bridges. Theses six studies carry out the following researches:

- **Study 1** investigates the use of blended cements by a life-cycle greenhouse gas emission evaluation from cradle to grave. The CO_2 capture during the service life and after demolition is included. This study is explained in detail in García-Segura et al. (2014a).
- **Study 2** examines the use of conventional vibrated concrete and self-compacting concrete in concrete I-beams. The cost and CO_2 emissions criteria are evaluated from raw material acquisition to construction, which can be considered from cradle to gate. After bridge construction, carbon capture due to concrete carbonation is considered. The optimization is carried out by a hybrid glowworm swarm optimization algorithm (SAGSO) that combines glowworm swarm optimization (GSO) and simulated annealing (SA). This study is explained in detail in García-Segura et al. (2014c).
- **Study 3** focuses on the design of precast-prestressed concrete road bridges with a double U-shape cross-section. Concrete strength is investigated as a

variable of the optimization problem, including high-strength concrete. Cost and CO_2 emissions are evaluated as objective functions from raw material acquisition to construction. SAGSO is used as optimization algorithm. This study is explained in detail in Yepes et al. (2015b)

- **Study 4** investigates the same structure and materials as study 3. However, the cost and embodied energy are used as objective functions in this case. A hybrid simulated annealing algorithm with a mutation operator (SAMO2) is used in this study. This study is explained in detail in Martí et al. (2016).
- **Study 5** examines the best designs of post-tensioned concrete box-girder pedestrian bridges. Concrete strength, including high-strength concrete is studied. The cost and CO_2 emissions are evaluated from raw material acquisition to construction, including carbon capture during use stage. A hybrid harmony search algorithm that combines threshold accepting (HHS) carries out the search for the sustainable designs. This study is explained in detail in García-Segura et al. (2015).
- **Study 6** proposes a decision-making technique to analyze and reduce the Pareto optimal set for a multi-objective optimization of a reinforced concrete I-beam in terms of cost, CO_2 emissions, and service life. Multi-objective simulated annealing (MOSA) is used as the optimization algorithm. The use of high-strength concrete is studied. The method combines the Analytic Hierarchy Process (AHP) and the distance minimization. This study is explained in detail in Yepes et al. (2015a).

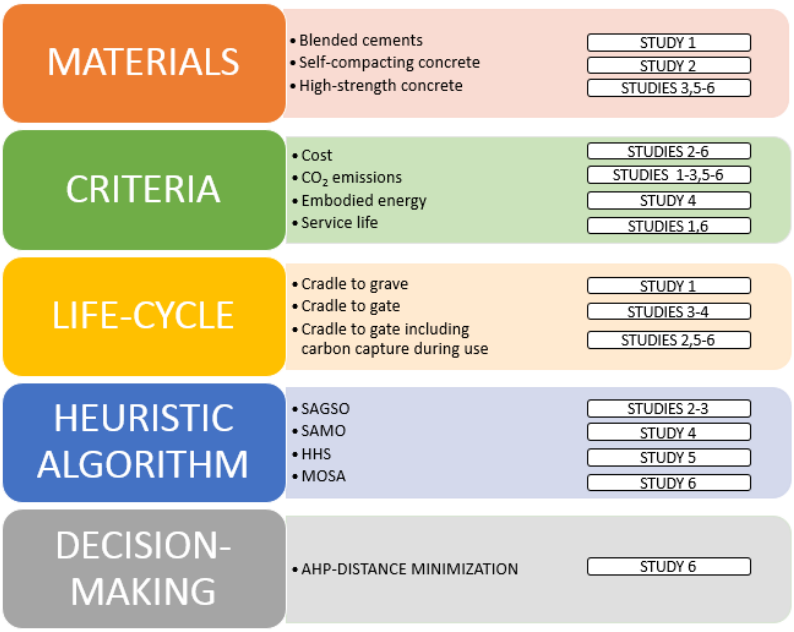

Figure 3.1. Framework of the previous studies

3.2. Study 1. Life-cycle greenhouse gas emissions of blended cement concrete including carbonation and durability

This study (García-Segura et al. 2014a) compares the life-cycle greenhouse gas emissions of several columns using blended cement. This study aims to check whether the reduction in CO_2 emissions of blended cements compensates the reduction in carbon capture and service life. The carbonation is taken into account as a negative emission during the service life and after demolition, and as a durability degradation. The results of this study show the appropriateness of using blended cements for a sustainable point of view. Even blended cement is not used for the post-tensioned concrete bridge, the results serve as a guide for the sustainable design of reinforced concrete structures. Besides, the life-cycle evaluation shows the relevant stages for an environmental assessment. The carbon capture during use and reuse stage also provides relevant knowledge.

Methodology

This study evaluates the CO_2 emissions and CO_2 capture for a reinforced concrete column during its service life and after demolition, considering its reuse as gravel filling material. The following stages are considered: obtaining raw materials and processing them, transport to the concrete plant, mixing, steel production of bars, transport to the building site, construction activities, demolition and crushed to be recycled as gravel filling material. Concrete service life is evaluated due to carbonation and the unavoidable steel embedded corrosion. Besides, carbonation deepens progressively during service life capturing CO_2. After demolition, the significant increase in surface area of the aggregate helps to speed up CO_2 absorption. It is considered complete carbonation after that. Service life is evaluated for the durability conditions and then, this length of time is used for the benchmark "emissions per year".

Main results

Portland cement is replaced with either blast furnace slag (BFS), a by-product of the steel industry, or fly ash (FA), a by-product of burning coal. Table 3.1 shows that the use of blended cements results in CO_2 savings. Nevertheless, the replacement by FA rather than BFS lowers the material emission factor, since FA needs less processing after being collected and shorter transport distances for the case study. On the other hand, concrete obtains fewer emissions using BFS, since the amount of cement that can be replaced is higher.

Figure 3.2 and 3.3 illustrates the evolution of CO_2 emissions through concrete life-cycle. Emissions acquire the maximum value after construction. Note that construction process emits few emissions. After that, carbonation during use stage decreases the total emissions by 22% in concrete with Portland cement. Comparing blended cements, carbonation of CEM II/B-V (35 % FA) during use stage is 71 % of Portland cement capture. Regarding CEM III/B (80% BFS), carbon capture is 22% of Portland cement capture.

Moreover, most importantly, the atmospheric exposure after recycling guarantees a complete carbonation and a huge reduction in CO_2 emissions. The crushed concrete aggregate (20-mm diameter) takes 44.44, 6.25, 177.78 or 100.00 years to carbonate, depending on whether it is exposed to rain, protected, wet or buried, respectively. These values depend on the carbonation rate of each exposure type.

Table 3.1. CO_2 balances of cement production and transport (based on García-Segura et al. (2014a))

CO_2 emissions (kg)				
		Production	Transport	Total
CEM PORTLAND	Portland cement	55.28	0.07	55.35
CEM II/B-S (35% BFS)	Portland cement	35.93	0,04	
	Blast furnace slag	1.23	1.17	
	Total	37.16	1.21	38.37
CEM III/A (50% BFS)	Portland cement	27.64	0.03	
	Blast furnace slag	1.76	1.67	
	Total	29.40	1.70	31.10
CEM III/B (80% BFS)	Portland cement	11.06	0.01	
	Blast furnace slag	2.81	2.67	
	Total	13.86	2.69	16.55
CEM II/A-V (20% FA)	Portland cement	44.23	0.05	
	Fly ash	0.05	0.07	
	Total	44.28	0.13	44.41
CEM II/B-V (35% FA)	Portland cement	35.93	0.04	
	Fly ash	0.09	0.13	
	Total	36.03	0.17	36.20

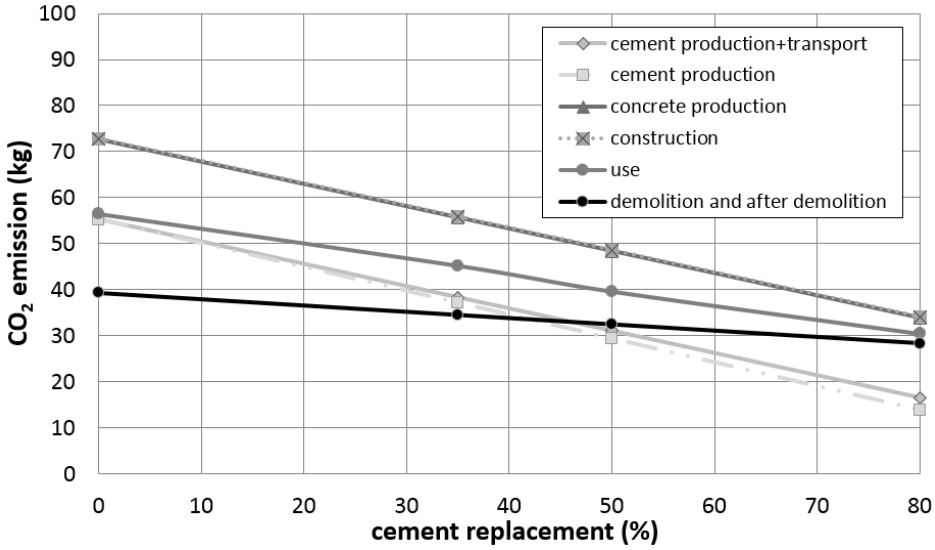

Figure 3.2. CO_2 emissions through concrete life according to BFS replacement (based on García-Segura et al. (2014a))

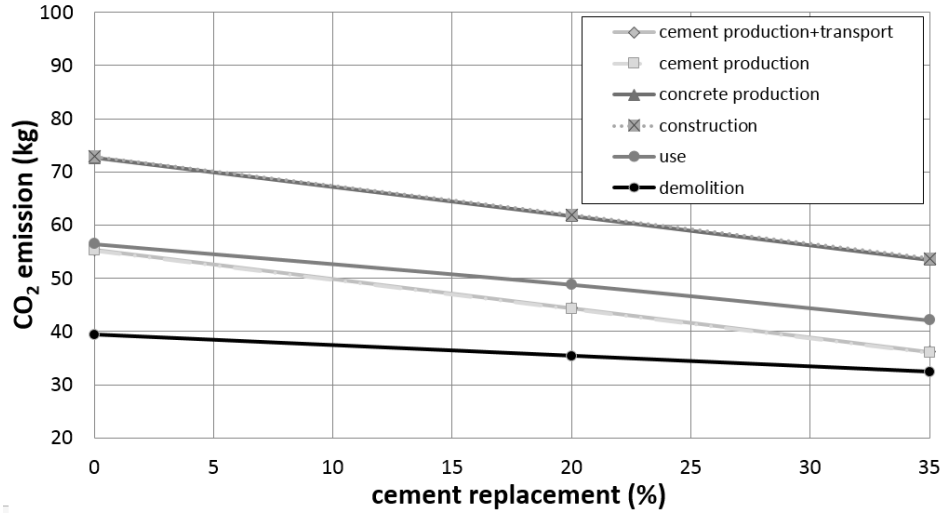

Figure 3.3. CO_2 emissions through concrete life according to FA replacement (based on García-Segura et al. (2014a))

Service life in CEM III/A (50 % BFS), CEM III/B (80 % BFS) and CEM II/B-V (35 % FA) is 10% shorter compared to Portland cement. Table 3.2 summarizes the CO_2 emissions per year. Even service life is shorter; fewer emissions per year are obtained using blended cement.

Table 3.2. Service life and CO_2 emissions per year (based on García-Segura et al. (2014a))

	Life (year)	CO_2 emissions per year (kg/year)
CEM PORTLAND	100.42	0.392
CEM II/B-S (35% BFS)	100.42	0.344
CEM III/A (50% BFS)	90.62	0.359
CEM III/B (80% BFS)	90.62	0.313
CEM II/A-V (20% FA)	100.42	0.352
CEM II/B-V (35% FA)	90.62	0.365

3.3. Study 2. Optimization of concrete I-beams using a new hybrid glowworm swarm algorithm

This study (García-Segura et al., 2014c) presents a new hybrid glowworm swarm algorithm (SAGSO) to optimize a simply-supported concrete I-beam defined by 20 variables. Eight different concrete mixtures are studied, varying the compressive strength grade and compacting system. Four mixes of self-compacting concrete (SCC) and four mixes of conventional vibrated concrete (CVC) represent four strength classes. Cost and CO_2 emissions of material production and placement are considered as the objective functions. Besides, carbon capture during use stage is taken into account. The proposed algorithm combines the ability to search in the entire solution space of glowworm swarm optimization (GSO) and the local search strategy of simulated annealing (SA). This study explores the advisability of using self-compacting concrete for an environmental point of view. In addition, the differences in the optimum designs will guide us towards more ecological designs of reinforced concrete structures.

Main results

The flowchart of SAGSO algorithm is illustrates in Figure 3.4. García-Segura et al. (2014c) explains in detail each point. SAGSO contains 13 variables that should be calibrated. The best values are obtained after 400 combinations of parameters for both cost and CO_2 emissions. SAGSO obtains better results than using the GSO and SA independently. Comparing GSO with GSO, SAGSO find high quality solutions with the same computing time. Regarding SA, SAGSO achieves better cost-optimized and emission-optimized solutions but the computer time increases 30 times. Authors also claim the importance of a good calibration to guarantee high quality solutions with a short computing time.

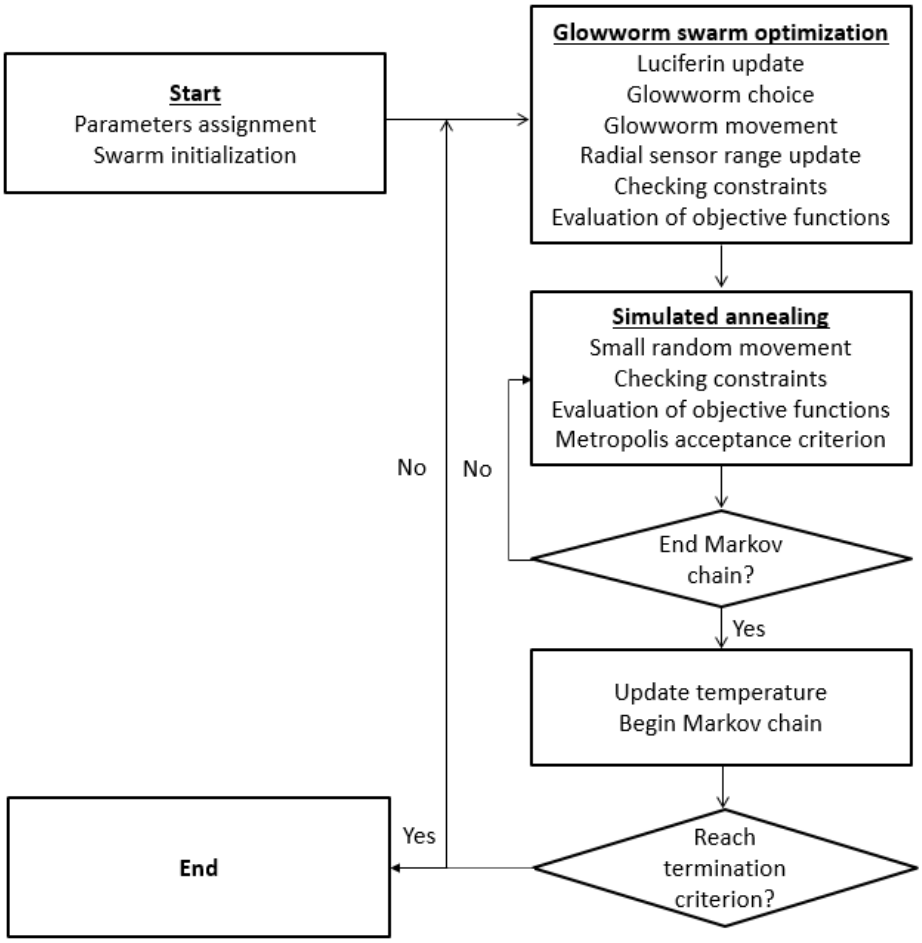

Figure 3.4. Flowchart of hybrid glowworm swarm algorithm (based on Yepes et al. (2015b) and García-Segura et al. (2014c))

Results regarding the cost-optimized and the emission-optimized beam are shown in Table 3.3. The emission-optimized beam achieves 26% fewer CO_2 emissions increasing the cost in 65%. A beam with larger section, greater amount of concrete, less steel and conventional vibrated concrete with the lower strength grade is more effective to minimize the emissions. It is worth noting that the higher exposed surface area, the more CO_2 capture. Thus, the exposed surface area of the emission-optimized beam is nearly double. Regarding the concrete type, the cost-optimized beam uses 54.2 MPa SCC and emission optimized beam acquires 31.10 MPa CVC. Plasticizer used for self-compacting concrete has more effect on CO_2 emissions than cost. Thus, results suggest that self-compacting concrete is not advisable for an environmental point of view. Regarding cost, few differences are obtained between these types of concrete.

Table 3.3. Best design solutions (based on García-Segura et al. (2014c))

	Cost-optimized	**Emission-optimized**
Depth (mm)	1570	2470
Concrete type	SCC3	CVC1
Amount of Steel (kg)	383.14	353.57
Volume of concrete (m^3)	4.54	8.44
Cost (€)	3155.17	5213.55
Emissions (kg CO_2)	3017.14	2217.75
Service life (years)	169.71	221.84

3.4. Study 3. Cost and CO_2 emission optimization of precast–prestressed concrete U-beam road bridges by a hybrid glowworm swarm algorithm

Study 3 focuses on the efficient design of precast-prestressed concrete road bridges with a double U-shape cross-section in terms of cost and CO_2 emissions. Hybrid glowworm swarm optimization algorithm (SAGSO) is used. The structural problem uses 40 variables to define the geometry, the concrete type for the slab and the beam, the prestressing and the reinforcement. Reinforced concrete between 25 and 100MPa, and prestressed concrete between 35 and 100MPa is used, respectively for the slab and beams. This study analyzes the sustainability based on a function of CO_2 emissions and cost during the production, transport and construction processes. More details about the optimization problem are explained in Yepes et al. (2015b). Findings indicate the main directions so that structural engineers may reduce CO_2 emissions in their structural designs. Even this type of bridge is different to the one studied in this thesis, the outcomes can be transferable and comparable.

Main results

The algorithm SAGSO has a good performance. Results show an average difference between the mean value and the minimum value after nine runs of only 2.9% for emissions and 1.8% for costs. These differences are sufficiently low for practical applications. Findings show that CO_2 emissions and cost are closely related. A euro reduction in cost results in savings of 1.75 kg in CO_2 emissions. Therefore, cost optimization leads to a material reduction and this, in turn, results in CO_2 savings.

Figure 3.5 illustrates the relationship between the span length and the best cost values when the objective function is either the amount of CO_2 or the monetary cost. A parabolic relation can describe the general cost trend for both objectives. Cost optimization is expressed as a function of span length as $C=48.088s^2+613.99s+31139$ with a regression coefficient $R^2=0.9999$. Likewise, the cost for emission optimization is expressed as $C=55.99s^2+163.96s+39134$ with $R^2=0.9998$. Regarding the relation with CO_2 emissions, Figure 3.6 depicts the results. The trend is represented by a parabolic function for both cost-optimized

solutions ($kgCO_2=63.878s^2+2429.3s+13052$ with $R^2=1$) and emission-optimized solutions ($kgCO_2=63.418s^2+2392.3s+13328$ with $R^2=0.9999$).

Comparing the cost and CO_2 optimization solutions, we can see some differences. CO_2 optimization finds better results with larger volumes of concrete of lower concrete grade, and greater and lesser amounts of passive reinforcement in the beams and the slab, respectively. Despite high-strength concrete is usually used for precast-prestressed concrete, concrete strength for short spans tends to be the minimum proposed. This is 25 MPa for slabs and 35 MPa for beams.

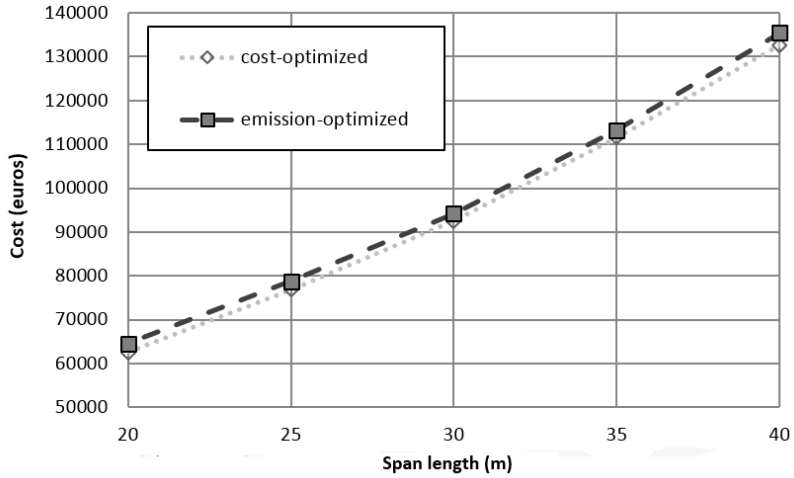

Figure 3.5. Cost of precast–prestressed concrete U-beam road bridges (based on Yepes et al. (2015b))

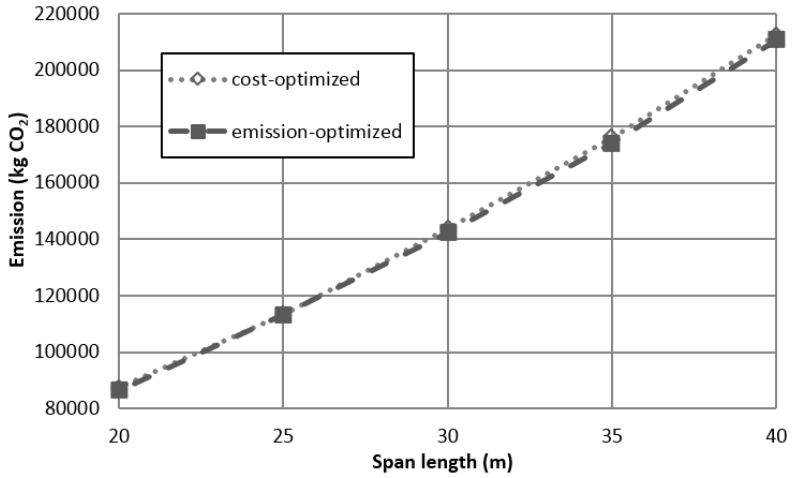

Figure 3.6. CO_2 emissions of precast–prestressed concrete U-beam road bridges (based on Yepes et al. (2015b))

Finally, a cost sensitivity analysis is carried out in a PC precast bridge with a 35 m span (see Figure 3.7). It is worth noting that while a 20% rise in steel costs leads to a 10.27% increase in the cost, a 20% rise in concrete costs only increases the cost up to 3.41%. The steel quantity increases in accordance with a lower steel cost and higher concrete cost. Regarding the volume of concrete, it decreases in accordance with a lower steel cost. However, the variation in the volume of concrete is almost insensitive to its rising price.

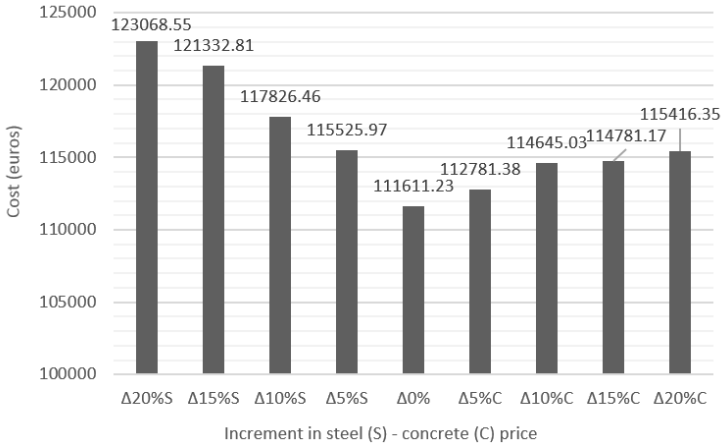

Figure 3.7. Cost sensitivity analysis according to the increment in steel (ΔS) and concrete (ΔC) prices (based on Yepes et al. (2015b))

3.5. Study 4. Structural design of precast-prestressed concrete U-beam road bridges based on embodied energy

This study (Martí et al., 2016) optimizes the previous structure using the economic cost and the embodied energy as objective functions. Besides, this study also considers the web inclination angle (*angl*) as design variable. A hybrid simulated annealing algorithm with a mutation operator (SAMO2) is used in this study. The outcome provides improved opportunities to learn about low-energy designs. The results regarding the most influential variables for the energy efficiency optimization are analyzed. In addition, the relationship between the criteria is discussed. Finally, findings indicate the differences between using CO_2 emissions and embodied energy as objective functions.

Main results

The energy and cost objectives of PC precast road bridges with a double U-shaped cross section and isostatic spans do not present conflicting behavior. An average cost increment of 3.23€ per square meter of deck is obtained when optimizing the energy. The optimization leads to the following rule of thumb: 1€ reduction implies a 4 kWh saving. The cost can be evaluated as a parabolic function of the span length. The equation $C=44.265s^2+1034.6s+12208$ (with a regression coefficient

R^2=0.9995) is used for energy optimization and C=48.958s^2+671.05s+17407 (R^2=0.9994) for cost optimization. Regarding the embodied energy, the amount of kWh can be calculated as E=191.69s^2+4333.2s+59141 (R^2=0.9996) for energy optimization and E=233.99s^2+2198.1s+99293 (R^2=0.9964) for cost optimization.

An average depth of the beam in relation to the span length is 1/18.15 and 1/17.51 for, respectively, cost and energy optimization, while Fomento (2000) recommends a ratio h1/L of 1/16 for this bridge design. Therefore, the optimization obtains smaller depths to reduce, in turn, the weight and the reinforcement required. This study decides to study the web inclination as variable, instead of fixing it as a parameter. Figure 3.8 shows the appropriateness of increasing the angle with the span length. The depth increases with the span length and consequently, the angle should be increased to maintain the slab span length in the transverse direction. Therefore, it is very important to keep slab span length and prevent unbalanced transverse bending in the slab.

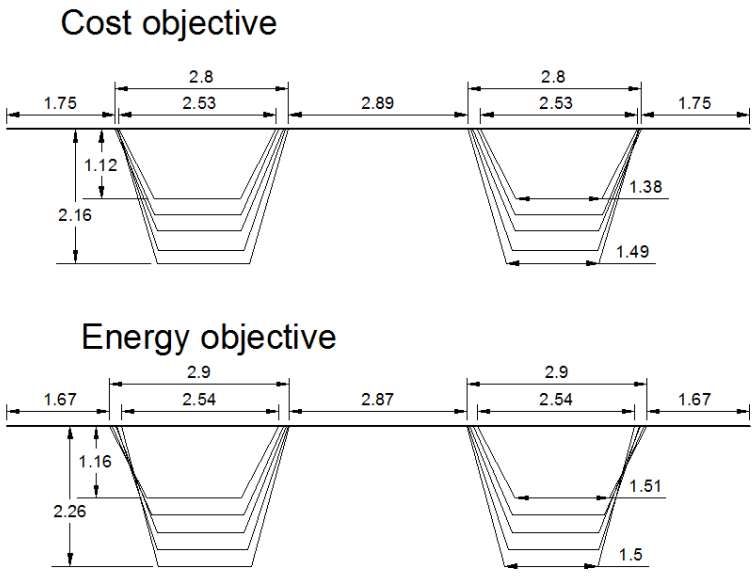

Figure 3.8. Mean cross-section dimensions for energy and cost objective (based on Martí et al. (2016))

On the other hand, Figure 3.8 compares cost and energy optimization. Results suggest that for an energy benefit it is better to take bigger beams (greater depth and width). Comparing the volume of concrete, the energy objective function achieves better results when the volume of concrete in both beam (see Figure 3.9) and slab (see Figure 3.10) is greater. Regarding the reinforcement, energy optimization reduces the quantity in the slab (see Figure 3.11). Therefore, results suggest that lesser amount of reinforcing steel and smaller length of the spans between the beams and the external cantilever are better for an energy point of view.

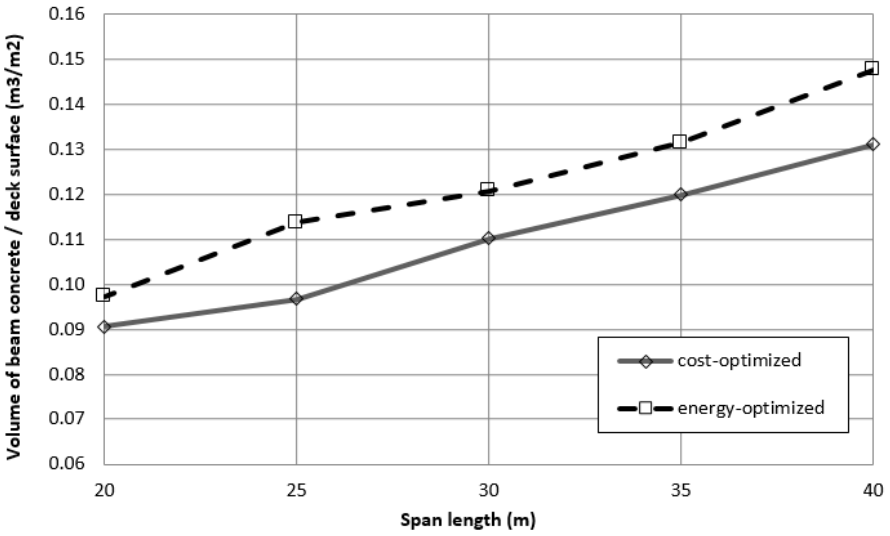

Figure 3.9. Mean beam concrete for energy and cost objective (based on Martí et al. (2016))

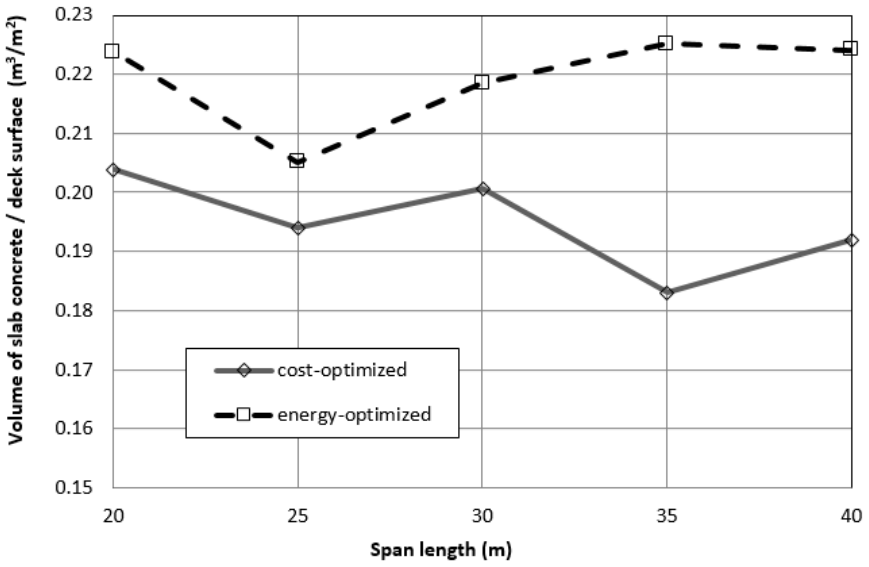

Figure 3.10. Mean slab concrete for energy and cost objective (based on Martí et al. (2016))

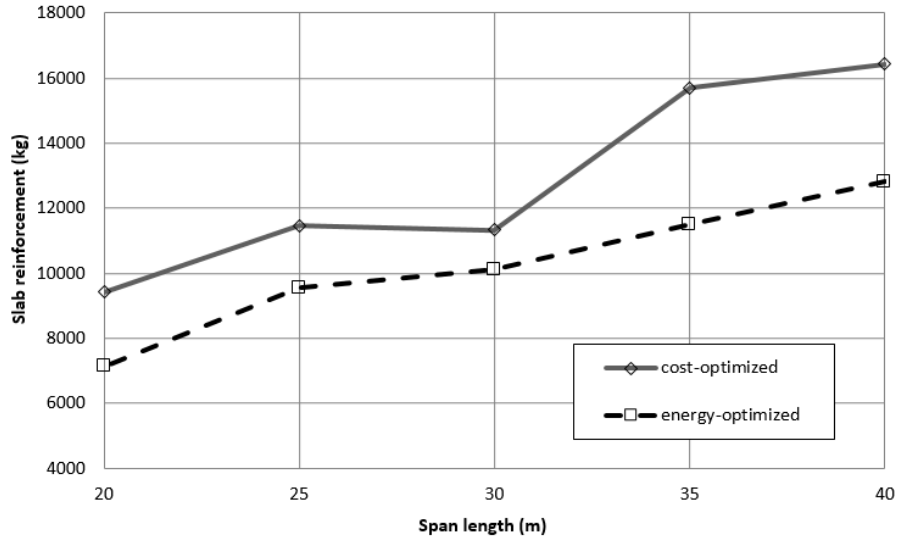

Figure 3.11. Mean slab reinforcement for energy and cost objective (based on Martí et al. (2016))

As for concrete type, the energy minimization does not show a clear difference in values compared to cost optimization. However, concrete used lower strength values in Yepes et al. (2015b) for the CO_2 emission criterion. It is important to remember that cement emissions are due to the energy demands and the limestone calcination. In contrast, the embodied energy is only because of the heat required to produce cement. Thus, high-strength concrete is less environmental friendly in terms of CO_2 emissions than in terms of energy.

3.6. Study 5. Hybrid harmony search for sustainable design of post-tensioned concrete box-girder pedestrian bridges

This study (García-Segura et al., 2015) studies the sustainable designs of post-tensioned concrete box-girder pedestrian bridges in terms of cost and CO_2 emissions. The cost and emissions take into account the material production, transport and placement. Concrete carbonation during use stage is also taken into account as a negative emission. The cost during usage is not taken into account since the structure is designed to withstand the service life. Both objectives are optimized separately. Then, results are compared. The variables define the geometry, concrete type, reinforcement and post-tensioning steel. The use of high-strength concrete is analyzed. A hybrid harmony search algorithm that combines threshold accepting optimization is used as optimization algorithm. Threshold accepting carries out a local search after a number of iterations without improving the best harmony. An experimental design method is used to adjust the algorithm parameters. The bridge is considered to be under conventional external ambient conditions. This case differs from the main study of this thesis in that a pedestrian bridge with different load conditions is analyzed. This simpler case is used to check

the performance of the algorithm, the design alternatives and the relationship between the objectives.

Main results

Hybrid harmony search algorithm obtained good results for the automatic design of post-tensioned concrete box-girder pedestrian bridges. A parametric study compares the best designs of five deck lengths, ranging from 90 to 130 m. Small differences between objectives are obtained due to geometrical restrictions. Findings indicate that the environmental goal also ensures economic solutions, given the emission-optimized results show 1% less pollution and 2% more expense compared to cost-optimized results.

Figure 3.12 shows the mean cost values per square meter of deck according to the deck length. A parabolic relation is used to describe the cost per surface of deck according to the deck length. For cost optimization, the relation is $C = 0.0146\ L^2 - 0.845\ L + 207.1$ with a regression coefficient $R^2 = 0.9885$. The relation for emission optimization is $C = 0.0257\ L^2 - 3.2912\ L + 345.75$ with $R^2 = 0.9885$. Figure 3.13 illustrates the mean emission values per square meter of deck according to the deck length. The emission relation can also be represented by a parabolic function for both cost-optimized ($E = 0.0734\ L^2 + - 10.67\ L + 812.93$ with $R^2 = 0.9914$) and emission-optimized solutions ($E = 0.0365\ L^2 + - 3.0631\ L + 422.2$ with $R^2 = 0.9938$).

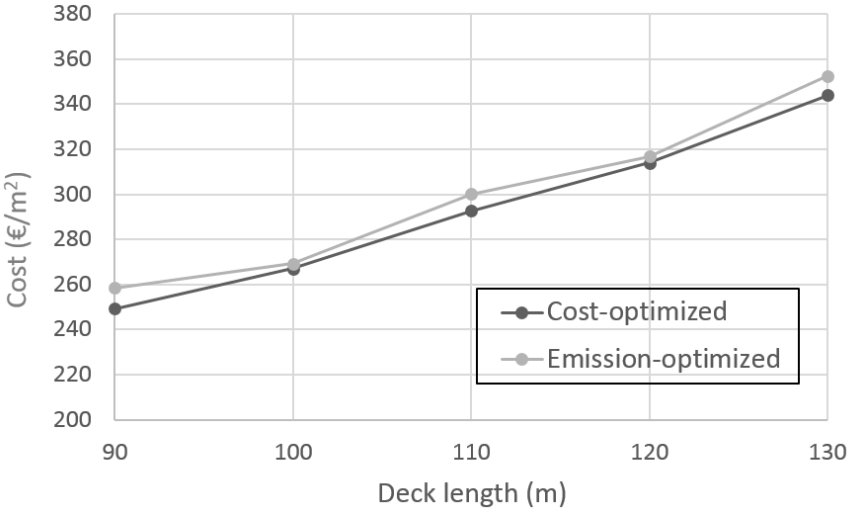

Figure 3.12. Mean cost of post-tensioned concrete box-girder pedestrian bridges (based on García-Segura et al (2015))

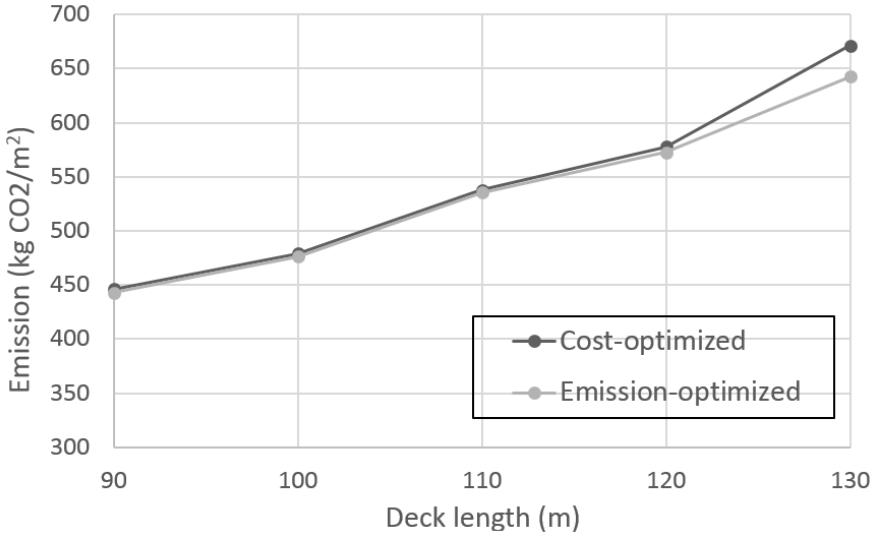

Figure 3.13. Mean CO_2 emissions of post-tensioned concrete box-girder pedestrian bridges (based on García-Segura et al (2015))

On the other hand, if costs and emissions per square meter of deck are represented as a linear function of the deck length, one meter increment results in 2.36 €/m^2 of deck and 5.49 kg CO_2/m^2 of deck for cost-optimized solutions. From an ecological point of view, increasing the deck by one meter results in 2.36 €/m^2 of deck and 4.96 kg CO_2/m^2 of deck.

Carbon capture is depicted in Figure 3.14. Carbonation represents less than 1% of the emissions. The conditions of geometry and service life do not lead to large quantities of carbon capture. To achieve more environmental benefits, concrete should be crushed and reused after demolition. The analysis of the main characteristics of the design shows that solutions with greater depths (see Figure 3.15), lower concrete strength (see Figure 3.16) and more strands (see Figure 3.17) are used when optimizing the emissions.

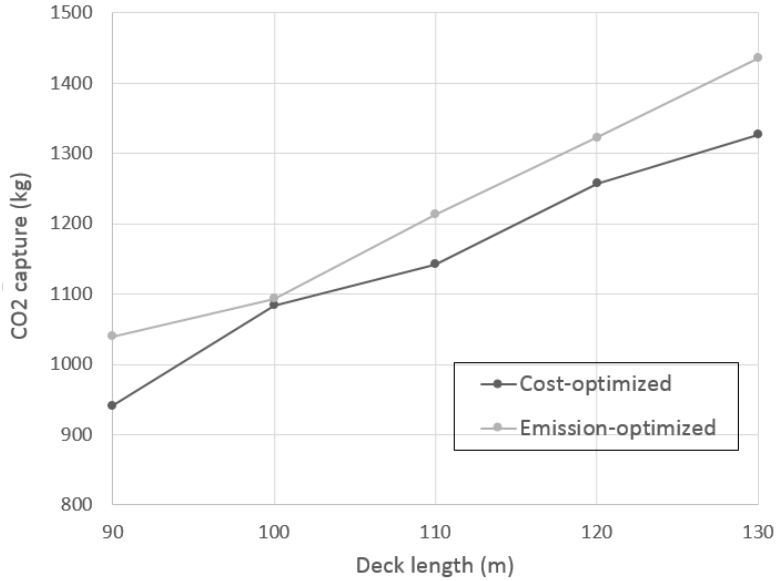

Figure 3.14. Mean CO_2 capture of post-tensioned concrete box-girder pedestrian bridges (based on García-Segura et al (2015))

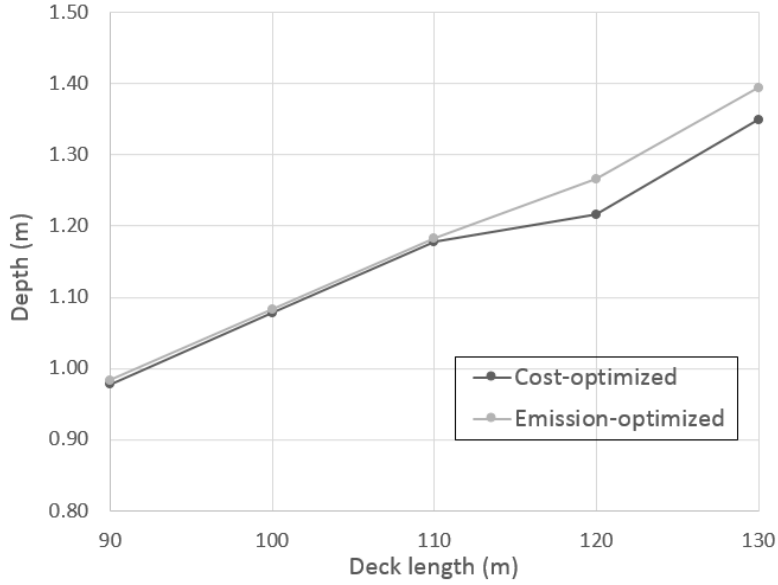

Figure 3.15. Mean depth of post-tensioned concrete box-girder pedestrian bridges (based on García-Segura et al (2015))

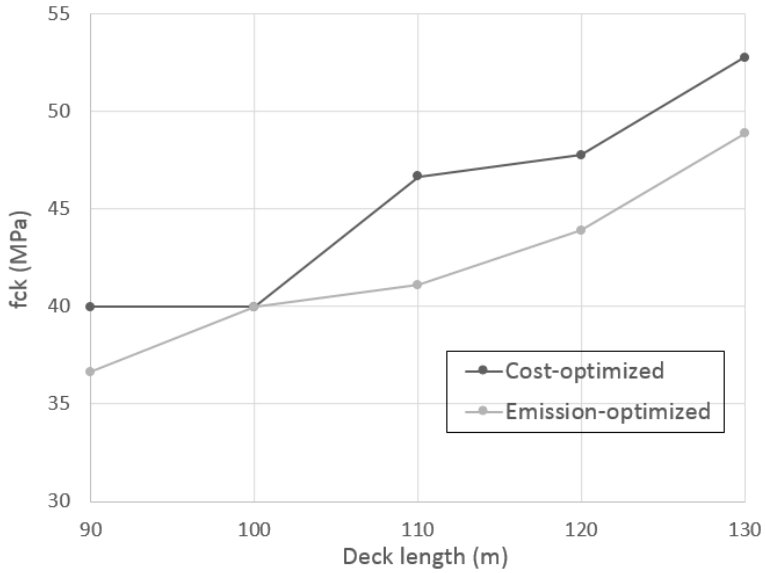

Figure 3.16. Mean concrete strength of post-tensioned concrete box-girder pedestrian bridges (based on García-Segura et al (2015))

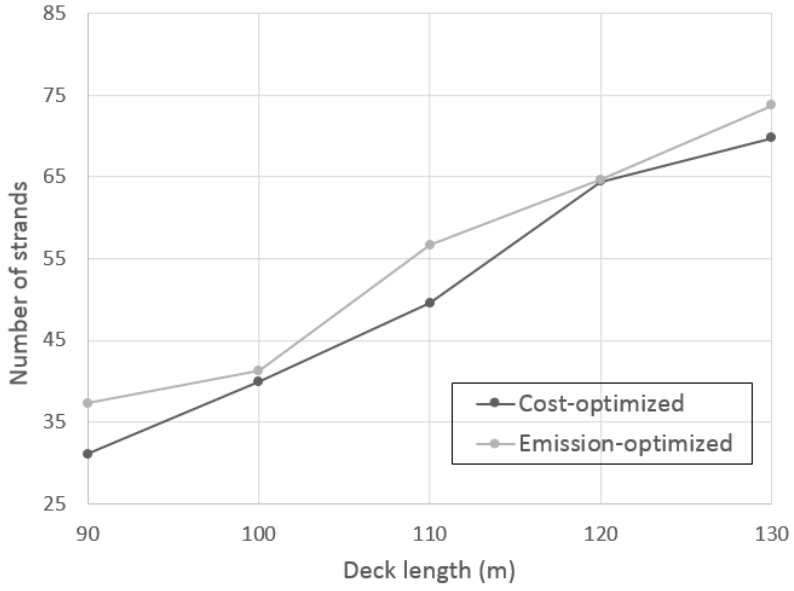

Figure 3.17. Mean number of strands of post-tensioned concrete box-girder pedestrian bridges (based on García-Segura et al (2015))

3.7. Study 6. A cognitive approach for the multi-objective optimization of RC structural problems

This study (Yepes et al., 2015a) aims to analyze and reduce the Pareto optimal set for multi-objective optimization of structural problems. Firstly, a multi-objective optimization of a simply supported concrete I-beam including several high-strength concrete mix compositions is carried out. The objective functions are the economic cost, the CO_2 emissions including carbonation, and the service life. This study considers carbonation as the main process in RC degradation. Multi-Objective Simulated Annealing (MOSA) is used as the optimization algorithm. Then, the Pareto set is filtered by obtaining random Analytic Hierarchy Process (AHP) pairwise comparison matrices and calculating the closest point to the ideal. The cognitive approach provides improved knowledge on the decision-making process.

Methodology

Figure 3.18 shows the methodology followed by this study. Three steps are conducted:

1. Pareto optimum solutions are obtained based on the variables, the parameters, the objective functions, the constraints and the algorithm selected.
2. Pareto set is filtered to compromise solutions. This process selects the closest solution to the ideal point according to random AHP pairwise comparisons. The weights are obtained from these random pairwise comparison matrices by applying the eigenvector method. Matrices that guarantee good consistency are saved. Thus, only those weights that belong to consistent matrices are used. Then, the closest solutions to the ideal are obtained using the three well-known metrics of the Minkowsky family: the Manhattan (p = 1), Euclidean (p = 2), and Tchebycheff ($p = \infty$) metrics. The solutions, which regardless of the criteria preferences, are further from the ideal point, are removed to facilitate the selection.
3. The decision-maker compares the importance of the criteria to achieve the sustainable goal and gives a numerical scale by means of AHP pairwise comparisons. The weights obtained to each criteria are allocated to the distance assessment. The preferred solution is obtained as the closest solution to the ideal point.

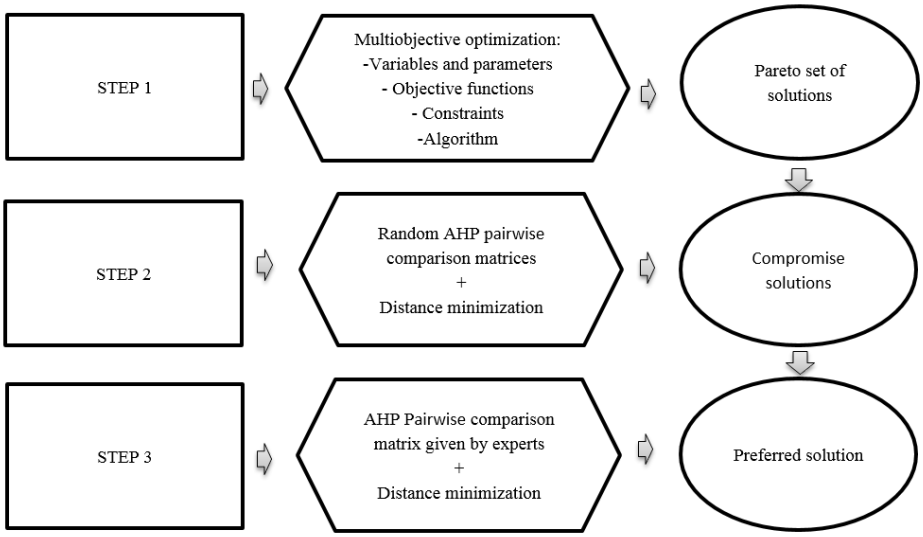

Figure 3.18. Methodology to filter the Pareto set and obtained the preferred solution (based on Yepes et al. (2015a)

Step 1 reduces the space of solutions to that of the optimum and feasible solutions. Step 2 hereafter selects the compromise solution as the one that lies geometrically closest to the ideal point. Figure 3.19 shows the compromise solution for a two-objective optimization in terms of the Euclidean distance. The ideal point is the theoretical best performance point that contains the best values for each objective. Note that if the relative importance of the objectives changes, a different compromise solution may be chosen.

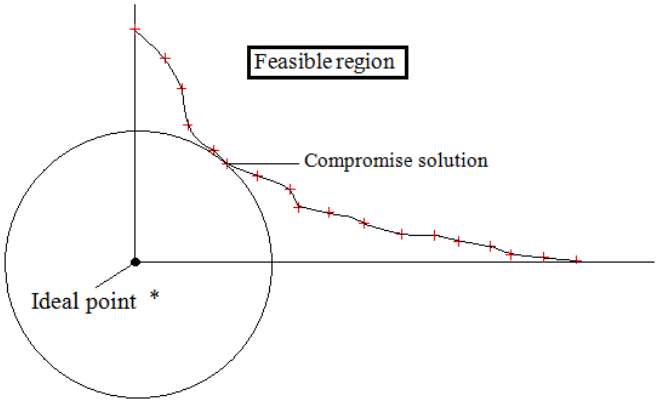

Figure 3.19. Compromise solution selection (based on Yepes et al. (2015a)

Main results

MOSA is calibrated using Metropolis and Glauber criteria. The Glauber criterion achieved the best results. Therefore, multi-objective simulated annealing with Glauber criterion (MOSA-G) is used for the Step 1. Compromise solutions are analyzed according to the relative importance of the compared criteria. The cognitive approach is carried out studying the stability of the obtained solution, the robustness of the proposed approach and the characteristics of the solutions.

Figure 3.20-23 illustrate the Pareto set as ranges of service life. Concrete strength is highlighted. Regarding service lives between 100 and 200 years (see Figure 3.20), concrete from 30 to 45 MPa presents the best results. In case service life between 200 and 300 years is preferred (see Figure 3.21), concrete from 45 to 55 MPa should be chosen. Nevertheless, for service life to 400 years (see Figure 3.22), 60 MPa concrete is also used. Concerning a service life of 400 to 500 years (see Figure 3.23), concrete of 50 to 80 MPa is the best choice. Finally, results show that 90 and 100 MPa concrete are not Pareto solutions.

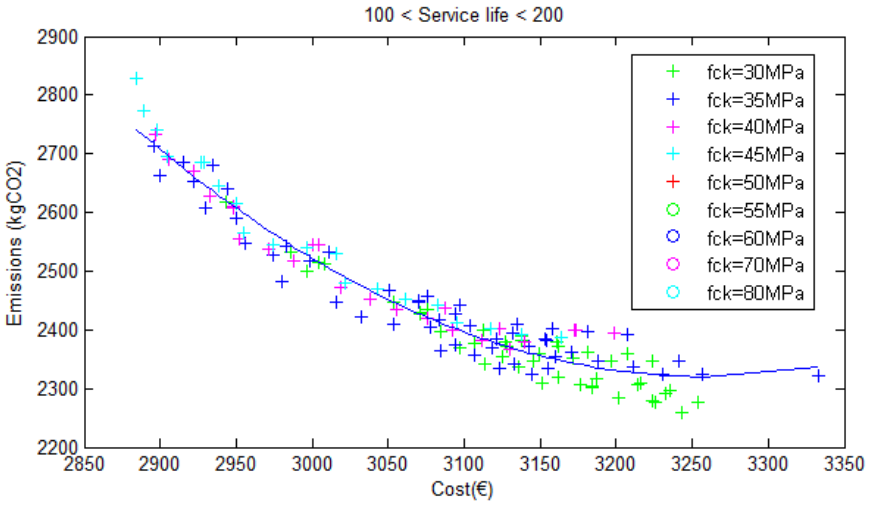

Figure 3.20. Pareto set for a service life between 100 and 200 years (based on Yepes et al. (2015a)

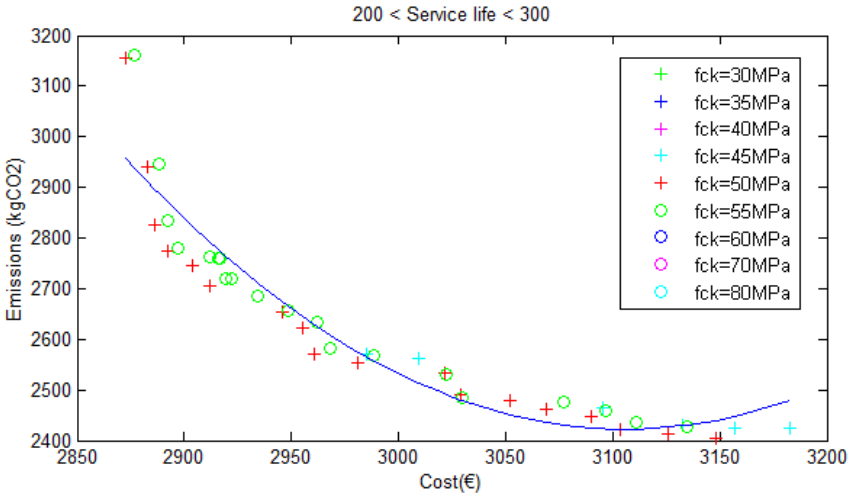

Figure 3.21. Pareto set for a service life between 200 and 300 years (based on Yepes et al. (2015a)

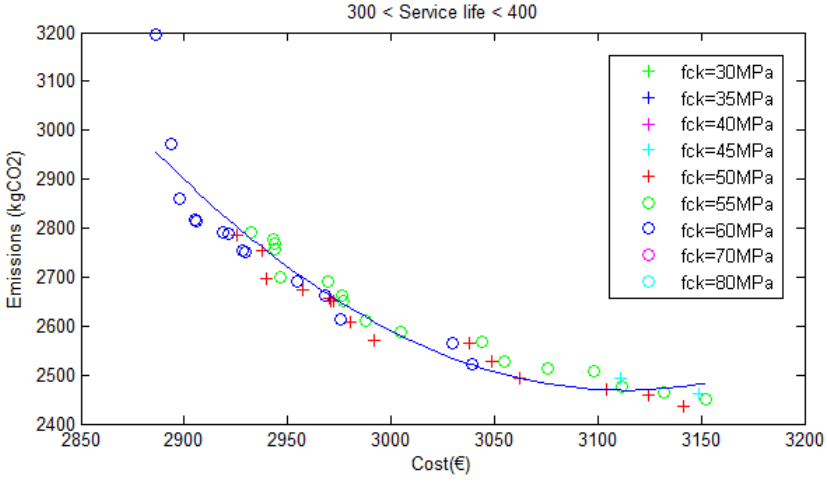

Figure 3.22. Pareto set for a service life between 300 and 400 years (based on Yepes et al. (2015a)

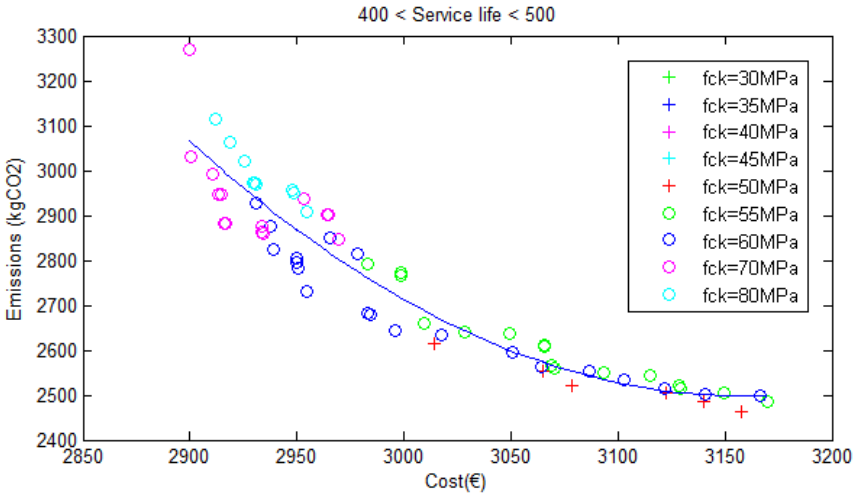

Figure 3.23. Pareto set for a service life between 400 and 500 years (based on Yepes et al. (2015a)

The following figures (Figures 3.24-26) provide a cognitive orientation of the compromise solutions according to the different types of concrete. Findings prove that this methodology has achieved the objective, which is to reduce the Pareto set and learn during this process. The results of the Step 2 are analyzed under the influence of the decision-maker and the metric used. Figure 3.24 shows the best solutions for the L_1 metric. The vertices represent the points where the weight of each criteria is equal to one. The 299 solutions of Pareto set are reduced to seven compromise solutions. All the solutions use high-strength concrete (fck > 50 MPa). Specifically, four solutions use 55 MPa concrete, one uses 60 MPa concrete, and two use 80 MPa concrete. Note that as the emission weight increases, the concrete strength decreases. This outcome is in accordance with the statement that high-strength concrete do not benefit the CO_2 reduction. Figure 3.25 depicts the results for the L_2 metric. In this case, the Euclidean metric reduces the set to 18 solutions. Regarding L_∞ metric, Figure 3.26 displays the 46 compromise solutions. Concrete of 55 MPa grade is the most used in both L_2 and L_∞ metrics.

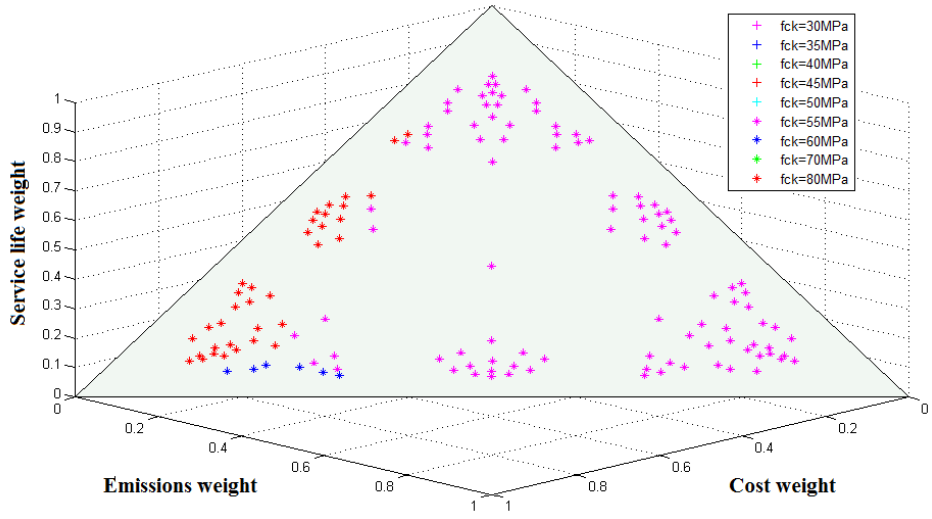

Figure 3.24. Compromise solutions for L_1 metric according to the concrete strength (based on Yepes et al. (2015a)

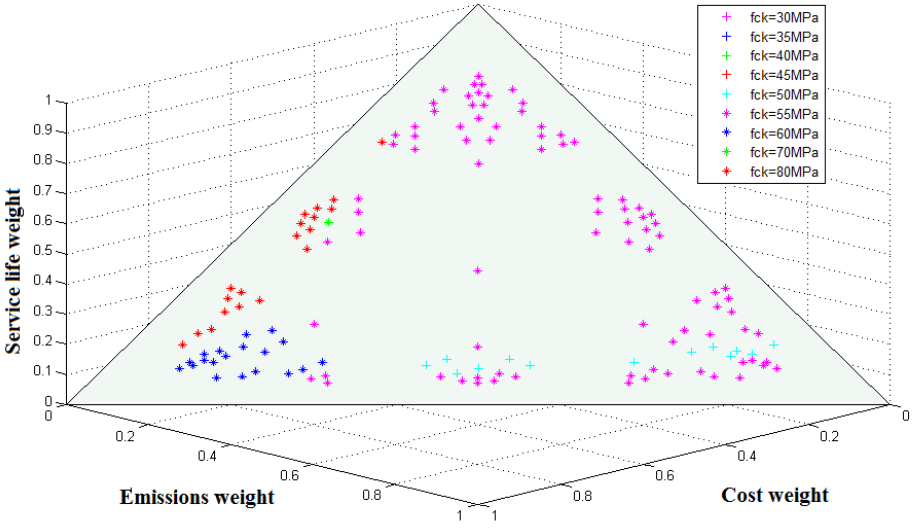

Figure 3.25. Compromise solutions for L_2 metric according to the concrete strength (based on Yepes et al. (2015a)

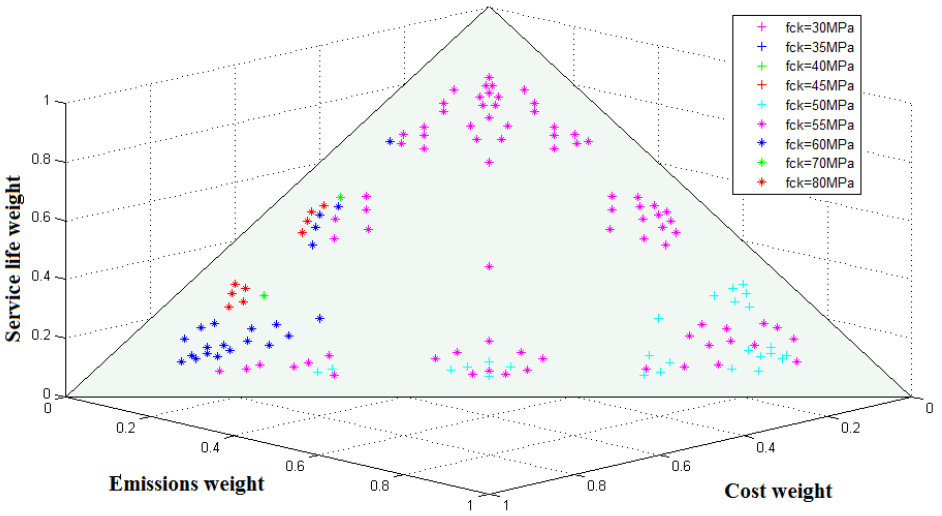

Figure 3.26. Compromise solutions for L∞ metric according to the concrete strength (based on Yepes et al. (2015a)

After that, Step 3 selects the preferred solution based on expert preferences. Yepes at al. (2015a) provides an example of a pairwise comparison matrix. Then, a preferred solution is chosen according this method.

3.8. Conclusions

This chapter explains the main results of six studies regarding the comparison of blended cements through a life-cycle greenhouse gas emission evaluation that includes the CO_2 capture during the service life and after demolition, the use of conventional vibrated concrete and self-compacting concrete in concrete I-beams, the emission and energy optimization of precast-prestressed concrete U-beam road bridges, the emission optimization of post-tensioned concrete box-girder pedestrian bridges and the reduction of Pareto solutions by a decision-making process. The main conclusions of these investigations are:

- **Blended cements** decrease the emissions per year despite the use of these cements entails a reduction in carbon capture and service life. It is crucial to reuse concrete as gravel-filling material to achieve a complete carbonation and reduce the CO_2 emissions.
- **Self-compacting concrete** is not advisable for an environmental point of view. Regarding cost, few differences are obtained between conventional vibrated and self-compacting concrete.
- **Emission optimization of RC I-beams** achieves better results using larger sections, greater amount of concrete, less steel and conventional vibrated concrete with the lower strength grade.
- Regarding **post-tensioned concrete**, small differences between objectives

are obtained. Emission-optimized results show 1% less pollution and 2% more expense compared to cost-optimized results. These differences show that solutions with greater depths, more strands and lower concrete strength are preferred from an environmental point of view.

- Concrete strength does not show a clear difference in values between energy and cost minimization. In contrast to **energy optimization**, the emission criteria prefers lower concrete strength. This outcome is attributed to the fact that emission criterion also considers the limestone calcination.
- Even common sense seems to await the outcome of more expensive solutions for sustainable designs, the range to which each criterion moves away from the structural efficiency and the volume of the feasible space determine the results. That is to say, structures with narrow feasible space in which the cost and emission minimization seek the reduction in material consumption, the **objective functions** are more likely to **search in the same direction.**
- Random AHP matrices can be combined with distance minimization to reduce the Pareto set and select a preferred solution. With this method, the consistency of the judgments is guaranteed and the sum of the weights provided by the matrix is always equal to one. The goal of facilitating the **decision-making process** is achieved.
- Regarding the **heuristic algorithms**, population-based algorithms with a local search strategy show promising results. However, SAGSO presents two problems: a high number of parameters with the subsequent importance of a good calibration, and a high computing time.

In view of these results, the following **considerations** will be taken into account for the multi-objective optimization of the post-tensioned concrete box-girder road bridges based on sustainable multi-objective criteria:

- Blended cements are not considered for the following studies since the Spanish code (Fomento, 2008) only covers the use of fly ash and silica fumes limited, respectively, to 20% and 10% of the weight of the cement for prestressed concrete. It is important to consider the carbonation during use stage and ensure the atmospheric exposure after recycling. The amount of carbon capture during the second life will depend on its use.
- Self-compacting concrete is not studied for the bridge road case. Nevertheless, this material should be considered when the construction characteristics require it.
- CO_2 emission is considered to achieve the sustainable goal. The relationship between cost and emission optimization depends on the case study, and particularly, to the space of feasible solutions.
- CO_2 emission evaluation takes into account the emissions derived from the energy use and other sources of emissions. Therefore, CO_2 emission is considered a more complete criterion, compared to energy.
- Hybrid harmony search algorithm showed its potential applicability for the design of sustainable solutions of post-tensioned concrete box-girder

pedestrian bridges. Nevertheless, this algorithm must be adapted to a multi-objective optimization problem.

- The preferences to a specific criterion are subject to uncertainty. Therefore, the decision-making process of Yepes et al. (2005) should be modified to take into account the uncertainty associated to the criteria comparison.

Chapter 4
Optimization problem

4.1. Aim of the study

This study focuses on the design of a real post-tensioned concrete box-girder bridge by an accurate method and taking into account sustainable criteria. Box-girder bridges are one of the most common types of continuous bridges. This cross-section can be found in beam, arc, portal frame, cable-stayed and suspensions bridges. Box-girder bridges have a number of advantages from both the resistance and construction perspective. Box-girder bridges with constant depth usually acquire spans lengths between 30 and 90 m.

Heuristic optimization is used as an automatic process for obtaining high-performing solutions. This method has proved its potential in solving complex and realistic structural problems. In this case, the variables needed to define the design form a solution space on the order of 10^{28}. Optimization technique provides the optimum designs that comply with the constraints and minimize the objectives. This technique gives rise to explore new designs through the combination of multiple variables. Besides, this approach guarantees that designs are not based on predefined rules, and therefore, each combination of the variables is explored. In addition, the constraints related to any important performance measure can be transformed to objectives. In this way, this procedure allows us to find solutions that hardly increase the cost and improve other objectives.

4.2. Problem definition

The structural problem involves a deck of three continuous spans of post-tensioned concrete (PSC) with a box-girder cross-section. Figure 4.1 shows the longitudinal profile of the bridge. The deck belongs to a road bridge located in a coastal region. The deck width hold a highway of two 3.5m-wide lanes, a 1m-wide inner verge and a 2.5m-wide outer verge. Besides, there should be 65 cm space to place the parapet on both sides of the deck. Therefore, the width is 11.8m. The external (L_2) and main (L_1) span have a length of 35.2 m and 44 m, respectively. This corresponds to a ratio between L_1 and L_2 of 0.8. The total span length is 114.4m. The construction is considered to be cast in place. The scaffolding is not considered, since it does not entail any change with respect to the optimal solution.

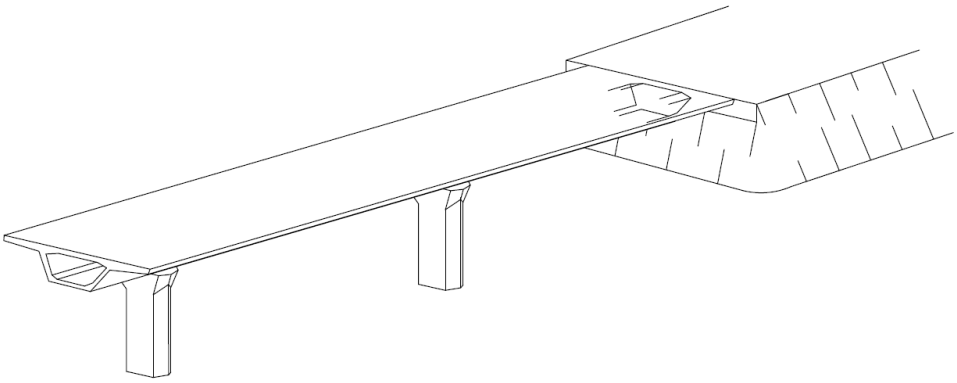

Figure 4.1. Longitudinal profile of the PSC box-girder road bridge

The multi-objective optimization problem aims to minimize or maximize the objective functions F_i of Equation 4.1, while satisfying the structural constraints G_j represented by Equation 4.2. Both the objective functions and structural constrains depend on the design variables x_1, x_2,…, x_n and the parameters p_1, p_2,…, p_m. Each design variable can adopt the discrete values, which range between d_{k1} and d_{kqk} (see Equation 4.3). The variables are discrete to guarantee a real bridge design.

$$F_i(x_1, x_2, \ldots., x_n; p_1, p_2, \ldots., p_m) \quad \textbf{Equation 4.1}$$

$$G_j(x_1, x_2, \ldots., x_n; p_1, p_2, \ldots., p_m) \leq 0 \quad \textbf{Equation 4.2}$$

$$x_k \in \left(d_{k1}, d_{k2}, \ldots., d_{kq_k}\right) \quad \textbf{Equation 4.3}$$

The objective functions are defined in Chapter 5. The constraints check all the serviceability limit states (SLSs) and ultimate limit states (ULSs) with which the structure must comply. In addition, the geometrical and constructability constraints of the problem should be guaranteed. Chapter 6 describes the bridge analysis and the corresponding constraints.

4.3. Parameters

The parameters are all fixed quantities that do not change during the optimization procedure. The parameters together with the variables must define the complete bridge design. The choice of the parameters leads to a particular case study. Varying the parameters, the optimum variables and the values of the objective functions change accordingly. In bridge design, the over-all geometry and the materials are defined in a previous stage according to the designer experience and the topographical and traffic conditions. Table 4.1 summarizes the parameters chosen for the optimization problem. The loads, transport distances and external ambient conditions are selected for a specific location and case study. In this case, 26 parameters are used to define the bridge problem

4.3.1. *Geometrical parameters*

Eight parameters are fixed for the geometry. The width is imposed by the road conditions. Span lengths are selected based on common values for highway bridges of box-girder cross-section and complying a ratio between the external and the main span of 0.8. This ratio has been chosen to balance the bending moments between spans under self-weight loads. Regarding the asphalt thickness, a mean value of 8.9 cm is considered.

Post-tensioning is applied by high-strength prestressing steel strands distributed symmetrically through the webs. Figure 4.2 illustrates the prestressing steel layout. The parabolic layout is defined by several points sorted in the following order: abutments, maximum eccentricity in the external span, point of inflection, piers, point of inflection and maximum eccentricity in the main span. While the point of inflection is variable, the distance from the abutments to the maximum eccentricity in the external span is set as $0.375 \cdot L_2$. The eccentricity in the piers and midspan is the maximum allowed, taking into account that the distance between the center of the duct and the reinforcing bars is 1.5 times that of the duct diameter. The maximum eccentricity in the external span is a design variable (see Section 4.4). The eccentricity of the point of inflection is calculated according to the other points. Table 4.2 summarizes the main points of the parabolic layout. A further consideration is that of the space for the duct placement. Figure 4.3 shows a cross-section of the bridge at the maximum eccentricity in the external span and over the piers. Over piers, the ducts are allocated in a line in the flanges and top slab. The lower points of layout are placed in rows of two.

Table 4.1. Main parameters of the analysis

Geometrical parameters (8)	
Pedestrian bridge width	A = 11.8 m
Number of spans	3
Main span length	L_1 = 44 m
External span length	L_2 = 35.2 m
Distance to the maximum eccentricity in the external span	0.375 L_2
Mean asphalt thickness	8.9 cm
Diaphragm thickness over abutments	2 m
Diaphragm thickness over piers	3 m
Material parameters (6)	
Maximum aggregate size	20 mm
Reinforcing steel	B-500-S
Post-tensioned steel	Y1860-S7
Transverse reinforcement diameter TR_9	12 mm
Strand diameter	Φ_s = 0.6”
Tensioning time	7 days
Loading related parameters (5)	
Reinforced concrete self-weight	25 KN/m^3
Asphalt layer self-weight	24 KN/m^3
Parapet self-weight	5 KN/m
Prestressing force in each strand	195.52 KN
Differential settling	5 mm
Transport parameters (5)	
Cement distance	32 km
Plasticizer distance	724 km
Aggregate distance	12 km
Silica fume distance	1420 km
Concrete distance	40 km
Code related parameters (2)	
Code regulation	EHE-08/IAP-11
External ambient conditions	IIIa

Table 4.2. Main points of the parabolic layout

Location	*x*	*z*
Abutment	0	0
Maximum eccentricity in the external span	$0.375 \cdot L_2$	$-e_p \cdot h/2$
Point of inflection	$L_2 - L_{PI} \cdot L_1$	
Pier	L_2	$h/2 - 1.5 \cdot \Phi_s$
Point of inflection	$L_2 + L_{PI} \cdot L_1$	
Maximum eccentricity in the main span	$L_2 + 0.5 \cdot L_1$	$-h/2 + 1.5 \cdot \Phi_s$

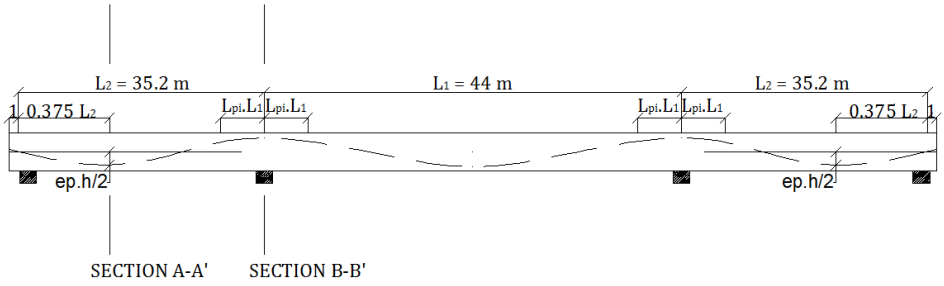

Figure 4.2. Layout of the post-tensioning steel

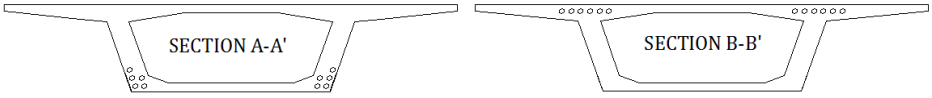

Figure 4.3. Duct allocation

4.3.2. *Material parameters*

The maximum aggregate size for the concrete is 20 mm. B-500-S is used for the reinforcing steel, which means that the characteristic yield strength is 500 MPa. Regarding the post-tensioning steel, Y1860-S7 is used. Strands have a maximum unit load of 1860MPa, seven wires and 15.7mm diameter (0.6 in.). The tension is applied after 7 days. Transverse reinforcement is shown in Figure 4.4. The diameters TR_1, TR_2,…,TR_8 are variables. However, TR_9 can only takes 12 mm diameter.

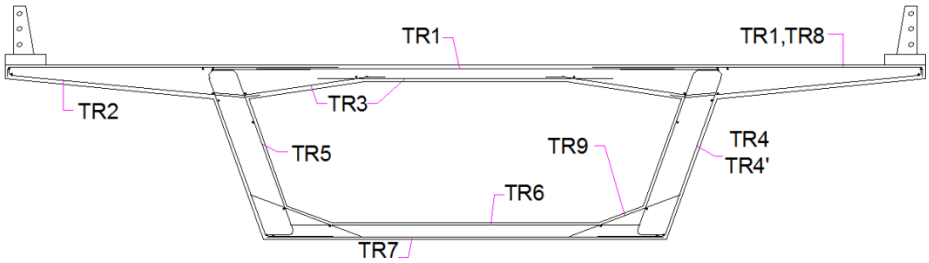

Figure 4.4. Transverse reinforcement

4.3.3. *Loading related parameters*

Bridge loads are defined by the Spanish code IAP-11 (Fomento, 2011), which is based on the Eurocode (European Committee for Standardisation, 2003b). Other actions are considered: reinforced concrete self-weight (25 KN/m^3), asphalt layer self-weight (24 KN/m^3), parapet self-weight (5 KN/m), prestressing force in each strand (195.52 KN) and differential settling between piers and pier-abutment (5 mm).

4.3.4. *Transport parameters*

Transport parameters are used to evaluate the cost and emissions of concrete. Concrete unit price and emissions are determined according to the compressive strength grade. To this end, the total cost and emission are assessed as the sum of every component. Values include the raw materials extraction, manufacture and transportation. The bridge is assumed to be placed in Valencia. The transport distances are doubled after considering the return trip. The distances for cement, plasticizer, aggregate and silica fume are shown in Table 4.1. Besides, the concrete is transported by mixer from the concrete plant to the building site.

4.3.5. *Code related parameters*

Bridge design follows the Spanish codes for actions IAP-11 (Fomento, 2011) and concrete design EHE-08 (Fomento, 2008). These codes have been adapted for the Eurocode content (European Committee for Standardisation, 2003b, 2005). The general exposure class relating to the corrosion of the reinforcements is IIIa (marine aerial). This exposure class corresponds to elements of structures located close to the coastline (l 5 km) and affected by chlorides.

4.4. Variables

Variables are defined to complete the bridge design. The values are assigned by the metaheuristic or stochastic algorithm. These values are discrete to guarantee that the bridge can be built. The optimal bridge design of a PSC box-girder is determined by the variables, regarding the geometry, concrete grade, reinforcement and post-

tensioning steel. The design variables and the possible values that they can adopt are listed below. Figure 4.5 and 4.6 illustrate the cross-section geometry and longitudinal reinforcement. An extra reinforcement in both transverse and longitudinal reinforcement is placed according to the distribution shown in Figure 4.7. The extra transverse reinforcement in the external layer of the web covers the support zone (0.2L on both sides). The extra longitudinal reinforcement in the top and bottom slab cover the pier zones (0.2L on both sides) and girder zones (the rest of the span), respectively. Note that the anchorage lengths are added to these values.

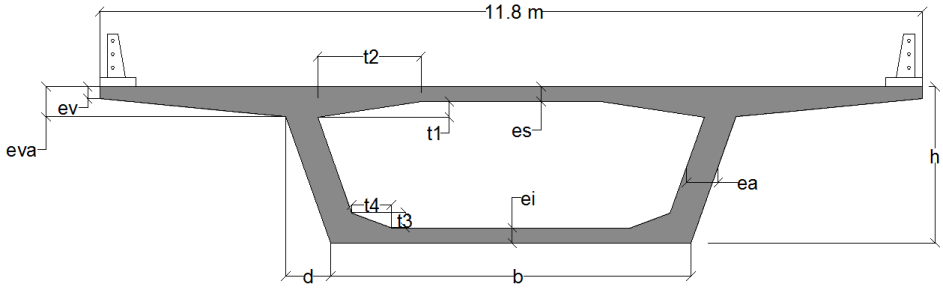

Figure 4.5. Cross-section geometry

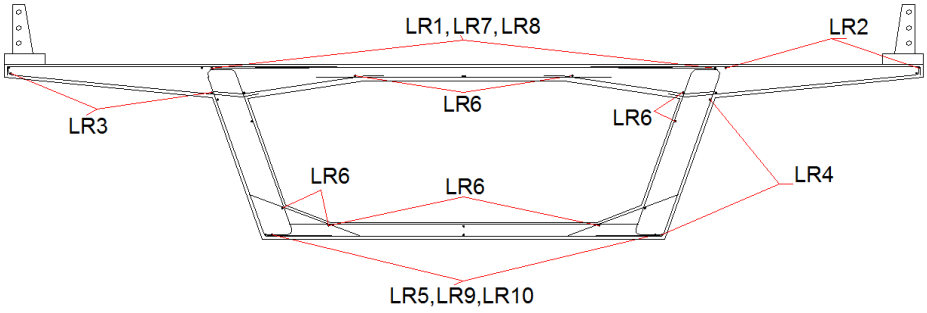

Figure 4.6. Longitudinal reinforcement

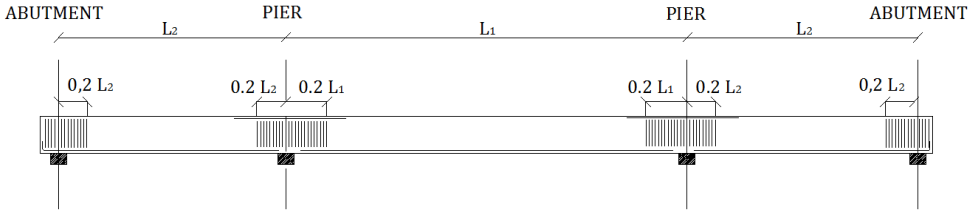

Figure 4.7. Extra reinforcement distribution

1) Depth (*h*)

The depth of the girder takes values from 1.45m to 4.4m, every 5cm. This corresponds a relationship between the span length and girder depth of L/30 and L/10. Therefore, 60 values are proposed.

2) Width of the bottom slab (*b*)

The width of the bottom slab takes values from 3.5m to 7.05m, every 5cm. These values correspond to percentages of 30% and 60% of the deck width. Thus, 72 values are proposed.

3) Width of the web inclination (*d*)

The width of the web inclination is determined from the web slope. The web slope takes values from 2 to 4, every 0.5. Once the web slope is defined, the width of the web inclination is calculated according to the depth minus thickness of the internal flange section (e_{va}). Thus, 5 values are proposed.

4) Thickness of the top slab (e_s)

The thickness of the top slab takes values from 20 cm to 40 cm, every 5 cm. Thus, 5 values are proposed.

5) Thickness of the external flange section (e_v)

The thickness of the external flange section takes values from 20 cm to 40 cm, every 5 cm. Thus, 5 values are proposed.

6) Thickness of the internal flange section (e_{va})

The thickness of the internal flange section takes values from 35 cm to 70 cm, every 5 cm. Thus, 8 values are proposed.

7) Thickness of the bottom slab (e_i)

The thickness of the bottom slab takes values from 20 cm to 40 cm, every 5 cm. Thus, 5 values are proposed.

8) Thickness of the web (e_a)

The thickness of the web takes values from 40 cm to 80 cm, every 5 cm. Thus, 9 values are proposed.

9) Concrete strength (f_{ck})

Concrete type is defined by its characteristic strength. This variable takes several grades: 35, 40, 45, 50, 55, 60, 70, 80, 90 and 100 MPa. Thus, 10 values are proposed. High-strength concrete has a compressive strength greater than 50MPa.

10) Eccentricity in the external span (e_p)

The eccentricity in the external span where the bending moment is maximum

($0.375 \cdot L_2$ from the abutments) is defined as a percentage of half of the depth. The eccentricity (e_p) takes values from 0.5 to 1, every 0.1. These values are later multiplied by h/2. Thus, 6 values are proposed.

11) Distance from the piers to the point of inflection (L_{PI})

The distance from the piers to the point of inflection is defined as a percentage of the span length. L_{PI} takes values from 0.05 to 0.2, every 0.05. These values are later multiplied by L_1. Thus, 4 values are proposed.

12) Number of strands (N_S)

The number of strands takes values from 160 to 320, one at a time. Thus, 161 values are proposed. Note that prestressing steel strands are divided symmetrically through the webs. Therefore, the number of strands should be even and the same in each tendon. Besides, the maximum number of strands per tendon is 31. This means that a module transforms the number of strands to a real number that follows this rule. For example, if the algorithm chooses 195 strands, this corresponds to a minimum of 6.29 tendons. As this number should be transferred to 8 tendons or 4 tendons/web, 195 strands divided by 8 tendons is equal to 24.375 strands/tendon. Therefore, 25 strands per tendon and 8 tendons are used. As a result, 200 strands will be the real number.

13-18) Diameter of the longitudinal reinforcement LR_1- LR_6

The longitudinal reinforcing steel is defined for the top layer of the top slab (LR_1), the top layer of the flange (LR_2), the bottom layer of the flange (LR_3), the external layer of the web (LR_4), the bottom layer of the bottom slab (LR_5) and the internal layer of the girder (LR_6). The diameter takes the following values: 10, 12, 16, 20, 25 and 32 mm. Thus, 6 values are proposed for each location.

19) Diameter of the longitudinal reinforcement LR_7

Besides, an extra reinforcement in the top layer of the top slab is proposed to adjust the differences in negative bending moment between the pier zone (L/5 on both sides of the piers) and the rest of the span. The extra reinforcement that covers the pier zone (LR_7) takes the following values: 0, 10, 12, 16, 20, 25 and 32 mm. Thus, 7 values are proposed. Note that the extra reinforcement can adopt the value 0, that is to say, there is no extra reinforcement.

20) Diameter of the longitudinal reinforcement LR_8

The extra reinforcement in the top layer of the top slab that covers the rest of the span (LR_8) takes the following values: 0, 10, 12, 16, 20, 25 and 32 mm. Thus, 7 values are proposed.

21) Diameter of the longitudinal reinforcement LR_9

Likewise, an extra reinforcement in the bottom layer of the bottom slab is proposed to adjust the differences in positive bending moment. The extra reinforcement that covers the pier zone (LR_9) takes the following values: 0, 10, 12, 16, 20, 25 and 32

mm. Thus, 7 values are proposed.

22) Diameter of the longitudinal reinforcement LR_{10}

The extra reinforcement in the bottom layer of the bottom slab that covers the rest of the span (LR_{10}) takes the following values: 0, 10, 12, 16, 20, 25 and 32 mm. Thus, 7 values are proposed.

23-30) Diameter of the transverse reinforcement TR_1 - TR_8

The transverse reinforcing steel is defined for the top layer of the top slab and flanges (TR_1), the bottom layer of the flange (TR_2), the bottom layer of the top slab (TR_3), the external layer of the web (TR_4), the internal layer of the web (TR_5), the top layer of the bottom slab (TR_6) and the bottom layer of the bottom slab (TR_7). Besides, there is an extra reinforcement in the top layer of the flanges (TR_8) to improve the efficiency over the flanges along the bridge length. The diameter takes the following values: 10, 12, 16, 20, 25 and 32 mm. Thus, 6 values are proposed for each location.

31) Diameter of the transverse reinforcement $TR_{4'}$

An extra reinforcement is defined in the external layer of the web ($TR_{4'}$) to cover the support zone (L/5 on both sides of the piers and abutment). It takes the following values: 10, 12, 16, 20, 25 and 32 mm.

32) Number of bars per meter for the longitudinal reinforcement (N_{LR})

The number of bars per meter is equal for all the longitudinal reinforcement, with the objective of simplifying the construction. The number of bars per meter takes the following values: 4, 5 and 6. Thus, 3 values are proposed.

33) Spacing of all the transverse reinforcing (S_{TR})

Likewise, the spacing of all the transverse reinforcing is equal. The spacing takes the following values: 15, 20 and 25 cm. Thus, 3 values are proposed.

34) Concrete cover (c_c)

Concrete cover is firstly fixed as 65mm to guarantee the durability conditions for a coastal environment. In this case, the concrete cover is not a variable and the bridge design uses 33 variables. In a second study, the concrete cover takes values from 3 cm to 7.5 cm, every 5 mm. Thus, 10 values are proposed.

Solution space

The solution space is defined by the set of combinations of values for the 33 or 34 variables, depending on the case. Such space is on the order of 10^{28} or 10^{29}, depending whether the concrete cover is considered as a variable or not.

Moreover, other values (t_1, t_2, t_3, t_4) are determined by the value of other variables (Equations (4.4–7)).

$$t_1 = e_{va} - e_s \quad \textbf{Equation 4.4}$$

$$t_2 = \frac{b + 2 * d}{5} \quad \textbf{Equation 4.5}$$

$$t_3 = e_i \quad \textbf{Equation 4.6}$$

$$t_4 = \frac{b}{10} \quad \textbf{Equation 4.7}$$

4.5. Heuristic algorithm

Despite many researches have investigated the best algorithm for different case studies, there is no consensus for the best algorithm. Structural optimization problems are non-convex, with a large design space of discrete variables. Population-based heuristic optimization methods are effective in such problems, outperforming gradient-based methods (Felkner et al., 2013). Other common outcome is that hybridization strategies benefit global search and convergence speed (Luo & Zhang, 2011; Shieh et al., 2011). That is, diversification and intensification techniques are combined. Our research group have proposed several hybrid algorithms (García-Segura et al., 2015; García-Segura et al., 2014c; Martí et al., 2013, 2016; Yepes et al., 2015b). As explained in Section 3.8, SAGSO obtained good quality results. However, the high number of parameters and the computation time make it less efficient. On the other hand, hybrid harmony search algorithm showed its potential applicability for the design of sustainable solutions of post-tensioned concrete box-girder pedestrian bridges (García-Segura et al., 2015). This algorithm combines harmony search and threshold accepting. The local search of threshold accepting improved the quality of solution about 8%, compared to the conventional HS.

Harmony search achieved the best results in the study of Alberdi & Khandelwal (2015), in which ACO, GA, HS, PSO, SA, and TS algorithms were compared for the design optimization of steel frames. These authors highlighted the efficiency of this algorithm in finding the optimal solution of problems with large and poorly organized variable spaces. HS algorithm is an effective metaheuristic algorithm in optimization of engineering problems (Nigdeli et al., 2015). HS has also been successfully used for the optimization of several structures (Akin & Saka, 2015; de Medeiros & Kripka, 2014; Kaveh & Shakouri Mahmud Abadi, 2010). Regarding multi-objective optimization, Sivasubramani & Swarup (2011) also pointed out that the proposed multi-objective harmony search method was able to give better distributed Pareto optimal solutions than NSGA-II method. Hajipour et al. (2014) demonstrated by statistical experiments that multi-objective harmony search algorithm worked better than multi-objective simulated annealing and multi-objective genetic algorithm, especially for larger size problems. These authors considered the time metric. Likewise, Pavelski (2012) stated that non-dominated harmony search outperformed NSGA-II.

On this basis, this study proposes multi-objective harmony search to find efficient designs of post-tensioned concrete box-girder road bridges. Besides, diversification-intensification techniques are applied to this algorithm to improve its performance.

4.5.1. *Harmony search*

The algorithm proposed by Geem et al. (2001), bases its strategy on the process of searching for the perfect musical harmony. In a music improvisation process, the musician looks for the musical harmony by playing notes from their memory, changing the previous ones a little, and trying new notes randomly. Similarly, HS algorithm seeks the best solution by taking the information of the harmony memory, using the pitch adjusting to carry out a small movement, and choosing randomly the value of the variable. These three procedures are contemplated by the algorithm. The following steps explain the procedure:

Step 1- Assignment of the algorithm parameters. The parameters governing the algorithm behavior are determined. These are the harmony memory size (HMS), harmony memory considering rate (HMCR) and pitch adjusting rate (PAR). Besides, the maximum number of improvisations without improvement (IWI) is commonly determined as a termination criterion. In addition, the design variable pool is provided for each variable.

Step 2- Memory initialization. Harmony memory matrix (HM) is filled with solutions randomly. The number of solutions is equal to HMS. Each value of the variable is randomly assigned from the design pool. Then, vectors that correspond to feasible solutions are saved. The matrix is as follows:

$$HM = \left(\begin{array}{ccc|c} x_1^1 & \cdots & x_n^1 & f(x^1) \\ \vdots & \ddots & \vdots & \vdots \\ x_1^{HMS} & \cdots & x_n^{HMS} & f(x^{HMS}) \end{array} \right) \quad \textbf{Equation 4.8}$$

where *n* is the number of variables and *f* is the objective function.

Step 3 - Improvisation of a new solution. New harmony vectors are improvised according to three procedures:

Option 1. Random selection: the values of the variables are chosen from a set of possible values in the design variable pools with probability (1-HMCR).

$$X_i' \in X_i \; with \; probability \; (1 - HMCR) \quad \textbf{Equation 4.9}$$

Option 2. Memory consideration: the values of the variables are chosen from the HM with probability HMCR.

$$X_i' \in \left\{ x_i^1, x_i^2, \ldots, x_i^{HMS} \right\} with \; probability \; HMCR \quad \textbf{Equation 4.10}$$

Option 3. Pitch adjustment: after the memory consideration the value is modified one position up or down with a probability PAR

$$X_i' \in x_i^j \pm 1 \; with \; probability \; PAR \quad \textbf{Equation 4.11}$$

This process is repeated for the total number of variables.

Step 4 - Harmony memory matrix update. The new solution replaces the worst harmony if its objective function value improves the worst one.

Step 5 – Termination criterion. The optimization process returns to Steps 3 if the iterations without improving the best harmony reaches IWI.

4.5.2. *Multi-objective harmony search*

Xu et al. (2010) proposed a multi-objective version of HS algorithm for the design of a reconfigurable mobile robot prototype. This approach has given rise to different versions. Ricart et al. (2011) presented two proposals of the Harmony Search for multi-objective optimization. Then, the algorithms were compared to NSGA-II (Nondominated Sorting Genetic Algorithm II), which is one of the most representative algorithms for multi-objective optimization. The results demonstrated that both proposals were competitive compared to NSGA-II.

There is a clear difference between mono-objective and multi-objective optimization. In a mono-objective problem, the ranking assignment is directly allocated from the better to the worse value of the objective function. However, the multi-objective optimization presents a set of optimum solutions called Pareto front. These non-dominated solutions cannot be improved without worsening the value of one objective. In this case, the ranking assignment is not straightforward. Ricart et al. (2011) proposed the Fonseca & Fleming (1993) method. The ranking of a solution is equal to the number of individuals that dominate the solution in question (n_d) plus one (see Equation 4.12). Individuals that belongs to the Pareto front have a rank of one, as they are non-dominated.

$$rank(\vec{x}) = 1 + \mathrm{n}_d \qquad \textbf{Equation 4.12}$$

The first proposal of Ricart et al. (2011) calculates the ranking at each iteration. When the ranking of the new solution is better than the worst ranked solution in HM, the new solution replaces the worst one. If there are several solutions with the worst ranking, one solution is chosen randomly. The second proposal generates a new matrix through Step 3. The Fonseca-Fleming ranking is evaluated to the joint matrix H_u, which contains the last and new HM matrices. After that, the best HMS solutions are saved.

This research follows the second proposal. However, the crowding distance metric is used instead of the random selection of solutions with the same ranking. Crowding distance evaluates the density of solutions surrounding a particular solution vector. Thus, this metric benefits the diversification, since the solutions with greater crowding distance, that is, they are further from other solutions, are preferred. The multi-objective optimization steps are the same as mono-objective optimization with the following changes:

Step 3 – Improvisation of a new solution. Improvisation is carried out for HMS solutions. These harmony vectors form the new harmony memory matrix (NHM).

Step 4 – Harmony memory matrix update. This step is divided into two processes.

- **Ranking assignment.** The ranking is assigned to H_u (HM ∪ NHM) through the Equation 4.12.
- **Selection of the best solutions.** H_u is sorted according to the ranking. The solutions with the lowest ranking are transferred to HM until the number of solutions with the next ranking is larger than the space of HM. Then, the crowding distance is evaluated according to the Equation 4.13. This metric estimates the perimeter of the cuboid formed by the nearest neighbors in the objective space as the vertices. Solutions are sorted for each objective (*m*). The crowding distance of a solution (*j*) is evaluated as the distance to the neighbors (*j+1*/*j-1*) sorted for each objective. The solutions with the greatest values of crowding distance are transferred to HM until the matrix is completed.

$$d_{I_j^m} = d_{I_j^m} + \frac{f_m^{I_{j+1}^m} - f_m^{I_{j-1}^m}}{f_m^{max} - f_m^{min}} \qquad \textbf{Equation 4.13}$$

Step 5 – Termination criterion. The optimization process returns to Steps 3 until the termination criterion is met. Different termination criteria can be proposed.

One option is ending when the iterations without changing the harmony memory reaches IWI. Other option is to measure the quality of Pareto front and ending when the quality improvement is sufficiently low.

The flowchart of the algorithm is presented in Figure 4.8.

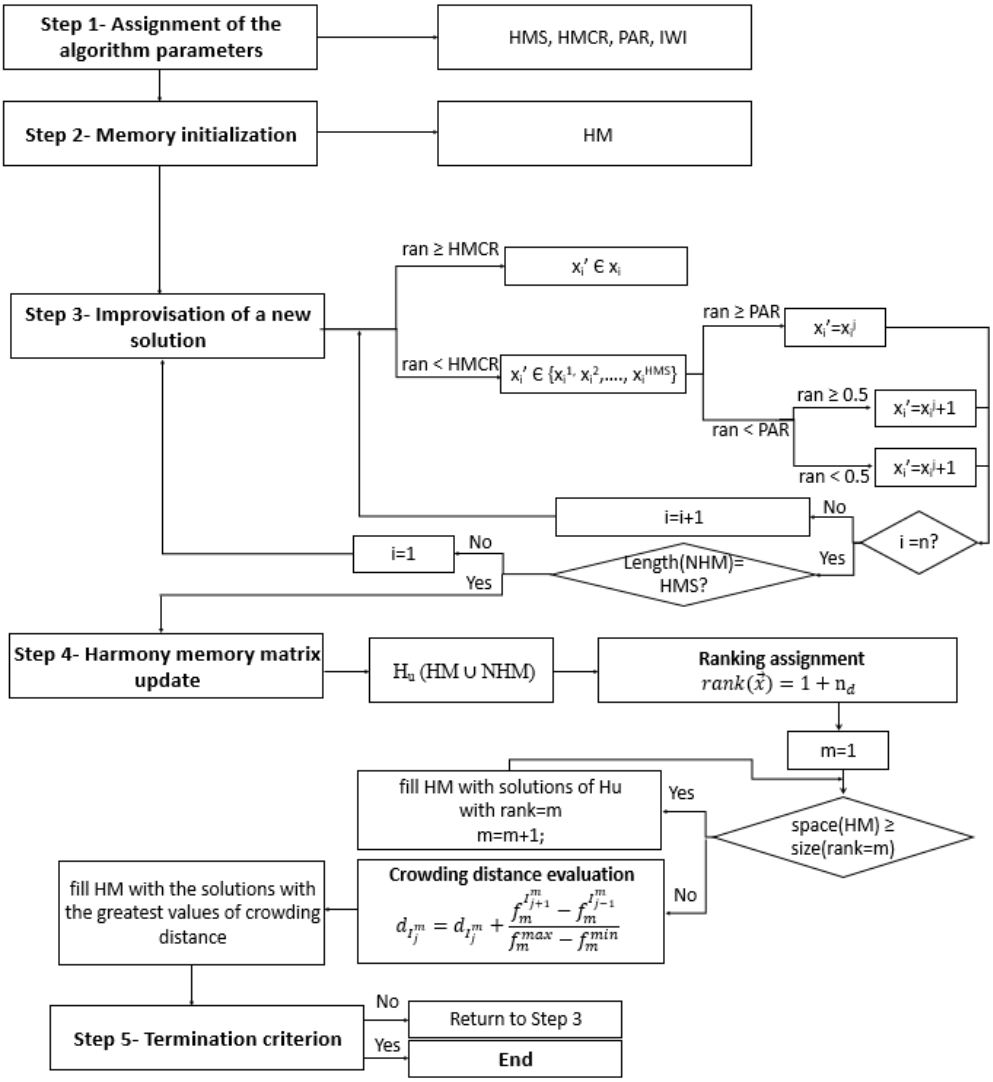

Figure 4.8. Flowchart of the multi-objective harmony search (based on García-Segura & Yepes (2016))

Chapter 5
Objective functions

5.1. Criteria considered for the sustainable design

The sustainable development requires a balance between the economic, environmental and social pillars. While economic and environmental criteria can be established as the cost and amount of emissions derived from an activity, social criteria are not straightforward determined. Social actors have different interests in view of the aims pursued. Safety, durability, serviceability and constructability can be selected as the target objectives when the objective is the bridge design. These criteria are also contemplated by the Spanish code (Fomento, 2008, 2011) and Eurocode (European Committee for Standardisation, 2003b, 2005). The codes guarantee a durability level according to the exposure class and structural importance. Regarding safety and serviceability, characteristic loads and partial safety factors determine a minimum threshold. Likewise, codes provide measures to avoid constructability problems.

The objective of this dissertation is to achieve efficient and sustainable designs of post-tensioned concrete box-girder road bridges. In the light of this, the economic cost, the CO_2 emissions, the overall safety factor and the corrosion initiation time are proposed as sustainable criteria. **Cost** optimization is essential to achieve a good design with the minimum economic resources. **CO_2** is the main greenhouse gas as accounts for 55% of the total greenhouse effect. Due to that, fib Bulletin "Guidelines for green concrete structures" (fib, 2012) proposes CO_2 as an environmental indicator. Likewise, other studies employed the CO_2 emissions for the environmental impact evaluation (Camp & Huq, 2013; García-Segura et al., 2015; García-Segura et al., 2014c; Park et al., 2013; Paya-Zaforteza et al., 2009;

Yepes et al., 2012; Yepes, et al., 2015b). The embodied energy has been also used as criteria in the structural optimization (Martí et al., 2016; Miller et al., 2015; Quaglia et al., 2014; Sattary & Thorpe, 2012; Yeo & Gabbai, 2011). However, as pointed in Section 3.8, the CO_2 emission evaluation takes into account the emissions derived from the energy use and other sources of emissions. Therefore, CO_2 emission is considered a more complete criterion.

Concerning the **overall safety factor**, this metric evaluates the minimum safety factor of the ultimate limit states. A value of one means strict compliance with the code. Optimization problems usually consider this criterion as a constraint, however, converting the structural safety constraints to objectives allows finding multiple trade-off solutions that hardly increase the cost and achieve improved safety. This is important when the structure is expected to be under increased loads, or the deterioration process may cause a reduction in structural safety. Besides, Neves & Frangopol (2005) pointed out that safety should be considered in the bridge management systems model deterioration, since condition state is not an accurate measure of the safety and serviceability of a bridge. From then on, both the condition and safety level have been used as objectives in the maintenance optimization (Chiu & Lin, 2014; Liu & Frangopol, 2005; Neves et al., 2006). This thesis studies how a design criterion can influence the long-term cost and emissions. Thus, the overall safety factor is considered as an objective function.

Durability is important to be considered to design for longevity and reduced long-term impacts. The Spanish code EHE-08 (Fomento, 2008) considers the durability limit state as "the failure occurring due to the characteristic working life of the structure not being reached, as a result of the concrete or reinforcement deterioration processes reaching such a degree that they prevent the structure from behaving in accordance with the assumptions under which it was designed". The working life, also called service life, is evaluated according to Tuutti (1982) model. The model distinguishes two phases: (1) the initiation of corrosion in which the aggressive agent penetrates in the concrete cover, leading to the loss of reinforcement passivity, and (2) the propagation of corrosion that begins when the steel is depassivated and ends when a limiting state is reached, beyond which consequences of corrosion can no longer be tolerated. This approach is widely accepted. However, there is no unanimous consensus for the propagation of corrosion phase. The code (Fomento, 2008) consider that this phase depends on the cover, the diameter of the reinforcement, and the exposure class. Other authors identify this phase with the loss of cross-sectional area of reinforcing or prestressing steel, the reduction of bond, or crack initiation and propagation (spalling, delamination) caused by expansive rust products (Stewart & Suo, 2009). Izquierdo López (2002) provided different limits for the propagation of corrosion.

This dissertation considers the durability, firstly, as a parameter and secondly, as an objective function. As a parameter, the durability conditions for a coastal environment demand the decompression limit state and a concrete cover of 65mm. As an objective function, the concrete cover is defined as a design variable and the corrosion initiation time is studied as an objective function. In this last case, bridge

designs have different durability levels and a **lifetime-reliability-based approach** is used to evaluate the maintenance required to satisfy a reliability target during a specified time horizon. The differences among the designs lead to alternative maintenance options that have different economic, environmental and societal impact. The **economic impact** is measured as the cost derived from the maintenance activities. The environmental impact takes into account the CO_2 emissions of the direct maintenance. As for the **societal impact,** the traffic disruptions during the maintenance actions are evaluated in terms of cost and CO_2 emissions due to the increase in travel time.

It is worth noting that the service life prediction of a structure is affected by several **uncertainties** due to the load effect, material properties, and damage occurrence and propagation (Frangopol & Kim, 2011). Besides, decisions regarding the bridge assessment are based on uncertainty (Stewart, 2001). While, system reliability analysis is not usually justified at the design level, the uncertainty consideration when assessing bridges could lead to considerable economic benefits (Wisniewski et al., 2009). Thus, variabilities in the corrosion initiation time and life-cycle criteria are incorporated in the model.

In view of all the above, this dissertation divides the objectives as those considered for the initial design and the others that are taken into account for the maintenance phase. The bridge life-cycle is evaluated by combining the initial objectives and those due to maintenance actions. Figure 5.1 displays the elements considered during the life-cycle. Direct and indirect maintenance actions are considered when design does not guarantee the minimum service life. Demolition and reuse are not taken into account since demolition technique and the following use are difficult to determine during the design stage. However, as section 3.8 pointed, it is recommended to reuse concrete as gravel-filling material to achieve a complete carbonation and reduce the CO_2 emissions.

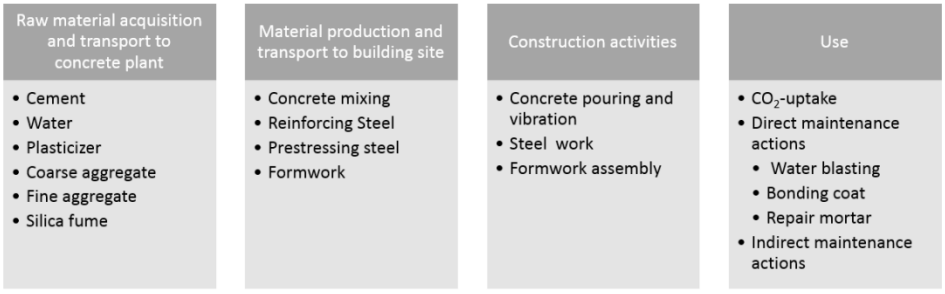

Figure 5.1. Life-cycle stages

5.2. Initial design objectives

5.2.1. *Economic cost*

Bridge design is often conditioned by the economic cost. The cost of the deck is evaluated as the cost of material production, transport and placement. The construction units considered are concrete, post-tensioning steel, reinforcing steel and formwork. It is worth noting that there are other units involve in the evaluation of the entire bridge cost. However, these are not considered since the parameters that do not vary during the optimization process do not provide information about the optimum solutions. In contrast, the volume of concrete, the amount of post-tensioning steel, the amount of reinforcing steel and the area of the formwork depend on the design variables.

Equation 5.1 measures the cost as the sum of each construction unit cost, which in turn is obtained as the product of the unit prices and the measurements. The unit prices of the materials include raw material extraction, manufacture, and transportation. Unit prices, shown in Table 5.1, are obtained from the Institute of Construction Technology of Catalonia (ITEC) database (BEDEC). This database belongs to the Institute of Construction Technology of Catalonia (Spain). The data is related to building, urbanism and civil engineering. It contains 750,000 items and provides the commercial costs for 83 Spanish companies.

The cost (C) is calculated according to the unit cost of concrete (C_{co}), the volume of concrete (V_{co}), the unit cost of reinforcing steel (C_{rs}), the weight of reinforcement steel (W_{rs}), the unit cost of prestressing steel (C_{ps}), the weight of prestressing steel (W_{ps}), the unit cost of formwork (C_f), the area of the formwork (A_f), the unit cost of CO_2 (C_{co2}), and the amount of CO_2 emitted (E).

$$C = C_{co} \cdot V_{co} + C_{rs} \cdot W_{rs} + C_{ps} \cdot W_{ps} + C_f \cdot A_f + C_{co2} \cdot E \qquad \textbf{Equation 5.1}$$

Concrete unit price is not obtained directly from the database, since the study differentiates the prices according to the concrete grade. Thus, the price is determined for each concrete grade from the aggregation of the concrete components. Table 5.2 and 5.3 show the concrete mix design according to the grade and the corresponding unit prices. Besides, the cost of concrete plant, transport of each component, transport of concrete and placement are taken into account (see Table 5.4). The bridge is considered located in Valencia. Transport distances are doubled after considering the return trip. Concrete components are transported from the nearest factory to the concrete plant. The transport distances for cement, plasticizer, aggregate and silica fume are 32 km, 724 km, 12 km and 1420 km, respectively. A mixer transports concrete from the concrete plant to the building site. This distance is considered as 40 km. Finally, the concrete cost for each grade is adjusted by a linear regression.

Table 5.1. Unit prices (based on García-Segura & Yepes (2016))

Unit measurements	Cost (€/measure)
Square meter of formwork	33.81
Kilogram of steel (B-500-S)	1.16
Kilogram of prestressing steel (Y1860-S7)	3.40
Cubic meter of concrete 35 MPa	104.57
Cubic meter of concrete 40 MPa	109.33
Cubic meter of concrete 45 MPa	114.10
Cubic meter of concrete 50 MPa	118.87
Cubic meter of concrete 55 MPa	123.64
Cubic meter of concrete 60 MPa	128.41
Cubic meter of concrete 70 MPa	137.95
Cubic meter of concrete 80 MPa	147.49
Cubic meter of concrete 90 MPa	157.02
Cubic meter of concrete 100 MPa	166.56
Tone of CO_2 emission	5.00

In addition, the cost of the CO_2 emissions (SendeCO2), is assessed from the emission objective. Law 1/2005, BOE number 59 (Jefatura del Estado, 2005), regulated the carbon market. EU stablished a policy to combat climate change after the Kyoto protocol. The EU emissions trading system is a tool for reducing industrial greenhouse gas emissions cost-effectively. The system put a limit on overall emissions from high-emitting industry sectors. This limit is reduced each year. Companies receive and buy emission allowances within this limit. They can buy limited amounts of international credits from emission-saving projects around the world. These limits ensure that they have a value (European Commission). Each allowance is equivalent to one ton of CO_2. Figure 5.2 shows the evolution of the cost of emission allowances during the last years.

Table 5.2. Concrete mix design according to the grade

Concrete grade	Cement (kg/m³)	Water (kg/m³)	Plasticizer (kg/m³)	Coarse aggregate (kg/m³)	Fine aggregate (kg/m³)	Silica fume (kg/m³)
35 MPa	300	162	4	848	1088	0
40 MPa	320	160	5	829	1102	0
45 MPa	350	157	5	795	1118	0
50 MPa	400	160	6	726	1136	0
55 MPa	457	160	7	918	876	0
60 MPa	485	160	9	1030	735	0
70 MPa	493	153	9	1077	678	37
80 MPa	497	149	10	944	820	50
90 MPa	517	155	10	944	875	52
100 MPa	545	136	11	1065	690	55

Table 5.3. Unit prices of concrete components

Cement (€/ton)	Water (€/ton)	Plasticizer (€/ton)	Coarse aggregate (€/ton)	Fine aggregate (€/ton)	Silica fume (€/ton)
98.91	1.25	1320	16.81	17.87	400

Table 5.4. Unit prices of concrete plant, transport and placement

Concrete plant (€/m³)	Truck (€/km/t)	Concrete mixer (€/km/m³)	Concrete placement (€/m³)
1.53	0.039	0.095	30.06

5.2.2. *CO_2 emissions*

Emissions (E), measured in kg CO_2, are evaluated with the same procedure as the economic cost. The construction units associated with the emissions are the same as the cost, with the exception of the CO_2 cost. The CO_2 emissions are defined in Equation 5.2, where E_{co} are the CO_2 emissions associated to concrete, E_{rs} are the CO_2 emissions of reinforcing steel, E_{ps} are the CO_2 emissions of prestressing steel, and E_f are the CO_2 emissions of formwork.

$$E = E_{co} * V_{co} + E_{rs} * W_{rs} + E_{ps} * W_{ps} + E_f * A_f \qquad \textbf{Equation 5.2}$$

Table 5.5 summarizes the unit emissions. Concrete unit emissions are also determined from each mix design. ITEC database (BEDEC) is taken into account for the unit emissions, with the exception of the plasticizer and silica fume. The plasticizer emission is taken from the European Federation of Concrete Admixtures Associations (2006). Regarding the silica fume, it is considered that this material do not emit CO_2 because it is a waste product from other material production (García-Segura et al., 2014a).

Table 5.5. Unit CO_2 emissions (based on García-Segura & Yepes (2016))

Unit measurements	CO_2 emission (kg/measure)
m^2 of formwork	2.08
kg of steel (B-500-S)	3.03
kg of prestressing steel (Y1860-S7)	5.64
m^3 of concrete 35 MPa	321.92
m^3 of concrete 40 MPa	338.90
m^3 of concrete 45 MPa	355.88
m^3 of concrete 50 MPa	372.86
m^3 of concrete 55 MPa	389.84
m^3 of concrete 60 MPa	406.82
m^3 of concrete 70 MPa	440.78
m^3 of concrete 80 MPa	474.74
m^3 of concrete 90 MPa	508.70
m^3 of concrete 100 MPa	542.66

Table 5.6. Unit CO_2 emissions of concrete components

Cement (kg/ton)	Water (kg/ton)	Plasticizer (kg/ton)	Coarse aggregate (kg/ton)	Fine aggregate (kg/ton)	Silica fume (kg/ton)
833	0.29	220	8	8	0

Table 5.7. Unit CO_2 emissions of concrete plant, transport and placement

Concrete plant (kg /m^3)	Truck (kg /km/t)	Concrete mixer (kg /km/m^3)	Concrete placement (kg /m^3)
0.37	0.197	0.517	0.82

Carbonation, considered as a CO_2 capture, was estimated by García-Segura *et al* (2014a; 2014c; 2015). Equation 5.3 shows the amount of CO_2 captured based on the predictive models of Fick's First Law of Diffusion and the study of Lagerblad (2005). The kg of CO_2 is calculated as the product of the carbonation rate coefficient (*k*), the structure service life (*t*), the quantity of Portland cement per cubic meter of concrete (*c*), the amount of CaO content in Portland cement (*CaO* is assumed to be 0.65), the proportion of calcium oxide that can be carbonated (*r* is assumed to be 0.75), the exposed surface area of the concrete (*A*), and the chemical molar fraction (*M* is 0.79). The carbonation rate coefficient and cement content per cubic meter of concrete are provided in Table 5.8 according to the concrete grade. Box-girder surfaces are considered exposed to rain, with the exception of the bottom slab. Therefore, the carbonation rate coefficient is given according to the rain exposure.

$$E_{CO_2} = k * \sqrt{t} * c * Ca0 * r * A * M$$ **Equation 5.3**

Table 5.8. Carbonation rate coefficient and cement content (based on García-Segura et al. (2015))

Concrete grade	***k* exposed to rain (mm/year$^{0.5}$)**	***k* protected from rain (mm/year$^{0.5}$)**	**Cement (kg/m^3)**
35 MPa	1.50	3.01	300
40 MPa	1.25	2.50	320
45 MPa	1.05	2.11	350
50 MPa	0.90	1.81	400
55 MPa	0.79	1.57	457
60 MPa	0.69	1.38	485
70 MPa	0.55	1.09	493
80 MPa	0.45	0.89	497
90 MPa	0.37	0.74	517
100 MPa	0.31	0.63	545

5.2.3. *Overall safety factor objective*

The overall safety factor (*S*) is evaluated as the minimum safety factor (γ_j) for the ultimate limit states (see Equation 5.4). To this end, torsion, flexure, transverse flexure and shear are considered. The factor γ_j corresponds to the ratio between the ultimate resistance of the structural response and the ultimate load effect of actions. Both the ultimate resistance and the loads effects are calculated according to the Spanish code (Fomento, 2008, 2011), which is based on the Eurocode (European Committee for Standardisation, 2003b, 2005). A deterministic analysis is carried out, considering the partial safety factors proposed by the code (Fomento, 2008, 2011). Note that a safety coefficient of one implies strict compliance.

$$S(\vec{x}) = Minimum\ \gamma_j(\vec{x})$$ **Equation 5.4**

5.2.4. *Corrosion initiation time*

The corrosion is initiated when the chloride concentration on the surface of the reinforcing steel exceeds a critical threshold value (C_r). The corrosion initiation time (t_{corr}) is the time required to achieve this threshold. The chloride content at a distance x from the outer surface of concrete at time t is calculated according to Equation 5.5 based on Fick´s second law. It depends on the surface content (C_o), the apparent diffusion coefficient (D) and the error function (erf). The model considers the uncertainties of the apparent diffusion coefficient, chloride concentration on the surface, concrete cover, and the critical threshold value.

The model suggested by Vu & Stewart (2000) and proposed by Papadakis et al. (1996) was considered for the diffusion coefficient. Vu & Stewart (2000) stated that even this model is not time-variant, it achieves the best fit. Equation 5.6 shows the apparent diffusion coefficient. It depends on the chloride diffusion coefficient in an infinite solution (D_{H20} = 1.6*10^{-5} cm^2/s for NaCl), the mass density of cement (ρ_c is considered to be 3.16 g/cm^3), the mass density of the aggregates (ρ_a is considered to be 2.6 g/cm^3), the aggregate-to-cement ratio (a/c) and the water-cement ratio (w/c).

$$C(x,t) = Co\left[1 - \text{erf}\left(\frac{x}{2\sqrt{tD}}\right)\right] \qquad \textbf{Equation 5.5}$$

$$D = D_{H_2O}0.15 \cdot \frac{1+\rho_c\frac{w}{c}}{1+\rho_c\frac{w}{c}+\frac{\rho_c}{\rho_a}\frac{a}{c}}\left(\frac{\rho_c\frac{w}{c}-0.85}{1+\rho_c\frac{w}{c}}\right)^3 \qquad \textbf{Equation 5.6}$$

Table 5.9 shows the parameters of the random variables and Table 5.10 provides a/c and w/c values according to the concrete grade. Model type and values of the random variables associated with corrosion are the same as those used by Vu & Stewart (2000), except for the coefficient of variation (COV) of the surface chloride content. A value of 0.3 is considered due to the reduction of the variability of the surface chloride content in a particular bridge compared to a group of bridges. The mean value of the surface chloride content depends on the distance to the coast. A value of 2.95 kg/m^3 was proposed for a distance up to 1000 m from the coast (McGee, 1999). The corrosion initiation time of the bridge is obtained as the mean value of the distribution obtained by Monte Carlo simulation.

Table 5.9. Model type and values of the random variables associated with corrosion (based on García-Segura et al., (submitted(b)))

Random Variables	Model type
Model error (D)	Normal (μ = 1, COV = 0.2)
C_o	Lognormal (μ = 2.95, COV = 0.3)
C_r	Uniform (0.6–1.2)
Model error for i_{corr}	Uniform (μ =1, COV =0.2)
Cover	Normal (μ = c_c, COV = 0.25)

Table 5.10. Aggregate-to-cement ratio and water-cement ratio for each concrete grade (based on García-Segura et al., (submitted(b)))

Concrete type	a/c	w/c
concrete 35 MPa	6.45	0.54
concrete 40 MPa	6.03	0.5
concrete 45 MPa	5.47	0.45
concrete 50 MPa	4.66	0.4
concrete 55 MPa	3.92	0.35
concrete 60 MPa	3.64	0.33
concrete 70 MPa	3.56	0.31
concrete 80 MPa	3.55	0.3
concrete 90 MPa	3.52	0.3
concrete 100 MPa	3.22	0.3

5.3. Maintenance objectives

5.3.1. *Economic impact*

The economic impact (C_{ms}) of maintenance actions considers the direct costs of maintenance applications. When costs over a different period are calculated, future costs should be transferred to present costs, taking into account the discount rate (v). In this case, the discount rate is applied to each maintenance action at the time (t). Note that the discount rate is not considered for the construction cost explained in Section 5.2.1, since the time of application is considered at year zero. Equation 5.7 illustrates the economic impact assessment.

Maintenance is applied to delay the damage propagation and consequently, increase the service life. The reduction in the reinforcing steel area due to the chloride-induced corrosion is formulated for each cross-section surface. In this line, the maintenance is scheduled in each cross-section surface separately. The maintenance cost (C_{msij}) is calculated for each surface i and maintenance action j (see Equation 5.8). The problem has to define the number of surfaces considered (N_i) and number of maintenance applications for each surface (N_{msi}).

This research considers minor concrete repair for the bridge maintenance. The chloride-contaminated concrete cover is replaced by a repair mortar. As a result, the degradation of the structural capacity is halted for a period equal to the corrosion initiation time of the new cover. The maintenance action consists firstly of removing the concrete cover and providing a proper surface for the coating adhesion. This is carried out by water blasting. Then, a bonding coat is applied between the old and new concrete. Finally, a repair mortar is placed to provide a new reinforcement corrosion protection. The maintenance activity is carried out by a truck-mounted platform. Thus, the maintenance cost (Equation 5.8) is calculated

as the cost of water blasting (C_{wb}), the cost of the repair mortar application (C_{rm}), the cost of the bonding coat application (C_{bc}), and the cost of the truck-mounted platform (C_{tp}). The measurements considered are the volume (V_{csi}) and the area (A_{si}) of concrete replaced on surface *i*. The thickness is considered equal to the concrete cover plus bar diameter.

Table 5.11 shows the prices of direct maintenance. A survey of Spanish contractors provided the prices of water blasting application (Hidrodemolición) and repair mortar (DRIZORO). The cost of repair mortar application from database (BEDEC) is added to the material price. The other prices regarding the truck mounted platform and bonding coat application are also obtained from database (BEDEC). These are the mean values of a lognormal distribution with a coefficient of variation of 0.2 (Dong et al., 2013). Likewise, a lognormal distribution with a coefficient of variation of 0.2 is also considered for the construction cost (Equation 5.1).

$$C_{ms} = \sum_{j=1}^{Nms1} \frac{C_{ms1j}}{(1+v)^{t_j}} + \sum_{j=1}^{Nms2} \frac{C_{ms2j}}{(1+v)^{t_j}} \quad \textbf{Equation 5.7}$$

$$C_{msij} = \left((C_{wb} + C_{rm}) * V_{csi} + (C_{bc} + C_{tp}) * A_{si}\right) \quad \textbf{Equation 5.8}$$

Table 5.11. Cost of the direct maintenance (based on García-Segura et al., (submitted(b)))

Mean cost	COV	Distribution
C_{wb} =11.5 (€/m^2/cm)	0.2	LN
C_{bc} =16.41 (€/m^2)	0.2	LN
C_{rm}=43.28 (€/m^2/cm)	0.2	LN
C_{tp}=53.71 (€/m^2)	0.2	LN

5.3.2. *Environmental impact*

The environmental impact of maintenance actions (E_{ms}) evaluates the CO_2 emissions due to the maintenance action. During the lifetime of the bridge, maintenance activities emit CO_2 gases. Equation 5.9 evaluates the environmental impact (E_{ms}) as the maintenance actions (E_{msij}) for all the surfaces and number of maintenance applications. The CO_2 emissions associated to the maintenance actions (see Equation 5.10) are obtained from the emissions of water blasting (E_{wb}), repair mortar application (E_{rm}), bonding coat application (E_{bc}) and truck-mounted platform (E_{tp}). The maintenance unit emissions are obtained from database (BEDEC). The mean value, COV and model type are summarized in Table 5.12.

$$E_{ms} = \sum_{j=1}^{Nms1} E_{ms1j} + \sum_{j=1}^{Nms2} E_{ms2j} \quad \textbf{Equation 5.9}$$

$$E_{msij} = \left((E_{wb} + E_{rm}) * V_{csi} + (E_{bc} + E_{tp}) * A_{si}\right) \quad \textbf{Equation 5.10}$$

Table 5.12. CO_2 emissions of the direct maintenance (based on García-Segura et al., (submitted(b)))

Mean CO_2 emission	COV	Distribution
E_{wb} =0.91 (kg/m^2/cm)	0.2	LN
E_{bc} =15.85 (kg/m^2)	0.2	LN
E_{rm}=25.5 (kg/m^2/cm)	0.2	LN
E_{tp}=142.09 (kg/m^2)	0.2	LN

5.3.3. *Societal impact*

The societal impact of maintenance actions is evaluated as the consequences of the traffic disruptions during the actions. These consequences are measured in terms of cost and CO_2 emissions. The traffic detour causes an increase in travel time that affects the bridge users. In this sense, users have higher cost of running compared to the normal situation. They must assume this increase in cost. In addition, the time loss has an economic value derived from the wage of car users, the truck driver compensation and cargo of trucks. From an environmental point of view, cars and trucks pollute the air. The CO_2 emissions of the traffic detour is calculated and added to the total emissions. This study considers that maintenance actions that take place about one year of difference are scheduled at the same time. In this case, the societal impact is computed once.

Equation 5.11 evaluates the cost associated to the societal impact (C_S) as the cost of running (C_{run}) and time loss (C_{time}) due to the increase in travel time. The running cost (see Equation 5.12) considers the cost for running cars ($C_{run,cars}$) and trucks ($C_{run,truck}$) per unit length according to the average daily truck traffic (T_{truck}). This equation also takes into account the average daily traffic (A_{DT}), the detour length (L_{detour}) and the detour time (T_{detour}). The cost for running is computed for all maintenance actions (Nm). Equation 5.13 illustrates the time loss cost, which depends on the wage compensation (C_{wage}), the truck driver compensation (C_{driver}), the value of a cargo (C_{cargo}), the average vehicle occupancies for cars (O_{cars}), the average vehicle occupancies for trucks (O_{truck}) and the speed at the detour (S).

$$C_{S=}C_{run} + C_{time} \qquad \textbf{Equation 5.11}$$

$$C_{run} = \sum_{i=1}^{Nm}\left[C_{run,cars}\left(1-\frac{T_{truck}}{100}\right) + C_{run,truck}\left(\frac{T_{truck}}{100}\right)\right]\frac{L_{detour}T_{detour}A_{DT}}{(1+v)^t} \qquad \textbf{Equation 5.12}$$

$$C_{time} = \sum_{i=1}^{Nm}\left[C_{wage}O_{cars}\left(1-\frac{T_{truck}}{100}\right) + (C_{driver}O_{truck} + C_{cargo})\frac{T_{truck}}{100}\right]\frac{L_{detour}T_{detour}A_{DT}/S}{(1+v)^t} \qquad \textbf{Equation 5.13}$$

Similarly, the environmental impact (E_S) of the increase in travel time is due to the CO_2 emissions for running (E_{run}). The running emissions are calculated according to the CO_2 emissions for running cars ($E_{run,cars}$) and trucks ($E_{run,truck}$) per unit length. Table 5.13 shows the cost and emissions associated to social impact of the indirect maintenance. The traffic condition and other values related to the social impact are summarized in Table 5.14. These values are those proposed by Dong et al. (2013).

$$E_S = E_{run} = \sum_{i=1}^{Nm} \left[E_{run,cars} \left(1 - \frac{T_{truck}}{100}\right) + E_{run,truck} \left(\frac{T_{truck}}{100}\right) \right] L_{detour} T_{detour} A_{DT} \quad \textbf{Equation 5.14}$$

The cost and emissions associated to the societal impact are added to the economic and environmental impact to account the total cost (TC_{ms}) and CO_2 emissions (TE_{ms}) due to maintenance actions (Equations 5.15-16).

$$TC_{ms} = C_{ms} + C_S \quad \textbf{Equation 5.15}$$

$$TE_{ms} = E_{ms} + E_s \quad \textbf{Equation 5.16}$$

Table 5.13. Cost and emissions of the indirect maintenance (based on García-Segura et al., (submitted(b)))

Mean cost	Mean CO_2 emission	COV	Distribution type
$C_{run,cars}$=0.07 (€/km)	$E_{run,cars}$=0.22 (kg/km)	0.2	LN
$C_{run,truck}$=0.34 (€/km)	$E_{run,truck}$=0.56 (kg/km)	0.2	LN
C_{wage}= 20.77 (€/h)		0.15	LN
C_{driver} =24.54 (€/h)		0.15	LN
C_{cargo} =3.64 (€/h)		0.2	LN

Table 5.14. Traffic conditions during the detour (based on García-Segura et al., (submitted(b)))

Unit measurements	Mean value	COV	Distribution
T_{truck} (%)	12	0.2	LN
A_{DT} (veh/day)	8500	—	Deterministic
L_{detour} (km)	2.9	—	Deterministic
T_{detour} (day)	7	—	Deterministic
S (km/h)	50	0.15	LN
O_{cars}	1.5	0.15	LN
O_{truck}	1.05	0.15	LN
v (%)	2	—	Deterministic

Chapter 6
Structural analysis and verification

6.1. Bridge analysis

The three-span box-girder bridge is designed as a continuous girder bridge. CSiBridge© is used to model and analyze the bridge. Shell elements are used for modelling the box-girder deck. A linear analysis without redistribution of forces is performed. The distortion of the cross section or the shear lag effects must be determined separately when using the beam theory. However, a three-dimensional computer model of finite-elements can avoid the mathematical complexity of the distortion of box-girder cross-sections (Hambly, 1991). Besides, the finite-element method allows the study of shear lag and the computation of effective flange breadths in box-girders. Numerous researchers use this technique to capture all aspects affecting the structure response. Sennah and Kennedy (2002) presented a review in analysis of box-girder bridges. For these reasons, shell elements are used to generate the entire FE model.

CSiBridge© has an Open Application Programming Interface (OAPI) to allow other software to be integrated with it. The finite-element (FE) mesh is created based on the specifications of a maximum segment length for discretization information and a maximum submesh size. The first parameter corresponds to the maximum length of longitudinal discretization for a section cut. Besides, a section cut is always applied over supports. CSiBridge© calculates section-cut forces by summing the forces which act on member joints at a section cut. As a result, the axial force, shear vertical, shear horizontal, torsion and moment about vertical and horizontal axis are evaluated at these sections. The second parameter defines the maximum submesh length in both directions. In addition, every edge of the

transverse section, like a change in thickness, is a condition for a FE division. The study considers a maximum segment length for discretization information of 3 m and a maximum submesh size of 1.5 m. These values are determined with the aim of obtaining accurate results without compromising the computing time. Figure 6.1 shows the finite-element mesh.

A reinforcement grid is embedded in the shell element. The grid is defined by the reinforcing steel variables. The post-tensioning steel is incorporated in the model through tendons. These tendons acquire the information of the parabolic layout, the prestressing force and the instantaneous loss parameters. Besides, material parameters regarding concrete, reinforcing steel and post-tensioning steel are defined. Diaphragms are assigned over each support.

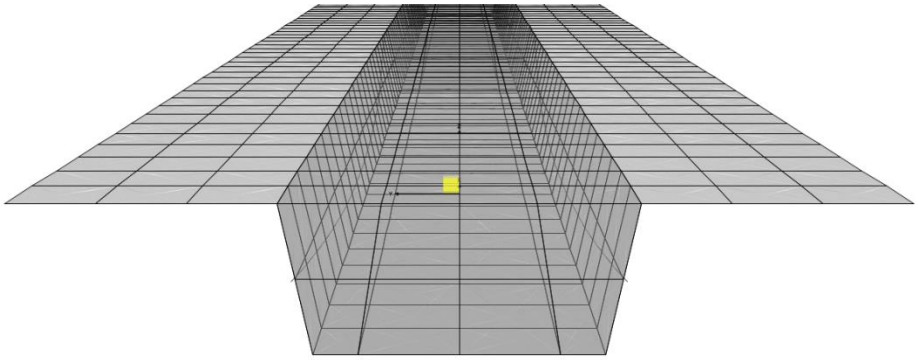

Figure 6.1. Finite-element mesh

Loads

Actions take into account the deck self-weight including the parapet and asphalt. The deck self-weight is directly applied by the software. Regarding asphalt load, two load cases are considered. One takes into account the mean asphalt thickness and the other case considers an increment of 50% of the thickness. The code IAP-11(Fomento, 2011) suggests this value to foresee a pavement rehabilitation. Load parameters are defined in Table 4.1. The traffic loads and thermal gradient are those proposed by IAP-11 (Fomento, 2011). The code divides the deck into virtual lanes with different applied loads. In addition, a differential settling in each support is considered.

As for the post-tensioned steel effect, the study considers two stages: tensioning and final life. The instantaneous losses are deducted from the prestressing force to evaluate the prestressing force at the tensioning stage ($P_i=P-\Delta P_{ins}$). In addition, the instantaneous and deferred losses are deducted from the prestressing force to evaluate the prestressing force at final life ($P_f=P-\Delta P_{ins}-\Delta P_{def}$).

Instantaneous losses of force are those which may arise during the tensioning activity and at the moment of anchorage the active reinforcements and depend on the characteristics of the structural element being studied. Instantaneous

losses include the losses due to friction, wedge penetration and elastic shortening of the concrete. To this end, the following parameters are considered: a straight friction coefficient of 0.21, a coefficient of friction curve of 0.0013 and a penetration of the wedge of 5 mm. Deferred losses take place over time, after the active reinforcements have been anchored. In this case, they are taken into account from day 7 (when prestressing activity takes place) to 100 years. These losses are due to the shortening of the concrete by creep and shrinkage and to the relaxation of the steel.

The prestressing forces and the effect of the loads are evaluated at each section, considering that finite-elements divide the deck in 40 sections. The instantaneous losses are evaluated directly by the CSiBridge©. The deferred losses are calculated from the stresses in the concrete in the fibre corresponding to the center of gravity of the prestressing steel due to the prestressing action and self-weight. The post-tensioning force and hyperstatic moment are adjusted to those at final life from the coefficient of the deferred losses. The section-cut forces due to each load are combined for the various design situations established by the code. In addition, the concomitant forces are assigned to each force combination. To this end, self-weights are considered as permanent loads; the differential settling and prestressing are considered as permanent loads of non-constant value; and the traffic loads and thermal gradient are considered as variable loads. IAP-11 (Fomento, 2011) provides the partial safety factors and combination factors according to the type of load. As both traffic and thermal gradient are variable loads, two cases are obtained considering each load as the decisive action.

6.2. Limit state evaluation

Limit states are checked based on the bridge resistance and load effects. Limit states follow the Spanish codes (Fomento, 2008, 2011), which have been adapted for the Eurocode content (European Committee for Standardisation, 2003a, 2005). Serviceability limit states of deflection and cracking are evaluated according to the following sections. The serviceability limit states of absence of cracking at prestressing stage and decompression limit state during service are required to guarantee the durability conditions for a coastal environment. Ultimate limit states of flexure, shear, shear between web and flanges, torsion, transverse flexure, transverse shear and punching shear are verified. In addition, the geometrical and constructability requirements are also examined. Note that EHE-08 code (Fomento, 2008) considers normal-strength concrete and high-strength concrete until 100MPa. On this basis, the concrete strength variable can take values until 100 MPa. Special equations and limitations are considered for high-strength concrete following the code.

6.2.1. *Serviceability limit state of deflection*

The EHE-08 (Fomento, 2008) states that the instantaneous and time-dependent deflection with respect to the precamber has to be smaller than 1/1400 of the main span length for the characteristic combination. The time-dependent deflection

considers the prestressing force at final life and the permanent loads, all affected by the creep coefficient.

IAP-11 (Fomento, 2011) pointes that the deflection due to frequent value for the live loads is restricted to 1/1000 of the main span length.

6.2.2. *Serviceability limit state of cracking*

6.2.2.1 Stresses during prestressing

During prestressing action, the absence of cracking during prestressing is checked:

- The appearance of compression crack: the compressive stresses in the concrete cannot exceed the 60% of the characteristic compression strength at t=7 days.

$$\sigma_c \leq 0.6 f_{ck,t} \qquad \textbf{Equation 6.1}$$

- The appearance of tension crack: the tension stresses in the concrete cannot exceed the characteristic tension strength at t=7 days.

$$\sigma_t \leq f_{ctm,flt} \qquad \textbf{Equation 6.2}$$

Stresses are evaluated due to the deck self-weight and the prestressing force at the tensioning stage.

6.2.2.2 Serviceability stresses

During service, the absence of cracking and decompression limit states are checked:

- The appearance of compression crack (Equation 6.1) under the characteristic combination. Note that the characteristic compression strength is evaluated at 28 days.

- The appearance of tension crack (Equation 6.2) under the frequent combination. The characteristic tension strength is evaluated at 28 days.

- The Decompression Limit State under the frequent combination of actions is verified. The fibers located 100 mm above and below the strands cannot be in a decompression state (European Committee for Standardisation, 2005).

Two situations are considered: initial service time and final life. These situations correspond to the prestressing forces of P_i and P_f, respectively. In addition, the partial factors for this load are 0.9 and 1.1 for favorable and unfavorable effect. All of these combinations are checked.

6.2.3. *Ultimate limit state of torsion*

The ultimate limit state of torsion requires the compliance of three maximum torsional moments: the one that the concrete's compressed struts can resist, the one that transverse reinforcements can resist and the one that the longitudinal reinforcements can resist. These three torsional moments must be greater than the

torsional moment on the section. Simultaneously, the longitudinal and transverse reinforcement required for the following load combinations are evaluated:

1. Longitudinal reinforcement to resist the maximum torsional moment (T_{max})
2. Longitudinal reinforcement to resist the minimum torsional moment (T_{min})
3. Longitudinal reinforcement to resist the torsion concomitant to the maximum bending moment (T_{bmax})
4. Longitudinal reinforcement to resist the torsion concomitant to the minimum bending moment (T_{bmin})
5. Transverse reinforcement to resist the maximum torsional moment (T_{max})
6. Transverse reinforcement to resist the minimum torsional moment (T_{min})
7. Transverse reinforcement to resist the torsion concomitant to the maximum shear force (T_{smax})
8. Transverse reinforcement to resist the torsion concomitant to the minimum shear force (T_{smin})

In addition, the minimum torsion reinforcement, the torsion combined with bending and axial loads and the torsion combined with shear are checked.

6.2.4. *Ultimate limit state of flexure*

Flexure limit state is calculated according to the methodology followed by Alcalá (2009). The ultimate strength is calculated by integrating the stresses in the concrete and in the active and passive reinforcements. Figure 6.2 illustrates the process of obtaining the stresses from the strains. The stresses are obtained from the limit strains that belong to a specific domain. Regarding the stress-strain design diagram for the concrete, the rectangular-parabola diagram is used (Fomento, 2008). The parabola has the vertex on the abscissa ε_{c0} (strain of the concrete under ultimate load in simple compression). Following the parabola, the rectangle has the vertex on the abscissa ε_{cu} (ultimate bending strain of the concrete). The ordinate of these vertexes corresponds to f_{cd} (design compression strength of the concrete). It is worth noting that these ultimate strains depend on whether the concrete has a characteristic design strength greater than 50MPa (high-strength concrete) or not. The reinforcing steel follows a bilinear stress-strain diagram with a second horizontal leg, which starts from the design yield strength of the steel. As for the active steel, the characteristic stress-strain diagram proposed by the code is followed. The prestrain of the active steel is taken into account to shift the origin of the stress-strain diagram. This prestrain is obtained from the pre-deformation of the active steel due to prestressing force at the tensioning stage and the strain of decompression in the concrete at the level of the fiber in the active steel due to self-weight and prestressing force.

To integrate the stresses in the concrete, the Gauss–Legendre quadrature methodology is performed (Bonet et al., 2004). The neutral fiber corresponding to the zero-tension is obtained from an iteration process based on the Bolzano theorem, which obtains it from three points (neutral fiber, tension). Once the neutral fiber for zero-tension is obtained, the maximum and minimum bending moment, depending on whether the curvature is positive or negative, are calculated. Flexure

limit state checks that bending force is within these limits.

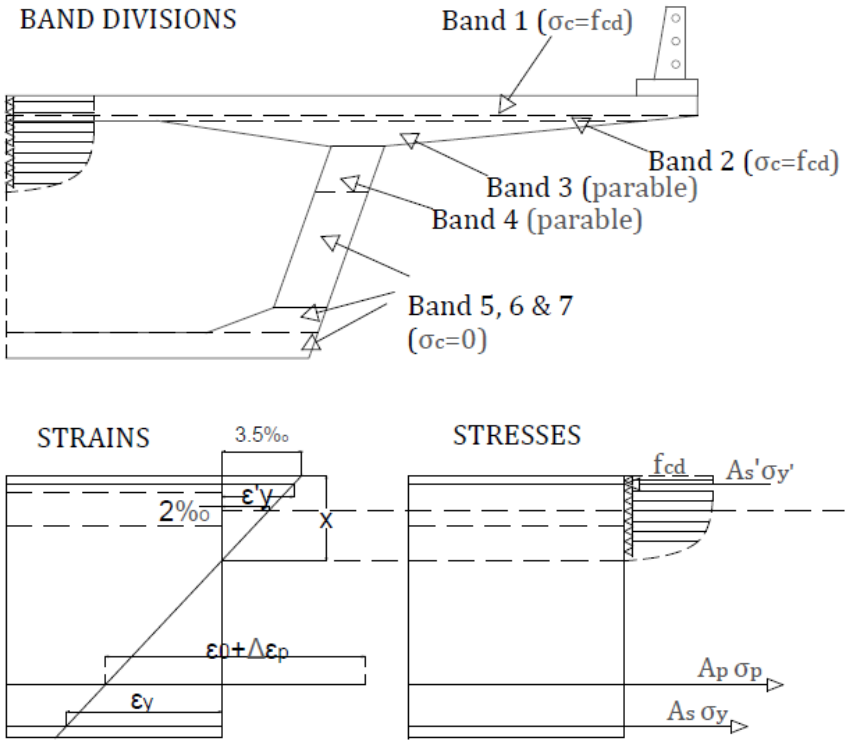

Figure 6.2. Strains-stresses in flexure limit state

The ultimate limit state of flexure is verified for the four first cases referred to in point 6.2.3. These are the bending moment concomitant to maximum torsional moment, the bending moment concomitant to the minimum torsional moment, the maximum bending moment and the minimum bending moment. The longitudinal reinforcement used to resist torsion is deducted in each case.

In addition, the Spanish code proposes a limitation for the longitudinal reinforcement based on a minimum bending moment related to the section failure due to pure or combined bending. Regarding the minimum geometric ratio, this is 2.8 per 1000 of the total concrete section. This ratio corresponds to the side under tension. Besides, a minimum reinforcement of 30% of the nominal reinforcement should be arranged on the opposite side.

6.2.5. *Ultimate limit state of shear*

Shear limit state is checked comparing the effective shear stress (V_{rd}) against the

ultimate shear force failure due to diagonal compression in the web (V_{u1}) and the ultimate shear force failure due to tension in the web (V_{u2}). Effective shear stress takes into account the design value of the shear force produced by external actions and the component of the prestressing tendons parallel to the section under study.

V_{u1} and V_{u2} are evaluated on each section of the deck, with the exception that V_{u2} is not evaluated on the sections over supports. In this case, the shear force is calculated on a section located at a distance of one effective depth from the edge of the support. Both the contribution of the web's transverse reinforcement and the concrete are taken into account to evaluate the shear strength V_{u2}.

Similar to the ultimate limit state of flexure, shear is verified for the last four cases referred to in point 6.2.3. These are the shear force concomitant to maximum torsional moment, the shear force concomitant to the minimum torsional moment, the maximum shear force and the minimum shear force. The transverse reinforcement used to resist torsion is deducted in each case. In addition, the minimum shear reinforcement proponed by the code (Fomento, 2008) is satisfied.

6.2.6. *Ultimate limit state of shear between web and flanges*

The mean longitudinal shear force per unit length is calculated as the ratio between the variation of the longitudinal shear force acting on the section of the flange and the corresponding length of variation. This force is compared to the ultimate longitudinal shear force due to diagonal compression and tension.

6.2.7. *Ultimate limit state of transverse flexion*

Transverse flexure is evaluated on the sections shown in Figure 6.3. These sections are characterized by a change in thickness and bending moment. Besides, the minimum transverse reinforcement is considered as the one associated to the minimum bending moment related to the section failure.

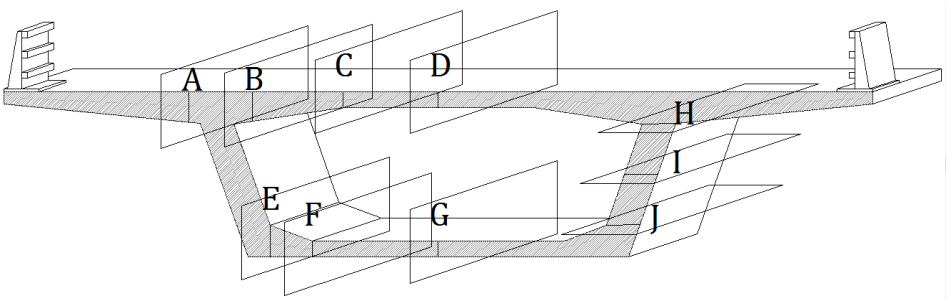

Figure 6.3. Sections studied for the transverse flexion limit state

6.2.8. *Ultimate limit state of transverse shear*

Transverse shear is checked on the same sections as transverse flexure. The shear force produced by external actions must be smaller than the ultimate shear force failure due to diagonal compression in the web and the ultimate shear force failure due to tension in the web considering the members without any shear

reinforcement.

6.2.9. *Ultimate limit state of punching shear*

Punching limit state is verified when slabs without any reinforcement for punching shear comply the equations of article 46 of the code (Fomento, 2008).

6.2.10. *Ultimate limit state of fatigue*

Spanish code (Fomento, 2008) proposes some verifications to check that the safety of an element or a structural detail with regard to fatigue. Steel should comply with the specifications of a fatigue test and variation in maximum stress.

Besides, Eurocode (European Committee for Standardisation, 2005) states that fatigue verification is generally not necessary in prestressing and reinforcing steel, in regions where, under the frequent combination of actions only compressive stresses occur at the extreme concrete fibers. Otherwise, the code proposes an equation to verify concrete under compression or shear.

6.2.11. *Geometrical and constructability constraints*

The Spanish code (Fomento, 2008) provides some recommendations for construction. Based on these specifications, the paper considers some geometric constraints. As an example:

- For the use of internal vibrators, the thickness of the top slab, external flange section and bottom slab must be enough to guarantee that the clearance between two consecutive isolated bars is equal to, or greater than, the larger of the following three values:
  - 20 millimeters
  - the diameter of the larger bar
  - 1.25 times the maximum size of the aggregate
- The thickness of the web must be enough to guarantee that the separation between the tendons will be such as to enable the proper positioning and compaction of the concrete and will guarantee correct bonding between the tendons or sheaths and the concrete. The code says that the clearances between sheaths or groups of sheaths in contact with each other, or between these sheaths and the other reinforcements, must be at least equal to the greatest of the following values:
  - the diameter of the sheath
  - the horizontal dimension of the sheath
  - 4 centimeters
- The design anchorage lengths. Particularly, due to the anchorage of passive reinforcements, the bottom slab reinforcement in pier zone (LR_5+ LR_9) must be greater than ¼ of the reinforcement in central span (LR_5+LR_{10}). The Spanish code (Fomento, 2008) states "In the case of girder end supports, at least a third of the reinforcement necessary for resisting the maximum positive moment shall continue as far as the supports; and at

least a quarter in the case of intermediates" In abutments, the reinforcement is the same as central span. Therefore, there is no constraint in that case.

In addition, the authors propose other geometric constraints.

- The slope of the web must be greater than t_3/t_4
- LR_2 cannot the greater than LR_1
- LR_3 cannot the greater than LR_2

6.3. Computer support tool

Eight modules that link CSiBridge© and Matlab© softwares carry out the optimization and bridge analysis and verification (see Figure 6.4). CSiBridge© is used for the finite-element analysis. Matlab©, as a control software, conducts the optimization process, the CSiBridge© management, and the limit states verification. The union of these modules enable bridge designers to define the fixed parameters, the variables and the objective functions that they want to optimize by a heuristic algorithm. The results show the optimum bridges according to the objective functions. Moreover, the output provides useful rules to guide engineers in designing post-tensioned concrete box-girder road bridges.

Module 1. This module updates the design variables based on the algorithm strategy. The algorithm parameters define a combination of rules and randomness that guide the search towards the optimum solution within the variable space. These parameters can be the same for the entire optimization process or they can be changed according to a strategy of diversification-intensification.

Module 2. This module receives the new solution vector and completes the design with the variable and parameter information. The bridge design is defined directly from the variables. The definition of the possible values of the variables is a competence of the designer. In addition, this module evaluates the section properties required for the limit state checking.

Module 3. This module writes a $br document with the structure information. This document is created prior to the optimization process. Later, the document is updated with the design changes affected by the new values of the variables of each iteration. CSiBridge© defines the design as a "bridge object". The $br document contains tables related to the bridge object definitions that allow users to easily change the bridge information.

Module 4. This module carries out three steps. The first step imports the $br document. The second step updates the model and the last step runs the model. All of these steps are performed through OAPI functions.

Module 5. After the structural analysis, this module extracts the results. OAPI functions are also used for this task. Firstly, the shell and point information are obtained. Then, OAPI functions report the area forces and stresses for a specified area element. These results are taken for each combination of loads. Design combinations are automatically added based on the design

code. In addition, the longitudinal forces for each combination are obtained at the superstructure section cuts. Regarding the bridge deflection, the joint displacements are taken for specific points.

Module 6. This module processes the previous analysis results, evaluates the bridge resistance, and checks the limit states. Module 4, 5 and 6 have been divided into blocks to achieve increased agility and versatility (see Figure 6.5). If any check is not verified the process returns to module 1. Otherwise, feasible solutions that comply all limit states continue to the next module.

Module 7. This module evaluates the objective functions according to the solution vector and the parameters.

Module 8. The last module obtains the Pareto optimum solutions. ´

This process is repeated until the termination criterion is reached.

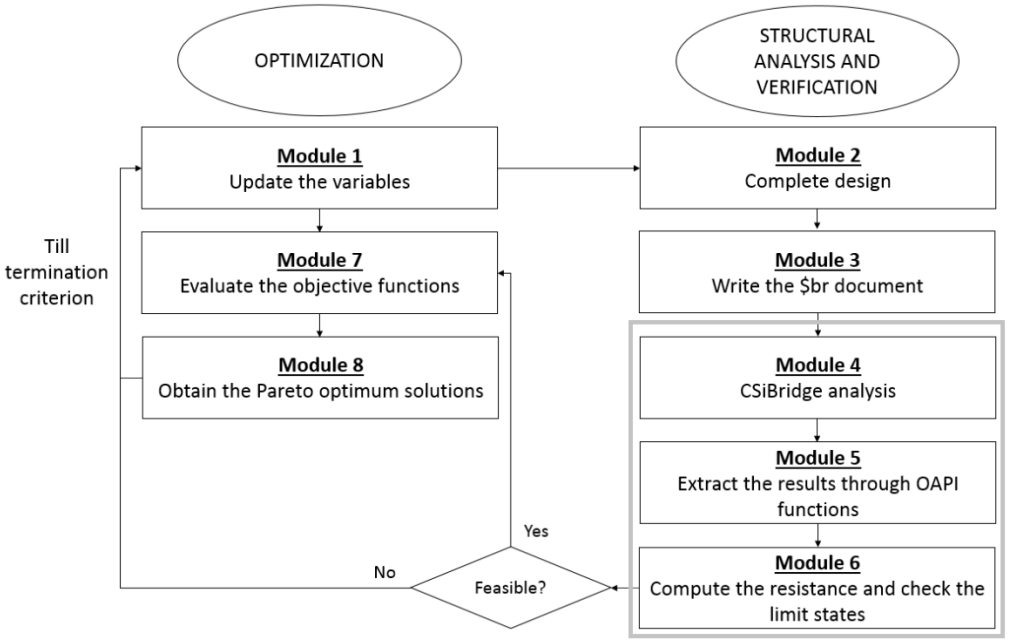

Figure 6.4. Modules of the computer support tool

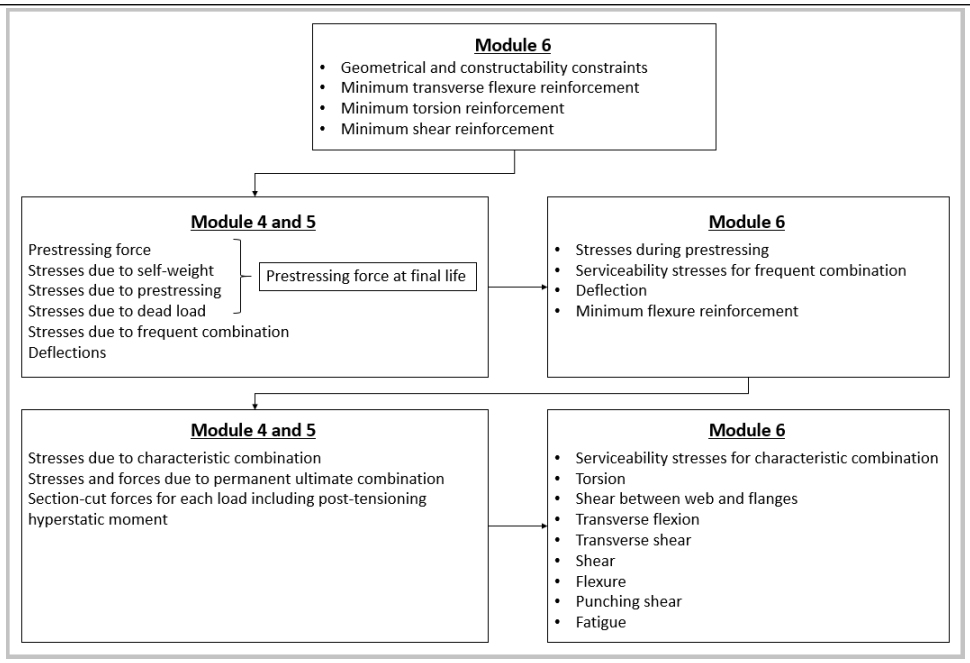

Figure 6.5. Analysis and checking blocks

Chapter 7
Multi-objective optimization of cost, CO_2 emissions, and safety

7.1. Aim of the study

This study (García-Segura & Yepes, 2016) focuses on the multi-objective optimization of post-tensioned concrete box-girder road bridges regarding cost, CO_2 emissions, and overall safety factor. The prior work of García-Segura et al. (2015) studied pedestrian bridges by a mono-objective optimization of the cost and CO_2 emissions. Findings indicated that the environmental goal also ensured economic solutions. The emission-optimized results showed 1% less pollution and 2% more expense compared to cost-optimized results. Similar results were obtained by other authors (de Medeiros & Kripka, 2014; Fraile-Garcia et al., 2016; Yepes et al., 2015b). They also stated that optimal solutions in terms of monetary costs had quite satisfactory environmental results. However, other studies found that these objectives were not clearly related (Camp & Assadollahi, 2015; García-Segura et al., 2014c). These differences can be attributed to the limit states or space of feasible solutions (as mention in Section 3.8). The environmental and economic costs of materials are not in any proportional relationship to one another. For instance, the concrete strength increment has a greater impact on the CO_2 emissions than the cost, since cement is a carbon-intensive material. In this regard, solutions designed according to an environmental goal could be more expensive. However, both objectives seek the material consumption reduction. In addition, the space of feasible solutions can be very narrow, not letting the objectives move away from the structural efficiency. In these cases, the objective functions are more likely to have a direct relationship.

This study aims to analyze the relationship between cost (C), CO_2 emissions (E)

and safety (*S*). Besides, the optimum value of the variables is investigated according to the objective functions. The inclusion of the safety function allows discovering useful knowledge regarding the best variables to improve safety. Other studies conducted by the author of this dissertation (García-Segura et al., 2015; Yepes et al., 2015b) carried out a parametric study of the span length. Results showed the dependence of the variables to the span length, and simultaneously, to the longitudinal load effect. However, a parametric study of the width is required to analyze these effects on the transverse direction. This paper proposes a multi-objective optimization that includes the safety factor to analyze all of these interactions in one analysis. The overall safety factor is evaluated as the minimum safety factor for the ultimate limit states of torsion, flexure, transverse flexure and shear. Thus, the outcomes will show if the variables are more influenced by the safety requirements or the differences between unit costs or emissions. For example, the increment in safety may lead to solutions of high-strength concrete for cost-optimization and conventional concrete for the emission-optimization.

On the other hand, this study provides an automatic design process for bridges through a commercial software for finite-element analysis. CSiBridge© and Matlab© are linked to optimize bridges. Eight modules update the design variables according to the algorithm strategy, complete the design, write the structure information, export it to CSiBridge©, run the model, extract the results, check the limit states, evaluate the objective functions and obtain the Pareto optimum solutions. This methodology provides the best bridge design based on the fixed parameters, design variables and the objective functions defined by the designer.

7.2. Definition of the problem

This study carries out a multi-objective optimization of post-tensioned concrete box-girder road bridges. The bridge design seeks a balance among the cost related to the construction materials and placement, the embedded emissions resulting from material production, construction and CO_2 capture, and the benefits achieved through improving structural safety prior to failure. To this end, a modified multi-objective harmony search is used to select the best variables regarding the geometry, concrete strength, reinforcement and post-tensioning steel. The algorithm parameters have been adapted to move from diversification to intensification. Diversification approach allows for the global search of a large variable space. Intensification, however, improves the convergence to the best solutions.

In this case, the durability conditions for a coastal environment (Fomento, 2008) are imposed by the parameters and the constraints. The durability of a concrete structure is its capacity to withstand, for the duration of its designed service life, the physical and chemical conditions to which it is exposed, and which could cause it to deteriorate as a result of effects other than the loads and stresses considered in its structural analysis. The code gives some considerations of durability at the design stage and the construction phase, as selection of suitable structural shapes, concrete quality, cover thickness, selection of raw materials,

correct placing and curing of the concrete, among others. Durability constraints are imposed to guarantee a service life of 100 years. The concrete cover is fixed as 65mm. The limitation corresponding to the decompression limit state during service and the absence of cracking during prestressing is checked. Besides, the compressive stresses in the concrete cannot exceed 60% of the characteristic compressive strength. It is worth noting that other requirements mentioned in the code that do not affect the optimization problem must also be satisfied. Use stage is considered finalized when service life takes place. Thus, maintenance activities are not included. During use stage, only carbon capture due to carbonation is considered. Bridge designs are obtained from the following optimization:

Given

A post-tensioned concrete box-girder road bridges with a width of 11.8m and three continuous spans of 35.2, 44 and 35.2m. The concrete cover is fixed as 65mm.

Goal

Find the optimal bridge design described by 33 variables regarding the geometry, the concrete grade and the reinforcing and prestressing steel, so that:

- The cost of the deck, which includes the cost of material production, transport and placement, as well as the cost of the CO_2 emissions, is minimized.
- The CO_2 emissions of the deck, which considers the embedded emissions due to the material production, transport and placement, as well as the CO_2 capture, is minimized.
- The overall safety factor with respect to the ultimate limit states is maximized.

Subject to

The requirements regarding the ultimate and serviceability limit states, and the constructability and geometric constraints described in Fomento (2008, 2011), which are based on the Eurocode (European Committee for Standardisation, 2003b, 2005). In addition, the durability constraints guarantee a service life of 100 years.

7.3. Results

7.3.1. *Multi-objective algorithm*

This study uses the multi-objective harmony search algorithm with a diversification-intensification strategy. Alberdi et al. (2015) compared the most common algorithms in the optimization of steel moment frames, and pointed out that harmony search and tabu search were the most robust algorithms. In addition, they outlined the benefits of combining intensification and diversification techniques. Murren & Khandelwal (2014) also claimed the appropriate incorporation of these two counterbalancing components to enhance the efficiency of the algorithm. Diversification promotes the exploration of the entire design

space. This, in turn, avoids trapping in local optima. Intensification improves the convergence. Therefore, this technique is applied in the latter part of the optimization process to improve the solution quality.

Multi-objective HS algorithm was explained in Section 4.5.2. Additionally, three phases of HM parameters are carried out to move from diversification to intensification. These phases reduce progressively the randomness as follows:

Phase 1: PAR=0.4, HMCR=0.7, HMS=50. The algorithm acquires the parameters proposed by García-Segura et al. (2015), excepting HMS. García-Segura et al. (2015) used the Design of Experiments methodology to adjust the algorithm parameters. The effect of each parameter on the algorithm performance was examined to find the best values. A harmony memory size of 50 solutions is enough to capture the variability. Besides, this reduction decreases the computation time and collects only high quality solutions. Note that when the number of solutions with ranking equal to one that is, belonging to the Pareto front, is greater than the value of HMS, the HMS value is increased to the number of Pareto solutions.

Phase 2: PAR=0.4, HMCR=0.7, HMS=50, fix the memory consideration. In Phase 1, the memory consideration selects the values of the variables from different HM solutions. In contrast, Phase 2 fixes the memory consideration to a unique random HM solution. Consequently, the movement is carried out around one random solution, which varies in every iteration.

Phase 3: PAR=0.4, HMCR=1, HMS=50, fix the memory consideration. In the last phase, the memory consideration is fixed and HMCR is equal to one. In this case, random selection is not allowed. A local search strategy is simulated fixing the memory consideration to a unique random HM solution and perturbing parts of existing designs by a small movement according to PAR. At the last part of the algorithm, finding a better random design is less likely. Therefore, this phase conducts a refinement process of local search.

After five harmony memory updates without improvement (Step 4 of Section 4.5.1), there is a phase transition. Lastly, the algorithm ends when the harmony memory is unchanged during a number of IWI equal to ten.

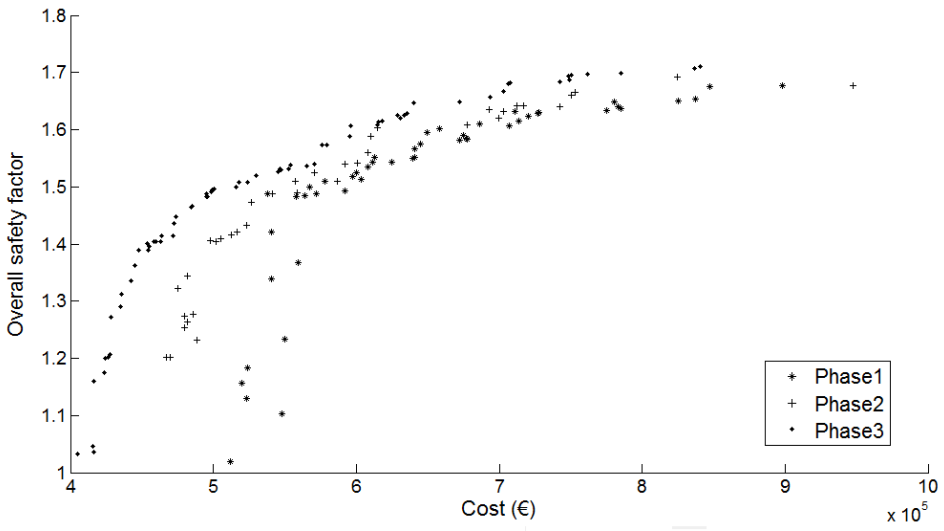

Figure 7.1. Multi-objective harmony search evolution (based on García-Segura & Yepes (2016))

Figure 7.1 illustrates the benefits of combining diversification and intensification. The parameters considered for Phase 1 lead to the exploration of the search space, and spread the solutions along the objective functions. Note that the diversity of the population is crucial for a multi-objective optimization. Phase 2, which is carried out after five memory updates without improvement, eliminates the combination of solutions. In terms of the algorithm, the memory consideration is fixed to one random solution. Thus, the algorithm improves the solution quality by generating new designs from parts of existing designs in the HM, and a random and mutation component. Figure 7.1 shows that the cheapest solutions are improved in both cost and overall safety factor during this phase. Finally, Phase 3 achieves solutions with a 13% and 18% reduction in cost and emissions compared to Phase2. This is done by intensifying the solutions by the pitch adjustment. It is worth noting that 1800, 1000 and 1700 feasible solutions are evaluated, respectively, during Phase 1, Phase 2 and Phase 3. The computational time to obtain an exact feasible solution is about 1500 s. This time is employed mainly for the finite-element analysis and extraction of results.

7.3.2. *Relationship between cost, CO_2 emissions and safety*

The Pareto set is formed by the solutions whose objective values cannot be improved without worsening the value of at least one objective. Generally, the Pareto front regarding three objectives forms a surface where each solution improves at least one objective. In contrast, Figure 7.1 shows that solutions stand nearly in a line. Thus, cost and emission objectives are not totally in conflict. The findings indicate that these objectives are closely related and therefore, reducing the material consumption reduces, in turn, both objectives. The analysis of the relationship between cost and CO_2 emissions as solutions request for increased

safety shows the degree of dependence of this relationship to the space of feasible solutions. Results show that the relationship is maintained for all safety levels and therefore, cost optimization is a good approach for emission minimization regardless of the safety level.

On the other hand, the relationship between the three criteria shows whether the variables are more influenced by the safety requirements, or conversely, the differences come from the unit costs or emissions. Findings indicate that structural efficiency has a great impact on the optimum design of road bridges. In addition, both cost and emission optimization leads to a reduction in material consumption and, therefore, to achieve an environmentally friendly design. Regarding the algorithm evolution, cost and emission objectives show stronger relationships as the algorithm progresses. Despite objectives are in conflict for random solutions, they are close to each other near their optima.

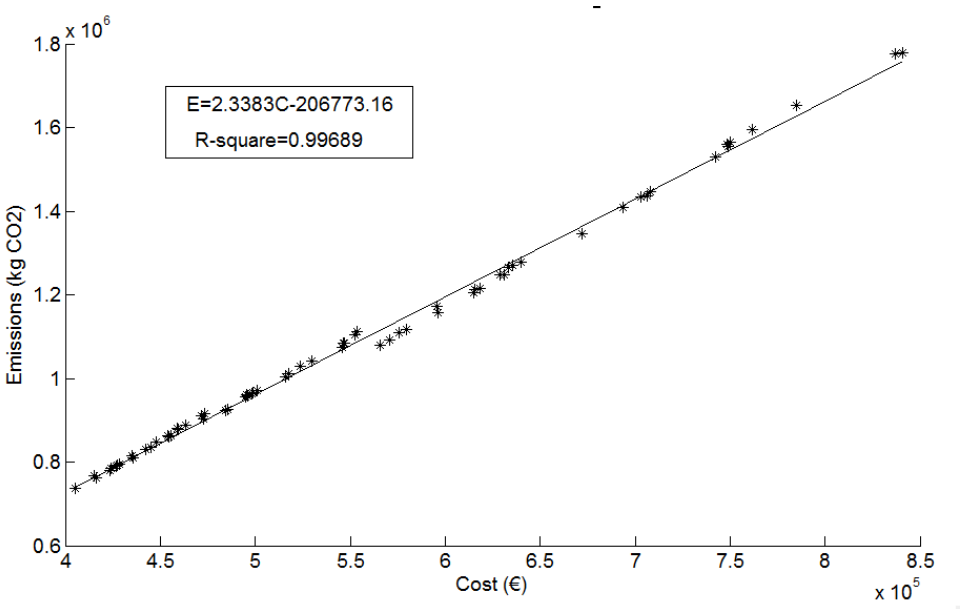

Figure 7.2. Pareto set of solutions for cost and CO_2 emissions (based on García-Segura & Yepes (2016))

Figure 7.2 depicts the relationship between cost and CO_2 emissions. This figure shows that minimum cost solutions coincide with minimum emission solutions. A good linear fit (E=2.3383C-206773.16 with a regression coefficient (R^2) equal to 0.99689) represents this relationship. In other words, when cost increases by one euro, the CO_2 emissions rise by 2.34 kg. During the following analysis, this relation can be used as a correspondence between the objectives. In addition, this outcome confirms that cost optimization is a good approach for emission minimization regardless of the safety level.

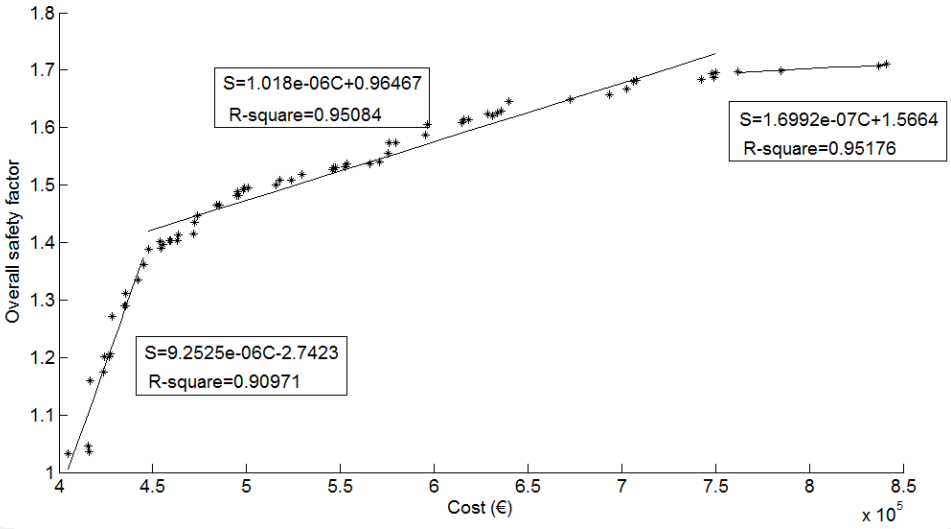

Figure 7.3. Pareto set of solutions for cost and overall safety factor (based on García-Segura & Yepes (2016))

As for the overall safety factor, the findings indicate that the increment in cost is not constant when increasing safety conditions. In a first step, the overall safety factor is improved with a small cost increment. As Figure 7.3 shows, a linear relation between both objectives (S=9.2525E-06C-2.7423 with a regression coefficient R^2=0.90971) is obtained until C=450,000 € and S=1.4. Increasing the overall safety factor by 10% results in a cost increment of 10,808 €. In a second step, the safety improvement is more expensive. The trend is represented by a linear relation until C=750,000 € and S=1.69 (S=1.018E-06C+0.96467 with a regression coefficient R^2=0.95084). This means that 98,232 € are needed to increase the overall safety factor by 10%. In a final step, the overall safety factor hardly increases when the cost increases. A linear relation between both objectives can be described (S=1.6992E-07C+1.5664 with a regression coefficient R^2=0.95176). Regarding the emissions, the trend is the same considering the correspondence between cost and emissions.

7.3.3. *Best designs*

Table 7.1 shows the cheapest solution, which has an overall safety factor of 1.03. This solution has a cost and emission of 405099.22 € and 735947.88 kg CO_2, respectively. The solution has a depth (h) of 2.3 m. Given that depth, the ratio between the main span length and the depth is 19.1. The web inclination width (d) is 0.45 m and the width of the bottom slab (b) is 4.45 m. Therefore, the ratio between the width of the bottom slab and the total width is 0.38.

The thickness of the top slab and that of the external flange is 0.25 m. However, the thickness of the bottom slab adopts a value of 0.35 m to increase the flexure capacity over the supports. The thickness of the internal flange section is 0.4 m. The

thickness of the webs is 0.6 m. Concrete acquires a grade of 35 MPa concrete. The distance from the piers to the point of inflection is 0.1 times the span length. The eccentricity in the external spans is set to a quarter of the depth. These points fix the layout of the post-tensioning steel. Regarding the quantities of concrete and steel, the amount of post-tensioned steel reaches 29676.21 kg and the amount of reinforcement is equal to 90294.37 kg. A concrete volume of 909.47 m^3 is needed.

Table 7.1. Cheapest solution

	Result values
Cost (€)	405099.22
Emissions (kg CO_2)	735947.88
Overall safety factor	1.03
***h* (m)**	2.30
***d* (m)**	0.45
***b* (m)**	4.45
e_s (m)	0.25
e_v (m)	0.25
e_i (m)	0.35
e_a (m)	0.60
e_{va} (m)	0.40
f_{ck} (MPa)	35.00
L_{pi}	0.10
e_p	0.50
Prestressing steel (kg)	29676.21
Reinforcing steel (kg)	90294.37
Concrete (m^3)	909.47

Figure 7.4 displays a box-plot for the variables of the optimum solutions. The analysis of the figure shows the best variables to be increased to improve safety. The percentiles [25^{th}, 50^{th}, 75^{th}] of the web inclination width are [0.5 m, 0.6 m, 0.8 m]. These values correspond to a web slope that ranges between 3.5 and 4. The slope is considered as the ratio between the width and the depth. Results indicate that the web slope remains approximately constant. This fact is explained by the fact that both the depth and the web inclination width increases in parallel to improve safety. The width of the bottom slab acquires values from 4.4 to 5.3 m, which is equivalent to a ratio of 0.37 and 0.45 of the width of the deck. The median value is 0.38. This means that 50% of values range from ratios of 0.37 to 0.38 the width of the deck. The width of the bottom slab should be increased to decrease the flange length, and therefore, the transverse flexure demand, only when the required overall safety factor is high.

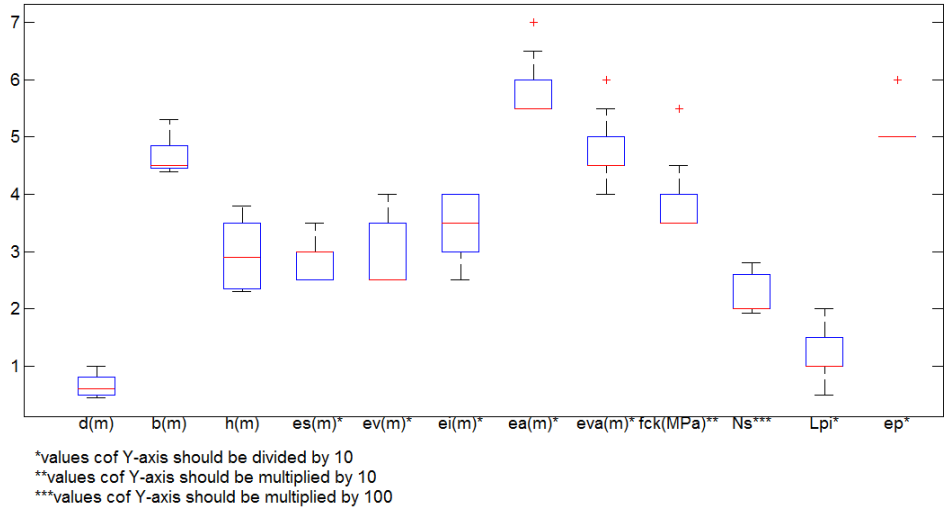

Figure 7.4. Box-plot of the design variables of Pareto solutions (based on García-Segura & Yepes (2016))

Concerning the depth, the minimum value is 2.3m and the interquartile range varies from 2.35 to 3.5 m. This corresponds to a relationship between the main span length and the depth of 19.1, 18.7 and 12.6, respectively. Fomento (2000) recommends a ratio L/h of between 18 and 20 for this type of bridge. Consequently, the depth of the optimum bridge design in terms of cost is within the range proposed by the guidance document, even if the case study is located in a coastal region. Note that for guaranteeing the decompression limit state, the depth is increased to increase, in turn, the inertia and reduce the stresses.

The thicknesses of the top and bottom slab and the external flange section range between 0.25 and 0.4 m. Most of the designs adopt a thickness of the top slab between 0.25 and 0.3. This indicates that increasing the thicknesses of the top lab is not advisable to improve structural safety, since it results in an additional weight. As for the thickness of the external flange, almost 50% of the values are 0.25 m and the other 50% are 0.3 m. Regarding the thickness of the bottom slab, the percentiles are [0.3 m, 0.35 m, 0.4 m]. Increasing this thickness improves the flexure capacity over the supports. The thickness of the web shows a narrow interquartile range from 0.55 to 0.6 m. Results indicates that the thickness of the web is not the most economic variable to increase the shear resistance, even this variable has an influence on the shear. The thickness of the internal flange section acquires values between 0.4 and 0.55 m. Transverse flexure impacts especially over the top slab, which is mainly affected by traffic loads. While it is not advisable to increase the thickness of the top slab, the thickness of the internal flange section is worth increasing to improve the transverse flexure.

Regarding the concrete strength, 50% of the Pareto solutions take the 35 MPa

grade, which is the minimum proposed. Despite there is an outlier solution of 55MPa, results suggest that increasing the concrete strength is not the best solution to improve safety. The use of high-strength concrete may lead to a reduction in depth or amount of reinforcement. Nevertheless, the constraints regarding serviceability limit states and minimum amount of reinforcement restrict both the depth and amount of reinforcement.

Concerning the post-tensioned steel, the interquartile range of the number of strands varies from 194 to 256. For the smallest values of overall safety factor, post-tensioned steel is adjusted to verify the decompression limit state. Afterwards, this variable is increased to contribute to the flexure capacity. The 25th percentile and median value of the distance from the piers to the point of inflection are equal to 0.1 of the span length. This value provides good results for most of the overall safety factors. As this distance is reduced, the post-tensioned steel effect in the piers is intensified. Finally, a ratio of 0.5 of half of the bridge depth is an adequate value for the eccentricity of the post-tensioned steel in the external spans to balance the stresses.

The limit states taken into account to evaluate the overall safety factor are flexure, shear, torsion and transverse flexure. The analysis of the evolution of these limit states indicates which are restrictive. Optimization, unlike the traditional design, seeks the value of the variables that minimizes all the limit states. The only limit states that are not critical are those whose influential variables are also variables of a most restrictive limit state. Such is the case of flexure (see Figure 7.5). Flexure factors take values around 1.4 until the overall safety factor reaches this value. This means that the variables affecting the flexure factor are conditioned by a more restrictive limit state. Results suggest that the decompression limit state is the state with the greater influence over variables such as depth and number of strands. For values greater than 1.4, the flexure factor is put on a par with the overall safety criteria. This indicates that flexure is a restrictive factor.

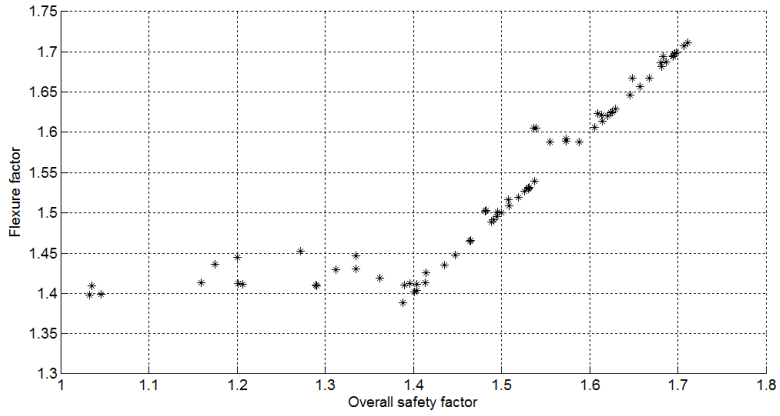

Figure 7.5. Relation between flexure factor and overall safety factor (based on García-Segura & Yepes (2016))

The analysis of the variables with respect to the safety improvement indicates the variables with a clear relationship. Figure 7.6-7.8 show the concrete volume, amount of post-tensioned steel and longitudinal reinforcing steel according to the overall safety factor. All of them show nearly constant values until the 1.4 overall safety factor and an increment after that. As stated previously, the depth and the post-tensioned steel are correlated to guarantee the decompression limit state. While both variables increase in steps, the longitudinal reinforcement is adjusted incrementally to achieve the overall safety factor required. Results suggest that increasing the depth and the number of strands is an economic option when it involves a large decrease in the longitudinal reinforcing steel. This situation happens around the 1.54 safety factor. Figure 7.9 reveals that the transverse reinforcing steel has a progressive increment, since it is influenced by shear, torsion and transverse flexure. The results suggest that to increase the overall safety factor to 1.4, the transverse reinforcement is mainly increased, and this has a little influence on the cost. From this point on, an increment in the longitudinal reinforcement, the post-tensioned steel, and the concrete volume (mainly due to the depth) are also needed. This second step entails high prices. Conclusively, results indicate that a bridge designer can improve the safety with a little cost increment by choosing the correct design variables.

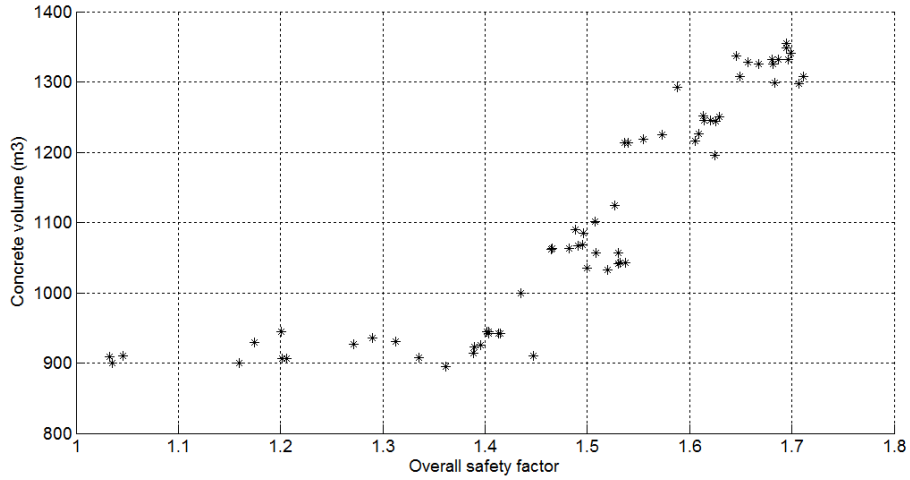

Figure 7.6. Volume of concrete according to overall safety factor (based on García-Segura & Yepes (2016))

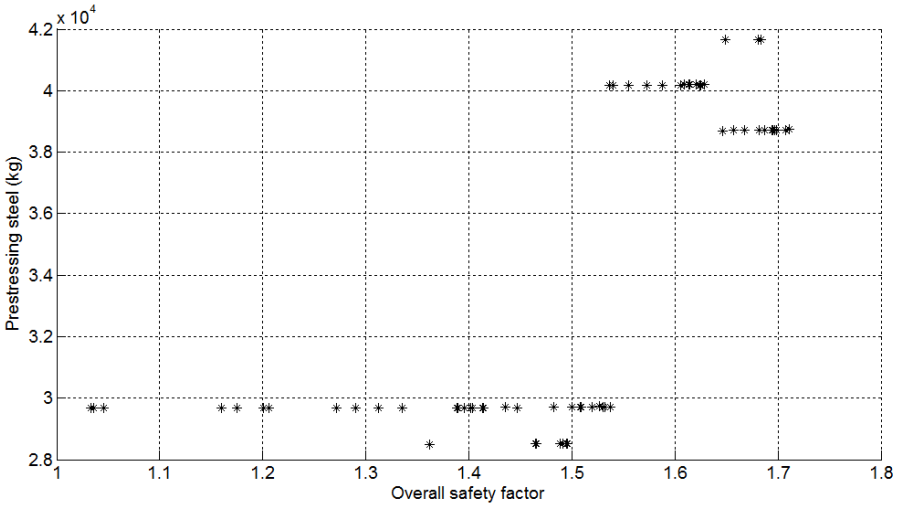

Figure 7.7. Amount of prestressing steel according to overall safety factor (based on García-Segura & Yepes (2016))

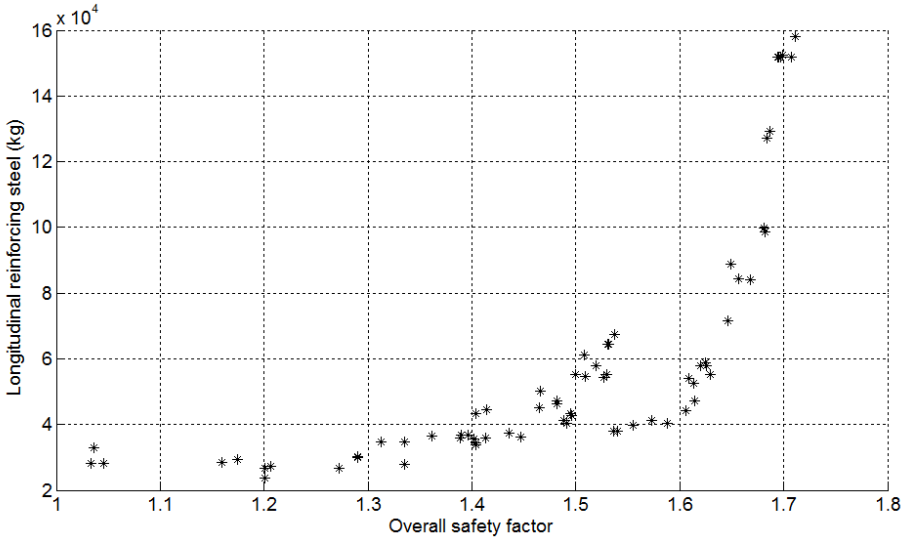

Figure 7.8. Amount of longitudinal reinforcing steel according to overall safety factor (based on García-Segura & Yepes (2016))

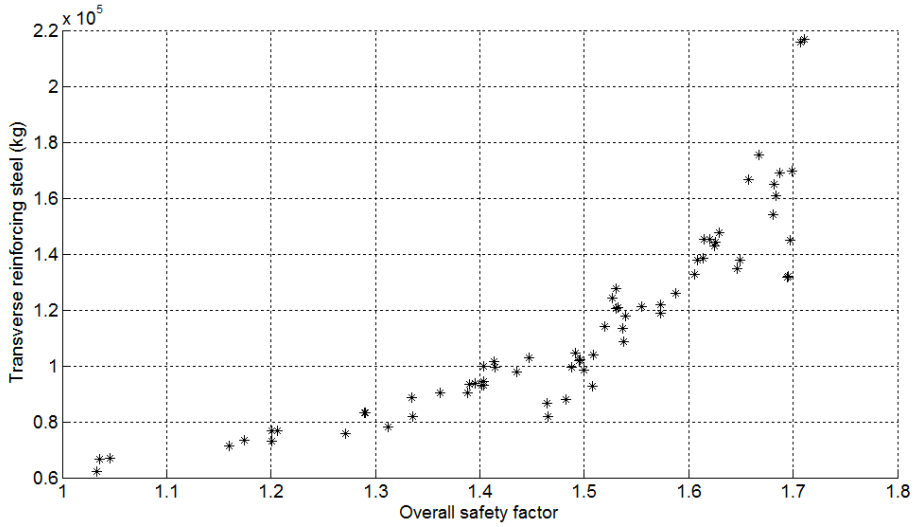

Figure 7.9. Amount of transverse reinforcing steel according to overall safety factor (based on García-Segura & Yepes (2016))

Finally, the optimum solution in terms of cost is compared with Fomento (2000) recommendations. The amount of reinforcement per surface of deck (66.89 kg/m^2) is smaller than the code suggestion (between 90 and 110 kg/m^2). However, the concrete volume per surface of deck (0.67 m^3/m^2) is greater than the recommendation (between 0.5 and 0.56 m^3/m^2). Likewise, the amount of post-tensioned steel per surface of deck (21.98 kg/m^2) is greater than the one recommended (between 13 and 19 kg/m^2) for this span length. It is important to remember that the bridge studied is located in a coastal region with restricting serviceability limit states. This case leads to greater cross-sections and amount of post-tensioned steel. Considering the cost of concrete, reinforcing and post-tensioned steel, the optimum solution reduces the cost by 3% and 14%, and the CO_2 emissions by 6% and 16%, compared to the average and maximum measurements proposed by the guidance document. These values are obtained from the most economical solution. As a final conclusion, the heuristic optimization found a cheaper and more environmentally friendly bridge, reducing the reinforcing steel but increasing the concrete volume and post-tensioned steel.

7.4. Conclusions

This study carries out a multi-objective optimization to find designs of the post-tensioned concrete box-girder road bridge that represent optimal trade-offs among the cost, CO_2 emissions, and overall safety factor. To this end, a computer tool links CSiBridge© and Matlab© software to integrate a finite-element analysis in a multi-objective optimization program with a limit state verification. The finite-element analysis is performed through shell elements, which incorporates the reinforcing steel as a reinforcement grid and post-tensioned tendons. The optimization provides

the best combination of variables, regarding the geometry, concrete strength, reinforcing and post-tensioned steel. The algorithm is improved by a combination of diversification and intensification strategies. The algorithm firstly explores random locations in the search space, to later conduct a refinement process around good solutions.

The analysis of the results provides information about the relation between objectives, the best variables to improve safety, and the critical ultimate limit states. The findings indicate that cost optimization is a good approach to achieve an environmentally friendly design, as long as cost and CO_2 emission criteria lead to a reduction in material consumption. In addition, this outcome is maintained regardless of the safety level. While objectives are in conflict for random solutions, they are close to each other near their optima. The Pareto set indicates, as a rule of thumb, that reducing costs by one Euro results in savings of 2.34 kg in CO_2 emissions. Besides, three linear relations between cost and the overall safety factor are highlighted. To increase the overall safety factor from 1 to 1.4, costs increase from 400,000 € to 450,000 €. After this point, the safety improvement is more expensive.

The inclusion of the safety function in the multi-objective optimization provides vital knowledge about the dependence of the variables to the safety level. This is important since the optimum value of variables depends on parameters like the width and span length. However, transforming the safety from a constraint to an objective, we can know the best values of the variables without limiting the design to a unique structural response due to a value of width and span length. The analysis of the Pareto front reveals the variables with smaller influence over the cost and emissions, which are better for improving safety.

Results suggest that the decompression limit state is a restricting limit state that conditions variables such as depth and number of strands. The depth, together with the thickness of the bottom slab, the post-tensioned steel, and the longitudinal reinforcing are the main variables providing the flexure capacity. However, the thickness of the top slab and external flange are not the best variables to improve safety, since it entails an additional weight. The ratio L/h of the most economical solution is 19.1. The thickness of the internal flange section should be increased and the flange length should be decreased to improve the transverse flexure performance. The slope of the web inclination remains approximately constant (between 3.5 and 4) for all the overall safety factors, as both the depth and the web inclination width increases in parallel to improve safety. The ratio between the width of the bottom slab and the deck acquires values around 0.38. The thickness of the webs is not the most economic variable to increase the shear resistance. Rather, the reinforcing steel is increased.

Regarding concrete strength, the use of high-strength concrete is advisable when it results in a reduction in depth or amount of reinforcement. However, as serviceability limit states and minimum amount of reinforcement restrict these variables, the use of high-strength concrete grade is not efficient for this case.

Comparing the best cost solution with the standards, the optimization tool found a cheaper and a more environmentally friendly bridge, by reducing the reinforcing steel but increasing the concrete volume and post-tensioned steel.

Chapter 8
Multi-objective optimization of cost, safety, and corrosion time by ANN

8.1. Aim of the study

In view of the results obtained in the previous study (Chapter 7), in that cost and emission objectives were closely related, this study (García-Segura et al., submitted(a)) does not consider the CO_2 emissions. However, in this case, the corrosion initiation time is included as objective function for further deepening in the durability requirements. Despite durability is a more common criterion when the management phase is studied, this research considers the durability objective in the design phase with the aim of designing for longevity and reduced long-term impacts. Therefore, a minimum service life is not imposed, in contrast to the previous study. Here, the concrete cover and concrete strength are variables to optimize the objective function of corrosion initiation time. The chloride-induced corrosion produces a degradation process and consequently, the reduction in structural safety. Thus, safety objective is important to be simultaneously considered in the optimization problem.

On the other hand, multi-objective optimization is a commonly used tool to find multiple trade-off solutions. However, a large computational time is needed to check the solutions to certain problems. The existence of many decision variables or the evaluation procedure, like the use of the finite-element method, increases the computational time (Deb & Nain, 2007). Meta-models to predict the objective functions and constraints have been developed to solve this problem (Deb, 2011). Giannakoglou (2002) stated that optimization procedures based on stochastic methods require huge time and proved the usefulness of surrogate or approximation models. Emmerich & Naujoks (2004) showed various metamodel-assisted multi-

objective evolutionary algorithms based on Gaussian field (Kriging) models. Deb & Nain (2007) analyzed the use of approximate models like artificial neural networks (ANNs) for multi-objective optimization. The results showed a saving in exact function evaluations of about 25 to 62%.

ANN is a machine learning method based on artificial neurons that learns from training examples and provides a response or output by approximating non-linear functions of their inputs. Several topics related to civil engineering have been conducted through the use of ANN. Researchers aimed to predict the structural behavior (Caglar et al., 2008; Erdem, 2010; Marti-Vargas et al., 2013; Sanad & Saka, 2001), to study the sensitivity of parameters (Cao et al., 2015; Hadzima-Nyarko et al., 2011), and to analyze the effects of the input parameters on the output (Shi, 2016; Zavrtanik et al., 2016). Chatterjee et al. (2016) used ANN for structural failure prediction. In this line, Protopapadakis et al. (2016) presented a neural detector with the aim of identifying the structural defects in concrete piles.

This study reduces the high computational cost required to evaluate the constraints of a real bridge optimization problem though the use of ANN integrated in a multi-objective harmony search (MOHS). ANNs are trained to predict the structural response in terms of the limit states based on the design variables, without analyzing the bridge response. The combined process of ANN+MOHS obtains an approximate Pareto front. After that, the Pareto is actualized and improved through exact analysis. The final Pareto set provides a complete set of alternative trade-off solutions of PSC box-girder road bridges with respect to cost, overall safety factor, and corrosion initiation time.

8.2. Definition of the problem

Given

A post-tensioned concrete box-girder road bridges with a width of 11.8m and three continuous spans of 35.2, 44 and 35.2m.

Goal

Find the optimal bridge design described by 34 variables regarding the geometry (including the concrete cover), the concrete grade and the reinforcing and prestressing steel, so that:

- The cost of the deck, which include the cost of material production, transport and placement, is minimized.
- The overall safety factor with respect to the ultimate limit states is maximized.
- The corrosion initiation time due to chloride is maximized.

Subject to

The requirements regarding the ultimate and serviceability limit states, and the constructability and geometric constraints described in Fomento (2008, 2011),

which are based on the Eurocode (European Committee for Standardisation, 2003b, 2005).

8.3. Methodology

The methodology proposed involves four steps that carry out the ANN training, obtaining of approximate Pareto set, updating of Pareto set and obtaining of exact Pareto set (see Figure 8.1). These steps follow two models. The first one is an approximate model that guides the optimization process and provides a near-optimum Pareto front. To this end, ANN is integrated in a multi-objective HS. This artificial neural network is trained by the data collected from previous studies. Then, the ANN is used to predict the limit state coefficients from the design variables, since the large computational time of a multi-objective bridge optimization comes from the structural analysis. The limit state coefficients evaluate the ratio between the resistance of the structural response and the ultimate load effect of actions for this limit state. The second model is an exact model that conducts a multi-objective optimization with a complete bridge analysis and verification. The Pareto set is updated and improved through this model. The combination of the two models aims to reduce the computing time while achieving a good performance. Finally, trade-offs between cost, safety, and corrosion initiation are obtained.

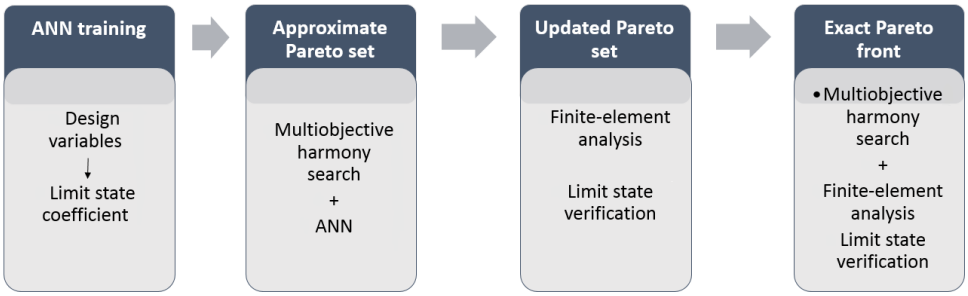

Figure 8.1. Methodology to integrated multi-objective harmony search with artificial neural networks (based on García-Segura et al. (submitted(a)))

The Neural Network is formed by many processing elements or neurons that use a backpropagation algorithm. The model learns from the input elements by adjusting the weights through an iterative process. The model outputs are compared with the targets and the errors are back-propagated. The multilayer feedforward network consists of one hidden layer of sigmoid neurons followed by an output layer of linear neurons. The neurons of the hidden layer are connected to all neurons in both the input and output layers (see Figure 8.2). The number of neurons in the input and output layers corresponds, respectively, with the number of input and output parameters. Inputs are multiplied by weights and combined linearly with an independent term or bias. Each hidden neuron follows this equation ($\sum x_i \cdot w_{i,j} + b$). Then, each neuron of the hidden layer produces an output by applying a tan-

sigmoid function to the linear combination. The output layer follows the same procedure. The accuracy of the network is measured by the mean square error (MSE) and the coefficient of determination (R^2).

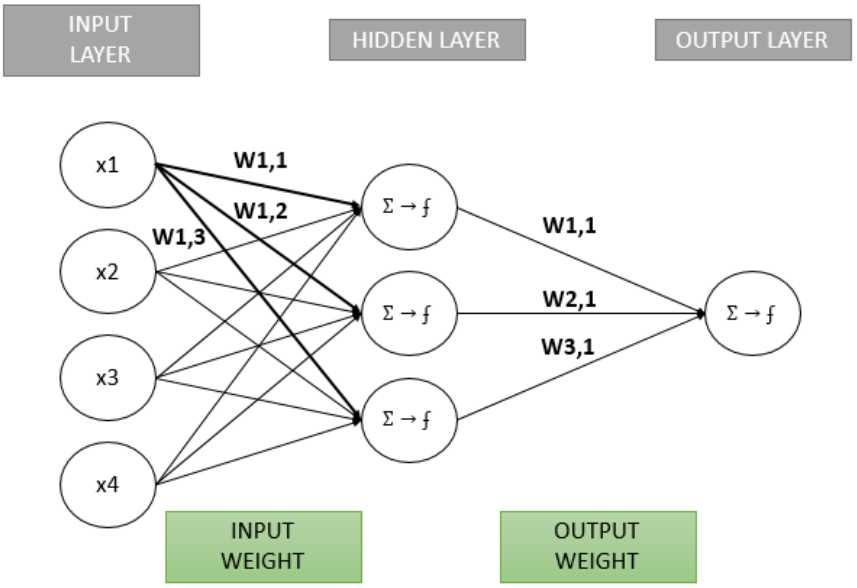

Figure 8.2. Neural Network

This study uses the multi-objective HS algorithm proposed by Ricart et al. (2011) with the crowding distance criterion to select the solutions with the same ranking. This criterion benefits the diversification, since the solutions with greater crowding distance are those further from other solutions. As proposed in the previous study (Chapter 7), this study checks several intensification-diversification strategies by changing the algorithm parameters. While diversification promotes to explore the entire design space to avoid trapping in local optima, intensification is needed to improve the convergence. The cases studied are explained in Section 8.3.2. The algorithm parameters and the use of penalty functions are studied.

As the approximate model (ANN integrated in a multi-objective HS) does not guarantee that solutions would be feasible after the exact evaluation, this study proposes penalties for the unfeasible solutions to worsen their aptitude. A review of penalty functions can be found in the study of Coello (2002). The penalty function used is $F_p = (K_p/f)\cdot F$, where F_p is the penalized cost; F is the non-penalized cost; f is a coefficient of unfeasibility with a value of less than one, and K_p is a coefficient. Thus, the cost is penalized by a coefficient that depends on the feasibility of the solution (f) and an extra coefficient that increases the cost for unfeasible solutions (K_p). The f factor is equal to the minimum limit state coefficient. Two values of K_p coefficient are studied (see Section 8.3.2).

To compare different Pareto fronts and establish a termination criterion, this study uses the hypervolume measure. The hypervolume is frequent applied for comparing the quality of results in multi-objective optimizations. Coello et al. (2006) reviewed a variety of indicators to measure the quality of Pareto front. Among them, the hypervolume measure or S-metric is of outstanding importance (Beume et al., 2007). This quality indicator evaluates the convergence towards the Pareto front as well as the representative distribution of points along the front. The hypervolume measure was originally proposed by Zitzler & Thiele (1998), who called it the size of dominated space. Then, it was described as the Lebesgue measure. The values should be firstly normalized to evaluate the hypervolume. In this case, the problem minimizes the cost and the negative value of corrosion initiation time and the overall safety factor. Thus, the values are divided by (20x10^6, 500, 2) to normalize the values of cost, corrosion initiation time, and the overall safety factor. After normalization, the utopia and antiutopia points are (0, –1, –1) and (1, 0, 0).

8.3.1. *Step 1. ANN training*

The neural network is trained using 4500 data. Each datum comprises 34 input variables and one output variable. The output variable refers to the limit state coefficients. As there are 17 limit states, the process is repeated 17 times, and therefore, 17 ANNs are obtained. The data are divided into training, validation, and test. The respective percentages are 70%, 15%, 15%. The ANN uses a Levenberg-Marquardt backpropagation algorithm with 10 neurons. The number of neurons is adjusted to provide the best performance. A neural network with a sufficient number of neurons can adjust the weights to provide a good fit. However, the excessive number of neurons can lead an overfitting model. In this last case, the model has a good fit for the model sample, while it has poor generalization ability for other data. The training process is finalized when the number of iterations reaches 1000, or the performance function drops below 10^{-8}, or the magnitude of the gradient is less than 10^{-10}, or the maximum number of validation failures exceeds 50.

Results of Step 1

Table 8.1 summarizes the results of the ANNs. The coefficient of determination R^2 and the MSE are used to analyze the relation between the output and targets and the network's performance. As Table 8.1 shows, the values of R^2 vary between 0.912 and 0.999. Regarding MSE, values are between 0.0001 and 0.088.

Table 8.1. Results of the network's performance (based on García-Segura et al. (submitted (a)))

Limit state	MSE	R^2
Stresses during prestressing	0.0213	0.976
Serviceability stresses	0.0039	0.996
Deflection (Fomento, 2008)	0.0036	0.996
Deflection (Fomento, 2011)	0.0001	0.999
Flexure	0.0574	0.942
Minimum flexure reinforcement	0.0704	0.930
Shear	0.0063	0.993
Minimum shear reinforcement	0.0116	0.988
Shear between web and flanges	0.0384	0.960
Torsion: longitudinal reinforcement	0.0096	0.990
Torsion: transverse reinforcement	0.0270	0.973
Minimum torsion reinforcement	0.0407	0.959
Torsion combined with shear	0.0012	0.999
Torsion combined with tension	0.0408	0.958
Transverse flexion	0.0479	0.952
Minimum transverse reinforcement	0.0877	0.912
Transverse shear	0.0627	0.937

8.3.2. *Step 2. Approximate Pareto set*

The multi-objective HS is combined with ANN to obtain an approximate Pareto set. As mentioned previously, ANN is used to obtain the coefficient of the limit states from the design variables. Based on those values, nine predictions of each output are carried out and the average value is obtained. The constraints check whether the coefficients of the limit states predicted are greater than one. The overall safety factor objective is also evaluated according to these predictions. The ANN+MOHS is performed for 20000 feasible iterations. The termination criterion of this step is set based on the hypervolume stabilization. Figure 8.3 shows that Pareto front tends to stabilize around 20000 iterations. Ten different cases regarding diversification-intensification strategies and penalty functions are examined during this step to improve the efficiency of the algorithm. Table 8.2 summarizes the algorithm parameters according to the case studied.

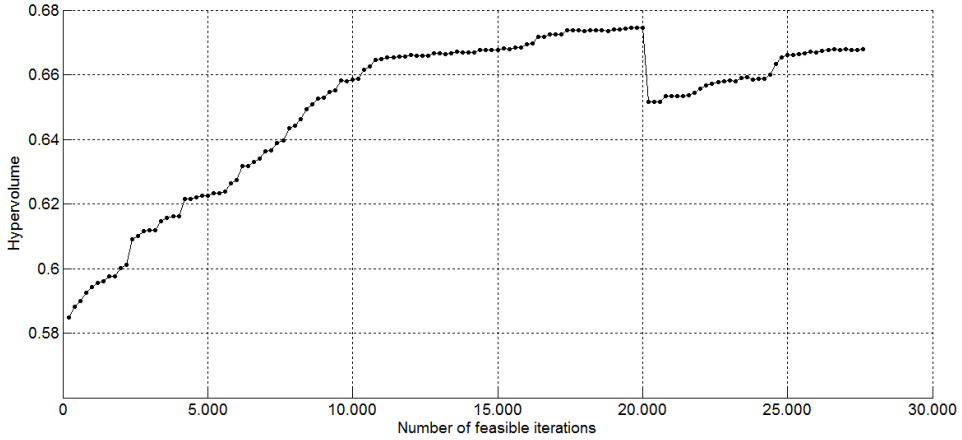

Figure 8.3. Hypervolume evolution of Pareto front (based on García-Segura et al. (submitted(a)))

Table 8.2. Algorithm parameters according to the case studied (based on García-Segura et al. (submitted (a)))

		HMS	HMCR	PAR	Fix memory consideration	K_p
Case 1		200	0.7	0.4	No	1
Case 2		200	0.85	0.4	No	1
Case 3		200	1	0.4	No	1
Case 4		200	0.7	0.4	Yes	1
Case 5		200	0.85	0.4	Yes	1
Case 6		200	1	0.4	Yes	1
Case 7		200	0.7	0.4	Yes	1.1
Case 8		200	0.85	0.4	Yes	1.1
Case 9		200	1	0.4	Yes	1.1
Case 10	Phase 1: 2500 iterations	200	0.7	0.4	No	1
	Phase 2: 2500 iterations	200	0.7	0.4	Yes	1
	Phase 3: 15000 iterations	200	1	0.4	Yes	1

Results of Step 2

In this step, the approximate Pareto set, which is obtained combining ANN and multi-objective HS, is studied through different cases regarding the algorithm parameters and the coefficient of penalty function. The values shown in Table 8.2 are analyzed. The hypervolume is used to evaluate the convergence and spread of solutions. Results are compared through this metric in Table 8.3. Case 10 presents the greatest hypervolume. This case corresponds to the progressive diversification-

intensification strategy.

Cases 1–3 and Cases 4–6 present increasing values of HMCR. In all of them, the case with the greatest hypervolume is the last one. This indicates that the greatest HMCR value performs better for this structural problem. When HMCR is equal to one, the random selection of the value of the variables becomes unlikely. Cases 4–6 fix the memory consideration to one solution. These cases achieve better results, compared to Cases 1–3. This means that combining the values of variables from different solutions is less effective than taking only one solution and perturbing some members. However, the progressive evolution of random selection and combination of solutions is analyzed in Case 10, obtaining the best value of hypervolume.

Regarding the penalty function, Cases 7-9 analyze a higher value of K_p coefficient (K_p equal to 1.1). In this case, the cost of unfeasible solutions is extra-penalized. Consequently, the hypervolume values are expected to be smaller. Thus, Case 8 is also studied in the next step to determine whether this case is definitely worse than Case 10.

Table 8.3. Hypervolume results for each case (based on García-Segura et al. (submitted (a)))

	Hypervolume		
Case 1	0.6286	**Case 6**	0.6744
Case 2	0.6322	**Case 7**	0.6225
Case 3	0.6373	**Case 8**	0.6589
Case 4	0.6504	**Case 9**	0.6583
Case 5	0.6612	**Case 10**	0.6748

8.3.3. *Step 3. Updated Pareto set*

In this step, the Pareto set is updated through an exact method. Specifically, the HM solutions, including the Pareto front, are updated. In the same way that there are Pareto solutions which may no longer be after updating, there are HM solutions with ranking greater than one which can belong to Pareto front after updating. In the updating process, CSiBridge© is used for the finite-element analysis and Matlab© verifies the limit states based on the load effects obtained from CSiBridge© and the bridge resistance evaluation. Afterwards, the feasible solutions are saved and ranked. The feasible solutions with ranking equal to one constitute the updated Pareto set. The following step departs from the exact solutions.

Results of Step 3

When actualizing the Pareto set, the limit state coefficients are modified. This, in turn, change the objective values and the hypervolume value. This step is carried out in Cases 8 and 10. The following hypervolume values are obtained:

Case 8: 0.6589 → 0.6499

Case 10: 0.6748 → 0.6520

Unsurprisingly, the hypervolume difference of Case 8 is smaller, since this case imposes a higher penalty on unfeasible solutions. Even so, the hypervolume remains smaller in Case 10 after the updating. Therefore, Case 10 is used to carry out the following step.

8.3.4. *Step 4. Exact Pareto front*

The last step (Step 4) conducts a multi-objective optimization through an exact method. Therefore, new harmony solutions are generated based on the HS strategy. Each new harmony is analyzed through a finite-element analysis and verified. The harmony memory is updated with the feasible solutions of highest ranking. It is worth noting that when the number of solutions with ranking equal to one that is, belonging to the Pareto front, is greater than the value of HMS, the HMS value is increased to the number of Pareto solutions. Finally, the optimization process finishes after ten consecutive harmony memory matrix updates (see step 4 of Section 4.5.2) with a difference in hypervolume value of less than 0.0005.

Results of Step 4

Figure 8.3 shows the Pareto performance results. The last step improves the hypervolume value from 0.652 to 0.668. Findings indicate that the percentage of exact function evaluations is about 37% of the total, when the exact evaluations for ANN training are taken into account. However, if the ANN training data are not considered, the percentage of exact function evaluations is 27%. It is worth noting the importance of this result, since the average time for obtaining an exact feasible solution is about 1500 s, while obtaining a solution through ANN takes about 4 s.

Figure 8.4 contains the Pareto set of solutions. These solutions cannot be improved without worsening the value of one objective. Results provide trade-off solutions from which the designer can select the most desirable one. There are solutions, which require higher initial cost, but these solutions have a longer lifetime thanks to the higher corrosion initiation time and improved safety. As a result, these solutions will need lower maintenance and repair costs. Codes recommend a service life target and safety level for all road bridges. However, this study gives multiple alternatives that can easily be adjusted to each need.

Analyzing Figure 8.4, we can see that the relationship between the cost and the overall safety factor presents a parabolic fit. This relation is maintained for each corrosion initiation time. It is important to note that the corrosion initiation time is limited to 500 years. Findings indicate that there are solutions whose cost is smaller than €500000 and they have an overall safety factor of around 1.5 and a maximum corrosion initiation time. This means that with a small cost increment, the safety and durability can be greatly improved. Considering that each solutions is the cheapest one for the safety and durability level, the best values of cross-section geometry, concrete grade, reinforcement, and post-tensioning steel for a safety and

durability target are known.

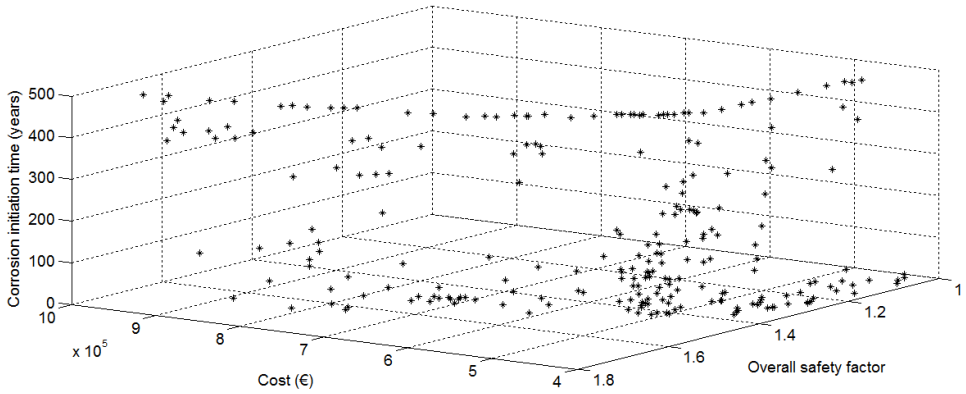

Figure 8.4. Pareto set for cost, overall safety factor and corrosion initiation time (based on García-Segura et al. (submitted (a)))

The variables with influence over the corrosion initiation time are the concrete strength and the concrete cover. Figure 8.5 shows the Pareto set according to the concrete grade. The figure illustrates a tendency towards increasing concrete strength to increase corrosion time. The average corrosion initiation times are 36.3, 88.3, 343.7 and 500 years for 35, 45, 55, 70, and 90 MPa, respectively. Concerning the overall safety factor, this objective do not present a clear relationship with concrete strength, since the same safety range can be obtained with different concrete grades.

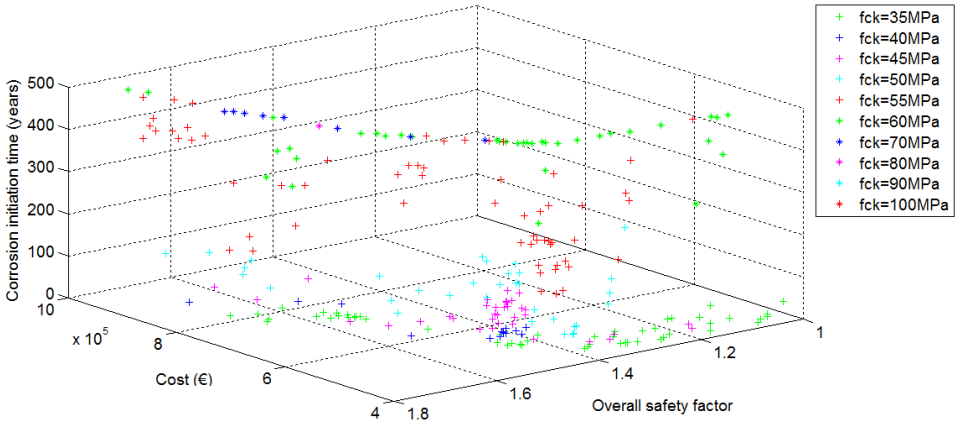

Figure 8.5. Pareto set according to the concrete grade (based on García-Segura et al. (submitted (a)))

Regarding the concrete cover effect, Figure 8.6 depicts the solutions according to this variable. It is worth mentioning that an increment in concrete cover has an effect on the corrosion initiation time that depends on the value of concrete strength. This relationship is represented by Figure 8.7. Selecting one concrete grade, the relationship between corrosion initiation time and concrete cover is almost linear. Both the slope and the y-intercept increase with the concrete strength. It is important to note that the higher concrete strength the higher is the increment. This means that the effect of increasing the concrete strength in 5 MPa is not the same for each concrete grade. For lower concrete grades, this increment hardly increases the corrosion time. However, a considerable increment is shown from 45 MPa. Considering that concrete strength has more economic impact than concrete cover, it is cheaper to increase the concrete cover for shorter service life targets. Nevertheless, an increment in concrete strength favors strategies of higher service life targets. Thus, there are optimum bridge solutions with the maximum corrosion initiation time that use high-strength concrete with the minimum cover. However, the opposite case is not obtained. As a conclusion, an optimum selection of a concrete cover and concrete strength can achieve the durability and cost goals.

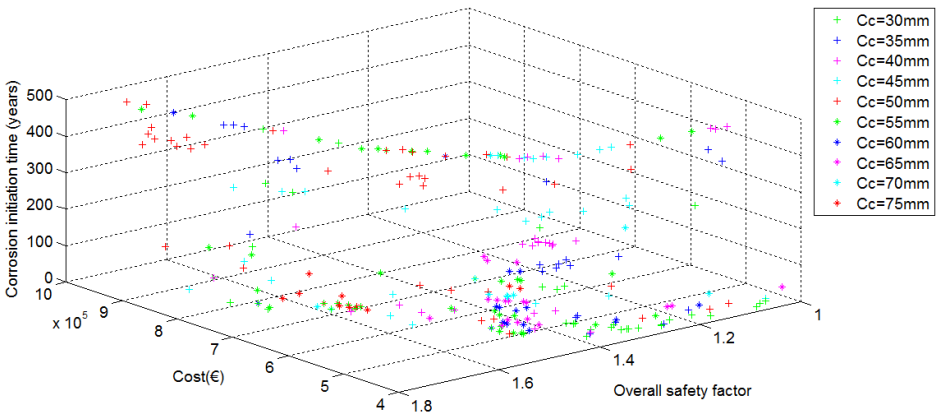

Figure 8.6. Pareto set according to the concrete cover (based on García-Segura et al. (submitted (a)))

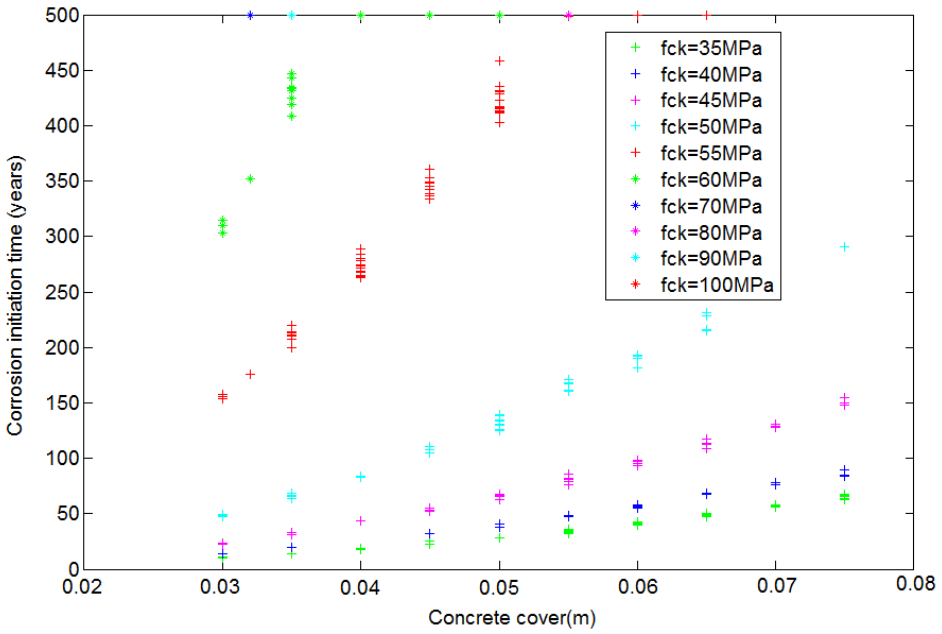

Figure 8.7. Relationship between corrosion initiation time and concrete cover according to the concrete strength (based on García-Segura et al. (submitted (a)))

8.4. Conclusions

This study provides trade-off solutions of post-tensioned concrete box-girder road bridges regarding the cost, the overall safety factor, and the corrosion initiation time. Results show solutions that are initially more expensive but have a longer lifetime and improved safety. Therefore, the designer can select the cheapest solution for a safety and durability target. A multi-objective optimization of a bridge analyzed by finite-elements requires high computing time. This study proposes a methodology to reduce the number of exact evaluations based on ANN.

The methodology implements four stages. In the first step, the ANN is trained by the limit state data of previous evaluations. As the neural network is formed by the input based on the design variables and the output based on the limit state coefficients, the ANN can be trained by the results of another optimization process with different objective functions. The aim is to learn from the relationship between the variables and the limit states, since the bridge analysis and evaluation is the most computationally intensive. The second step combines a multi-objective HS with ANN to obtain an approximate Pareto front, which provides a good search direction. The third step actualizes the Pareto set of solutions through a finite-element analysis, limit state verification, and objective evaluation. Finally, a multi-objective optimization is conducted from the updated Pareto set by exact evaluations.

The results of ANN give values of the coefficient of determination R^2 between 0.912 and 0.999. The results of the second step show the best hypervolume value for the combination of parameters that follow a transition from diversification to intensification. The progressive elimination of the combination of solutions and the random selection achieve the best results. The methodology show a percentage of exact function evaluations of about 37% or 27%, depending on whether or not the training data are considered. This acquires even more importance when the computational time is reduced from about 1500 s when obtaining an exact feasible solution to 4 s when using ANN. Conclusively, findings indicate that ANN is a good tool to reproduce the structure response and reduce the computational cost. Nevertheless, finer models to converge closer to the true Pareto front are needed.

The Pareto front provides a set of optimum bridge solutions between the cost, the overall safety factor, and the corrosion initiation time. Focusing on corrosion initiation time, a good combination of both concrete strength and concrete cover could achieve the durability and cost goals. The effect of increasing the concrete strength is not the same for each concrete grade. For lower concrete grades, this increment hardly increases the corrosion initiation time. Therefore, an increment in concrete strength favors strategies of longer service life targets, while an increment in concrete cover favors strategies of shorter service life targets.

Chapter 9
Maintenance lifetime optimization

9.1. Aim of the study

This study (García-Segura et al., submitted(b)) starts from the results of the previous study (Chapter 8). The multi-objective optimization obtained a set of optimum bridge solutions considering initial cost, overall safety factor and corrosion initiation time. As solutions have different service lives, maintenance actions must be effectively planned throughout the life-cycle of structures to achieve a service life target with the minimum economic, environmental and societal impacts. In this case, a service life target of 150 years is considered. The degradation process due to chloride-induced corrosion reduces the reinforcing steel area. Consequently, structural safety varies with time. A lifetime-reliability-based approach is used to evaluate the structural performance. The maintenance actions delay the damage propagation and extends the life-span. Thus, a maintenance optimization is carried out aimed at minimizing the economic, environmental and societal impacts of the bridge while satisfying the annual reliability target at 4.7 during the bridge service life.

As noted in Section 5.1, the service life prediction of a structure is affected by several uncertainties, like load effect, material properties and damage occurrence and propagation (Frangopol & Kim, 2011). The partial safety factors have been adopted by a great amount of design codes, including the Eurocode, to take into account the uncertainties arising from geometry, material properties, load effects, and design models. During the planning of maintenance actions, stakeholders should also be aware of the uncertainties that are involved in the deterioration process and potential inspections or interventions (Frangopol, 2011). Wisniewski et

al. (2009) stated that a proper consideration of uncertainties can lead to significant economic benefits for both initial design and life-cycle performance. Thus, this study conducts a lifetime reliability-based approach for the optimization of sustainable post-tensioned concrete box-girder road bridges subjected to chloride attack in a coastal zone.

The optimization variables define the maintenance plan in each cross-section surface. The maintenance optimization follows the three pillars of sustainability criteria, i.e. economic, environmental and societal impacts. The economic impact of maintenance actions comes from the material and construction costs arising from the maintenance actions. The environmental impact takes into account the CO_2 emissions derived from the materials and construction activities. The societal impact evaluates the consequences of traffic disruptions during maintenance actions. This study assesses the societal impact according to the economic and environmental consequences of such traffic disruptions. Therefore, two mono-objective optimizations are conducted with costs and CO_2 emissions due to maintenance actions as objectives. A harmony search algorithm is used for the optimization. Finally, the sustainability of PSC box-girder road bridges in a coastal zone is evaluated through the comparison of some important features regarding the life-cycle cost and CO_2 emissions of the initial designs under consideration.

9.2. Definition of the problem

Given

Post-tensioned concrete box-girder road bridge designs from the previous study, as well as the effect of concrete repair on the chloride-induced corrosion.

Goal

Find the optimal time of the first application and the number of applications on surface 1 (t_1 and n_1) and surface 2 (t_2 and n_2), as illustrated in Figure 9.1, so that:

- The economic costs of maintenance actions, which takes into account the direct and indirect maintenance costs, are minimized.
- The CO_2 emissions of maintenance actions, which are caused by the direct and indirect maintenance, are minimized.

Subject to

The annual target reliability index of 4.7. This constrain ensures that the annual reliability index of the bridge is above the threshold during the entire service life.

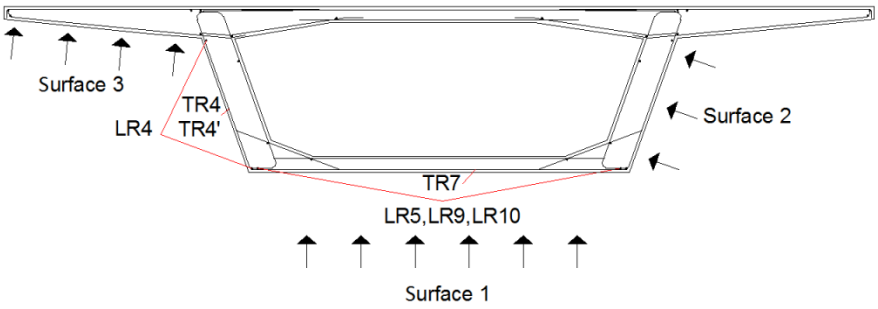

Figure 9.1. Surfaces affected by corrosion propagation (based on García-Segura et al. (submitted(b)))

9.3. Methodology

The methodology used is explained in the following sections. Figure 9.2 shows a flowchart of this methodology. Firstly, several solutions of the Pareto front regarding initial cost, overall safety factor and corrosion initiation time are chosen. These solutions have different levels of safety and durability. A deterioration process analysis is conducted over these solutions. These bridges are subjected to chloride-induced corrosion that reduces the reinforcing steel area. A numerical model is used to reflect the material degradation process. Secondly, the reduction in structural safety due to the corrosion process is evaluated based on reliability indices. To guarantee a good structural performance, a value of 4.7 is considered as reliability threshold at 1-year reference period, as proposed in the Eurocode (European Committee for Standardisation 2002). If reliability index is under this value during the prescribed service life of 150 years, an optimization process is carried out to seek the best maintenance actions to keep the structural reliability above the threshold value. Otherwise, no maintenance is required. Maintenance actions are scheduled as design variables. The objectives reflect the economic, environmental and societal impacts of the maintenance activities. The economic and environmental impacts of maintenance actions consider, respectively, the direct costs and emissions of maintenance applications. The societal impact is evaluated as the costs and emissions of the traffic disruptions during the actions. Therefore, these impacts are evaluated in terms of cost and CO_2 emissions. A mono-objective optimization minimizes the total cost and CO_2 emissions due to maintenance actions while guarantying a structural reliability greater than 4.7. The initial cost and emissions are not considered since the optimal maintenance solutions do not depend on these terms. Finally, once the maintenance is optimized, the life-cycle cost and emissions are calculated. The initial costs and emissions, which include material and construction costs and emissions, are combined with the maintenance cost and emissions. Bridge designs are compared based on the reliability-based life-cycle assessment

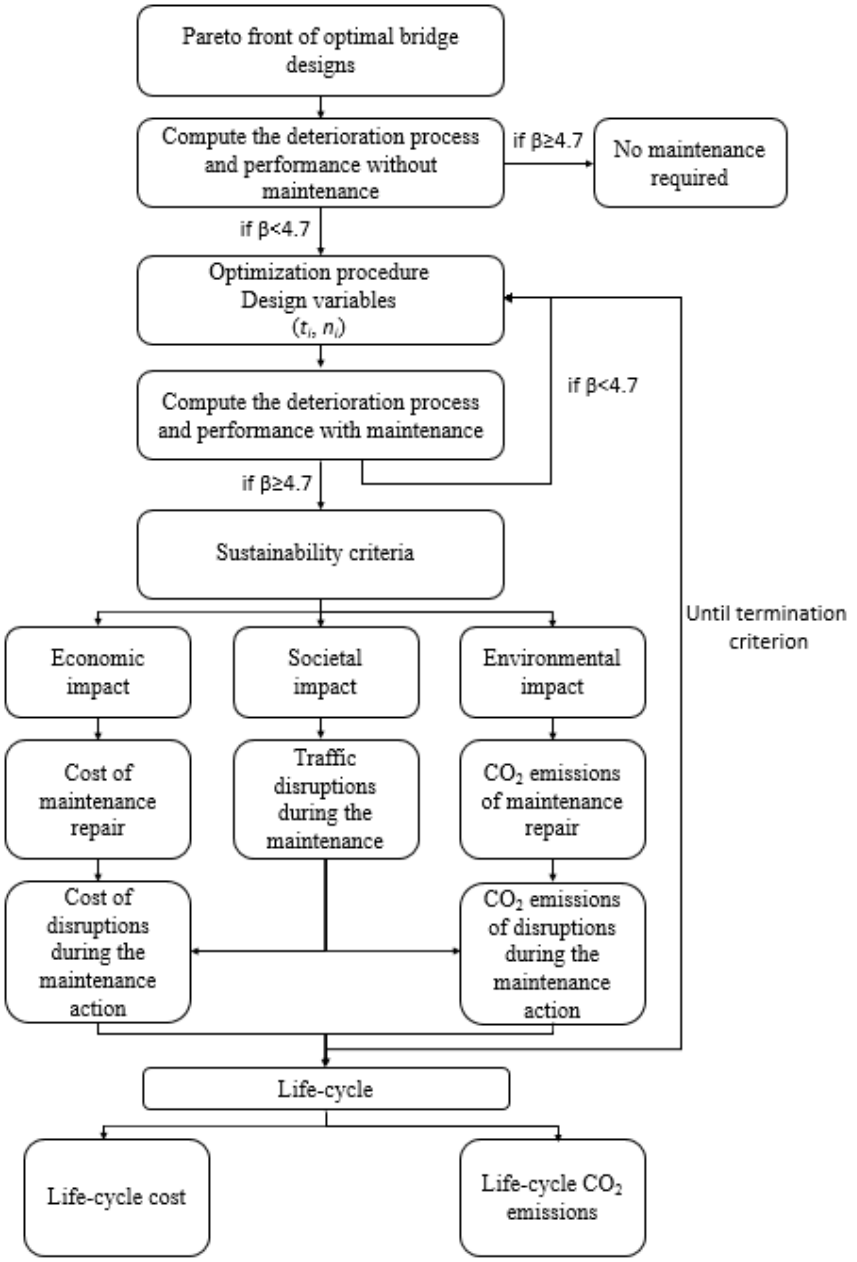

Figure 9.2. Flowchart of the methodology (based on García-Segura et al. (submitted(b)))

9.3.1. *Deterioration process*

The deterioration analysis considers uniform corrosion of the reinforcing steel. The corrosion rate is expressed as a time-dependent variable. This variable is based on the corrosion initiation time and the corrosion rate at the start of corrosion propagation ($i_{corr}(1)$), as shown in the following equations (Vu & Stewart, 2000):

$$i_{corr}(t) = i_{corr}(1) \cdot 0.85 \cdot (t - t_{corr})^{-0.29} \quad \textbf{Equation 9.1}$$

$$i_{corr}(1) = \frac{37.8(1 - w/c)^{-1.64}}{C_c} \quad \textbf{Equation 9.2}$$

$$D_b = D_{b0} - 2 \cdot \int_{T_i}^{t} 0.0116 \cdot i_{corr}(t)dt \quad \textbf{Equation 9.3}$$

The reinforcement diameter decreases after the corrosion initiation time (t_{corr}) according to the assumption of uniform corrosion. Note that 1 μ/cm^2 is equivalent to 0.0116 mm/year. It is considered that the pavement thickness increases the cover of the top slab. As a result, the reinforcement located near this surface is not critical. The bottom surface of the flanges (see Surface 3 in Figure 9.1) barely affects the ultimate limit state. Hence, both the top surface and the bottom surface of the flanges are not considered in the deterioration analysis. Consequently, the corrosion propagation affects mainly the reinforcement located in the bottom slab (surface 1 in Figure 9.1) and the webs (surface 2 in Figure 9.1). The longitudinal and transverse reinforcement beneath surfaces 1 and 2 are considered for the deterioration process. The limit states affected by the reinforcing steel corrosion are explained in Table 9.1.

Table 9.1. Limit states and reinforcement affected by chloride-induced corrosion (based on García-Segura et al. (submitted(b)))

Surface	Reinforcement diameter	Limit state
1	LR_5, LR_9, LR_{10}	Torsion
		Flexure
	TR_7	Transverse flexure
		Torsion
2	LR_4	Torsion
	TR_4, $TR_{4'}$	Transverse flexure
		Torsion
		Shear

9.3.2. *Lifetime performance*

The lifetime performance of the bridge is computed through the reliability indices (β) evaluated by the First Order Second Moment (FOSM) method as follows:

$$p_f = P_r[(R - S) < 0] \quad \textbf{Equation 9.4}$$

$$\beta = -\Phi^{-1}(p_f) \qquad \textbf{Equation 9.5}$$

$$\beta = \frac{\bar{R} - \bar{S}}{\sqrt{\sigma_R^2 + \sigma_S^2}} \qquad \textbf{Equation 9.6}$$

where p_f is the probability of failure; Φ^{-1} is the inverse standard normal cumulative distribution function; R is the generalized structural resistance, S is the generalized action effect; $\bar{R}$ and $\bar{S}$ are, respectively, mean values of R and S; and σ_R and σ_S are the standard deviations of R and S.

Table 9.2 depicts the statistical parameters for material properties and loading variables. A normal distribution describes the uncertainties inherent in concrete and steel properties (Ellingwood et al., 1980). Mean values are calculated considering that characteristic values correspond to the 95th percentile of material strength distributions. The generalized structural resistance is evaluated following the structural code EHE-08 (Fomento, 2008). It is worth noting that no partial safety factors are considered for the resistance evaluation.

Concerning the action effect, the mean value of load effects can be determined by the coefficient of variation (COV) and the characteristic value. The permanent loads are represented by normal distributions and characteristic values correspond to the 50 % quantile (Gulvanessian, 2003). The variable loads are described by Gumbel distributions. According to that, the relation between the characteristic value and the mean annual extreme can be obtained as follows:

$$Q_K = \mu \cdot \left[1 - V\frac{\sqrt{6}}{\pi}[0.577 + ln(-\ln(1-p))]\right] \qquad \textbf{Equation 9.7}$$

where Q_K is the characteristic value; μ is the mean annual extreme; V is the coefficient of variation and p is the probability of being exceeded. The characteristic values for the temperature-gradient effects and traffic load effects are obtained from IAP-11 (Fomento, 2011) and Eurocode (European Committee for Standardisation, 2003a, 2003b). The characteristic value of the temperature-gradient effects load corresponds to an annual probability of being exceeded of 0.02 (European Committee for Standardisation, 2003a). Therefore, p is 0.02 in Eqn. 8.2. The coefficient of variation of the temperature load is 40% based on available measurement data of existing bridges (Crespo-Minguillón & Casas, 1998; Gulvanessian & Holický, 2002). Regarding the traffic load, the annual characteristic value is 90% of the 50-year characteristic value (Sanpaolesi & Croce, 2005). The characteristic value corresponds to a probability of exceedance of 5%. The coefficient of variation for traffic loads is 0.15 (Bouassida et al., 2010; Nowak, 1993).

Table 9.2. Statistical parameters for material properties and loading variables (based on García-Segura et al. (submitted(b)))

Random Variables	Model type
Reinforcing steel strength	Normal (COV=0.098)
Prestressing steel strength	Normal (COV=0.025)
Concrete compressive strength	Normal (COV=0.18)
Concrete tension strength	Normal (COV=0.18)
Permanent	Normal (COV=0.1)
Gradient	Gumbel (COV=0.4)
Traffic load	Gumbel (COV=0.15)

9.3.3. *Design variables*

Four design variables of maintenance optimization are considered: the time of the first application on surface 1 (t_1), the number of applications on surface 1 (n_1), the time of the first application on surface 2 (t_2) and the number of applications on surface 2 (n_2). Both the time interval between applications on surfaces 1 and 2 are considered constant. The time-dependent evolution of the reliability index depends on the values of design variables. This study considers that bridge maintenance is conducted through concrete repair. It consist of removing the old concrete cover and replacing it with repair mortar. As the concrete cover returns to its initial non-contaminated state, it requires a period equal to the corrosion initiation time of the new cover to reach the same status of the structural capacity. Thus, the degradation of the structural capacity is halted for a period equal to the new corrosion initiation time (t_{corr2}). This value depends on the new water cement ratio and the thickness of the cover. This study considers a water cement ratio of 0.4 and a thickness of 30 mm. The new cover has a different corrosion rate. As a result, the structure after concrete repair deteriorates at a different speed.

9.3.4. *Optimization algorithm*

The mono-objective optimization of maintenance actions is conducted by a modified harmony search algorithm. Harmony search, proposed by Geem et al. (2001), establishes an analogy between optimization algorithm and the search for the best musical harmony. The algorithm parameters are: harmony memory size (HMS), harmony memory considering rate (HMCR), pitch adjusting rate (PAR) and the maximum number of improvisations without improvement (IWI). The algorithm is explained in Section 4.5.1. In conventional HS, memory consideration choose each variable from a random HM solution. This study improves the algorithm performance by selecting design variables merely from two random HM solutions. The first two variables, which are related to the maintenance of surface 1, are chosen from one random selection from the HM. The following two variables, which are related to the maintenance of surface 2, are taken from another random

selection. Thus, memory consideration selects the maintenance of each surface from a random HM solution. The calibration process suggested HMS=10, HMCR=0.9, PAR=0.4 and IWI=50.

9.4. Results

Cost and emission objectives are evaluated similarly (see Section 5.3). However, the time effect of economic costs results in different incentives for cost-based and emission-based maintenance optimization. The effect of the discount rate leads to less present value for costs at a later time. According to that, there is an incentive to take maintenance actions as late as possible. In contrast, CO_2 emissions are the same irrespective of the time of maintenance actions. Thus, the number of maintenance actions should be the smallest possible to achieve the minimum CO_2 emissions. Note that an earlier maintenance action may result in a better structural performance. In conclusion, the emission optimization generally favors strategies of earlier maintenance actions, while cost optimization gives incentives to postpone the maintenance actions on both surfaces provided that this does not lead to an increase of required maintenance actions.

The nine representative solutions selected from the Pareto front of initial design optimization are presented in Figure 9.3. These solutions are classified into three levels for the overall safety factor and six levels for the corrosion initiation time. The values of 1.1 and 1.2 mark the limits for the overall safety factor. Regarding the corrosion initiation time, 15, 30, 45, 60 and 75 are the boundary markers. Table 9.3 shows the objective values of these nine solutions and Table 9.4 summarizes the main variables of these Pareto solutions. Table 9.3 summarizes the levels of the overall safety factor and the corrosion initiation time associated to each solution.

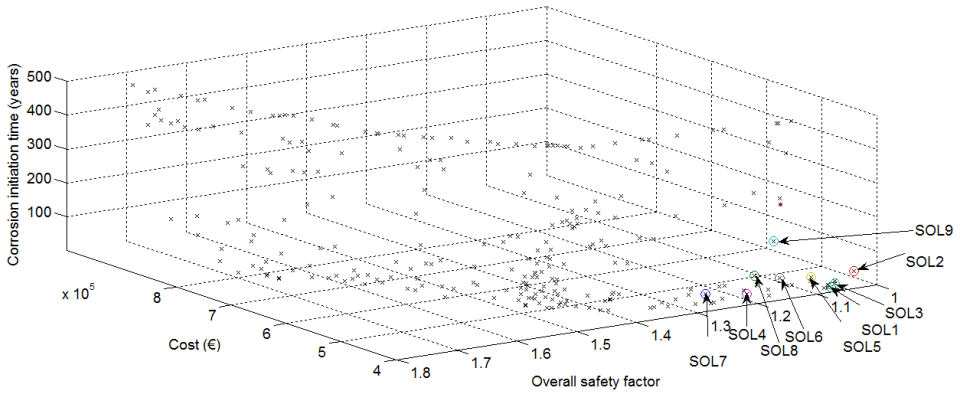

Figure 9.3. Representative solutions of the Pareto optimal set (based on García-Segura et al. (submitted(b)))

Table 9.3. Objective values of Pareto solutions (based on García-Segura et al. (submitted(b)))

	C_{ini} (€)	S	t_{corr} (years)
SOL1	401260.99	1.07 (L1)	10.45 (L1)
SOL2	401399.55	1.03 (L1)	47.41 (L4)
SOL3	401947.90	1.06 (L1)	18.26 (L2)
SOL4	406159.66	1.21 (L3)	23.81 (L2)
SOL5	409807.04	1.10 (L1)	41.04 (L3)
SOL6	416612.17	1.14 (L2)	48.15 (L4)
SOL7	416828.32	1.27 (L3)	35.09 (L3)
SOL8	418635.77	1.18 (L2)	65.68 (L5)
SOL9	423569.85	1.15 (L2)	153.90 (L6)

Table 9.4 shows the depth (h), concrete cover (c_c) and concrete grade (f_{ck}) of these solutions. Besides, Table 9.4 shows the amount of reinforcing steel, concrete and prestressing steel per square meter of deck. Solution 9 (SOL9) has a corrosion initiation time greater than the length of the service life (150 years). Therefore, this solution does not require any maintenance action. The other representative solutions are subjected to an optimization process. This procedure examines the optimum maintenance actions.

Table 9.4. Characteristics of Pareto solutions (based on García-Segura et al. (submitted(b)))

	h (m)	c_c (mm)	f_{ck} (MPa)	Reinforcing steel (kg/m^2 deck)	Concrete (m^3 /m^2 deck)	Prestressing steel (kg/m^2 deck)
SOL1	2.30	30	35	67.10	0.670	21.99
SOL2	2.30	65	35	66.89	0.674	21.98
SOL3	2.30	40	35	70.03	0.665	21.11
SOL4	2.65	30	45	70.44	0.662	19.80
SOL5	2.30	60	35	76.81	0.636	21.10
SOL6	2.60	30	50	72.31	0.678	19.80
SOL7	2.30	55	35	81.36	0.635	21.10
SOL8	2.65	35	50	74.67	0.674	19.80
SOL9	2.55	30	55	78.50	0.638	20.46

Figure 9.4 shows the time-variant evolution of the reliability index of solution SOL1 affected by the transverse reinforcement corrosion. The representative value

of the entire bridge reliability index corresponds to the smallest reliability index. The longitudinal reinforcement is less affected by the chloride attack, as rebars are placed further from the surface. Thanks to this increment in concrete cover, the corresponding limit states are less critical for the structure failure. Figure 9.4 shows that transverse flexure in surface 2 presents the smallest initial reliability index. However, the reliability index regarding the torsion is affected the most by the steel corrosion of transverse reinforcement with respect to surface 2. The reliability index reduces significantly (from 8.6 to 5.5) from t_{corr} to t_2 (year 25). The maintenance application at year 25 delays the deterioration process for about 50 years. This length of time is the one required for the chloride to penetrate through the new concrete cover and to reach the threshold concentration. Overall, two maintenance actions are required for solution SOL1 to finish the service life with a reliability index greater than 4.7.

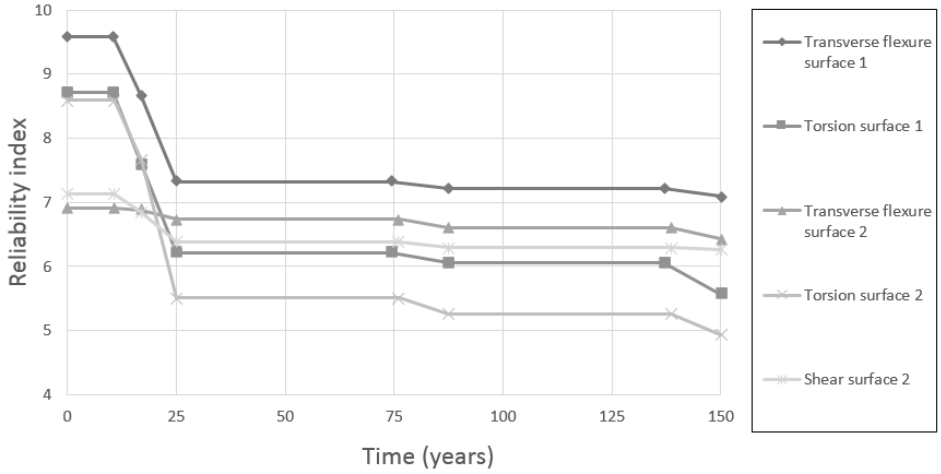

Figure 9.4. Reliability index evolution of the limit states affected by maintenance application (based on García-Segura et al. (submitted(b)))

Table 9.5, 9.6 and 9.7 show the results of cost optimization. Table 9.5 provides the optimum maintenance plan of the representative solutions. It is important to note that most of the solutions present simultaneous maintenance actions for surfaces 1 and 2. Thus, it is advisable to conduct maintenance activities over both surfaces at the same time. These results indicate that maintenance is planned to reduce the societal impact, since the societal impact is halved when the maintenance actions on both surfaces coincide. In addition, the number of maintenance actions should be as small as possible to reduce the economic, environmental and societal impacts. In this regard, the results promote the sustainability.

Results suggest that it is usually cheaper to reduce the total number of maintenance actions even at the price of advancing the first maintenance date. Thus, although the economic costs and CO_2 emissions are optimized separately, both objectives lead to the same number of maintenance actions, and therefore the same amount of CO_2

emissions. Fixing this number of maintenance actions and delaying the first maintenance date, the cost is also minimized. Consequently, cost optimization in general can lead to optimal solutions with respect to CO_2 emissions, and therefore, the following tables show the results of cost optimization.

Table 9.5. Optimum maintenance plan of the eight representative solutions (based on García-Segura et al., (submitted(b)))

	TC (€)	**TE** (kg CO_2)	t_1 (years)	n_1	t_2 (years)	n_2
SOL1	813350	1453093	25	2	25	2
SOL2	532289	1097023	70	1	70	1
SOL3	743009	1449714	35	2	35	2
SOL4	619797	1496228	65	2	65	2
SOL5	621560	1325939	60	1	60	2
SOL6	485022	1163320	105	1	105	1
SOL7	663944	1334575	50	1	50	2
SOL8	468838	1170615	120	1	120	1

Tables 9.6 and 9.7 show, respectively, the mean values of total life-cycle costs and life-cycle emissions. The order of the total life-cycle cost from least to greatest is SOL9, SOL8, SOL6, SOL2, SOL4, SOL5, SOL7, SOL3 and SOL1. This order coincides with the one of the corrosion initiation time, with the exception of the solution SOL4. The findings suggest that, despite a slight increase in the initial cost, the increment in corrosion initiation time generally reduces the life-cycle cost. Comparing SOL4, SOL5 and SOL7, solution SOL4 uses 45MPa concrete with 3 cm of cover, while the other solutions use 35MPa and greater concrete cover. Thus, even SOL4 belongs to a lower level of corrosion initiation time; the increment in concrete strength achieves a better life-cycle performance. This result indicates that, for similar corrosion initiation time, increasing the concrete strength, instead of concrete cover, may reduce the number of required maintenance actions and consequently, lower the life-cycle cost and emissions. In other words, even both the increment in concrete strength and concrete cover results in a better durability level, the increment in concrete strength has better life-cycle results for designs with similar corrosion initiation time.

Concerning the life-cycle emissions, the order of the total life-cycle emissions from least to greatest is SOL9, SOL2, SOL6, SOL8, SOL5, SOL7, SOL3, SOL1 and SOL4. In this case, the order does not follow exactly the one for the corrosion initiation time. The amount of CO_2 emissions due to maintenance depends on the total number of actions, independently of the time of applications. Thus, solutions designed with greater corrosion initiation time, which delay the maintenance actions but do not eliminate it, confer no particular advantage from the environmental point

of view.

On the other hand, the results are compared according to the initial safety level. The findings indicate that safety level has less influence on the life-cycle cost. The safety factor with respect to the critical limit state in initial design do not necessarily govern the life-cycle reliability level due to different deterioration rates. As a result, a bridge design with higher initial safety level does not always guarantee a lower life-cycle cost or emissions.

Table 9.6. Mean life-cycle costs of the nine representative solutions (based on García-Segura et al. (submitted(b)))

	C_{ms1} (€)	C_{ms2} (€)	C_{run} (€)	C_{time} (€)	C_{ini} (€)	TC (€)
SOL1	134628	107392	11045	66598	400966	813350
	39051	31148	3204	19318		
SOL2	55209	44037	4527	27264	401250	532289
SOL3	116330	78369	9046	54643	401870	743009
	37251	25098	2897	17499		
SOL4	53809	60348	5007	30085	406220	619797
	23192	26011	2158	12967		
SOL5	76256	56918	5534.9	33310	410260	621560
		23347	2270.4	13664		
SOL6	24413	27748	2271	13704	416886	485022
SOL7	92540	65389	6753	40347	417120	663944
		24294	2509	14990		
SOL8	18077	20276	1681	10153	418650	468838
SOL9					425710	425710

Table 9.7. Mean life-cycle emissions of the eight representative solutions (based on García-Segura et al. (submitted(b)))

	E_{ms1} (kg CO_2)	E_{ms2} (kg CO_2)	E_{run} (kg CO_2)	E_{ini} (kg CO_2)	TE (kg CO_2)
SOL1	170832	141393	44969	738705	1453093
	170832	141393	44969		
SOL2	171045	141564	44904	739510	1097023
SOL3	177518	130747	44938	743308	1449714
	177518	130747	44938		
SOL4	145803	175193	45038	764160	1496228
	145803	175193	45038		
SOL5	185880	146132	44841	758113	1325939
		146132	44841		
SOL6	145951	177822	44997	794550	1163320
SOL7	185963	141371	44997	775843	1334575
		141371	45030		
SOL8	146359	175847	44963	803446	1170615
SOL9				817966	817966

9.5. Conclusions

This study carries out a maintenance lifetime optimization of a set of alternative trade-off solutions of a bridge design through a probabilistic-based approach. This approach allows designs with longer corrosion initiation time or improved safety level to be compared according to the life-cycle perspective. In this regard, the benefits of designing with different objectives, i.e. the lowest initial costs, the longest corrosion initiation time, or the maximum safety, is analyzed. To that end, several bridge optimized solutions in terms of cost, corrosion initiation time and structural safety are selected. A chloride-induced corrosion process deteriorates the reinforcing steel and decreases the structural capacity. The optimum sustainable maintenance is calculated to maintain the structure reliability over the threshold during the service life. The optimization aims at minimizing the economic, environmental and societal impacts of the bridge. The economic and environmental impact considers the cost and CO_2 emissions due to direct maintenance. The societal impact of traffic disruptions is computed in terms of cost and CO_2 emissions.

The optimization variables control the initial application and the number of maintenance actions. This, in turn, restricts the deterioration of structural performance and the economic, environmental and societal impacts. The time of initial application, together with the discount rate, influences the present cost. Therefore, advancing the first maintenance date, results in a better structural performance but at a greater cost. In contrast, the time of application has no influence on the environmental impact. Thus, the strategy to minimize the maintenance emissions consists of achieving the smallest number of maintenance actions.

Results indicate that cost minimization also results in CO_2 emission optimization. These results are explained by the fact that both emission and cost minimization seek to reduce the total number of maintenance applications. Nevertheless, cost optimization has an additional incentive to delay the first application date. Therefore, fixing the number of maintenance applications and delaying the first maintenance date, the cost is also minimized.

Other important outcome is that the deterioration of each surface is different due to their distinct deterioration conditions. In spite of this, results recommend not adjusting the optimum maintenance over each surface separately. Maintenance actions over all surfaces should be scheduled at the same time to reduce the impact of traffic disruptions imposed on society.

Analyzing the limit states affected by the corrosion, the ones affected by the corrosion of the transverse reinforcement are more critical than the ones associated with the longitudinal reinforcement. In addition, results show that the time-variant reliability must be studied over each limit state, as the initial critical limit state may no longer be relevant when deterioration is considered.

Finally, findings indicate that it is advisable to design for longevity in order to reduce the long-term impacts. Bridge designs with greater corrosion initiation time have greater initial cost. However, this strategy decreases the life-cycle cost. In contrast, designs with higher initial safety level do not always result in a better life-cycle performance. Comparing concrete strength and concrete cover, the increment in concrete strength can give better life-cycle results for designs with similar corrosion initiation time.

Chapter 10
AHP - VIKOR under uncertainty

10.1. Aim of the study

This work raises the issue of decision-making after obtaining a Pareto front from a multi-objective optimization process. A previous study of the author (Yepes et al., 2015a) proposed a method for analyzing and reducing the Pareto optimal set. This method analyzed and filtered the Pareto optimal through random Analytic Hierarchy Process (AHP) pairwise comparison matrices and the three Minkowsky metrics. Finally, the decision-maker's preference was introduced by a pairwise comparison matrix based on conventional AHP method and a preferred solution was selected.

AHP is a decision analysis technique that incorporates expert preferences through pairwise comparisons of the different criteria. Besides, the method has the particularity of measuring the inconsistency from the calculations performed on the pairwise judgment. The decision is accepted if the consistency is verified. Therefore, this method guarantees the consistency of judgments. However, the relative importance between two elements is difficult to be defined by deterministic numbers due to the uncertainty in the behavior of the different elements under consideration (Dabous & Alkass, 2010). This work proposes a modified AHP that takes into account the uncertainty associated to the criteria comparison.

A hybrid multi-criteria decision-making method called AHP-VIKOR under uncertainty is suggested to reduce the set of solutions. This methodology helps experts to assign weights to criteria and study the best solution to different conflict aspects. The methodology proposed starts from a set of optimal solutions. The methodology is applied to the case study of Chapter 8. The multi-objective

optimization considered the objectives of initial cost, overall safety factor and corrosion initiation time. Then, the numerical scale of the pairwise comparisons is extended to an uncertainty range. A triangular distribution represents the decision-maker's preferences with a range of uncertainty associated to the pairwise comparison values. A Monte Carlo simulation is carried out to obtain the AHP values and consequently the weights. Then, the closest solutions to the ideal are obtained by VIKOR method.

10.2. Methodology

AHP is a decision analysis technique that incorporates expert preferences through pairwise comparisons using Saaty´s fundamental scale (Saaty, 1987). This verbal scale is transferred into a numerical scale. Table 10.1 shows the correspondences. Firstly, the decision-making problem is decomposed into a hierarchical model of a goal and the corresponding criteria that are evaluated for their importance to the goal. In this case, the sustainability goal is based on the initial cost, overall safety factor and corrosion initiation time criteria. Then, a matrix is filled by values that represent the relative importance of the compared elements based on their contribution degree to the higher level. To accept an AHP matrix, the consistency of the judgments should be verified. The eigenvector method gives the weights for each criteria (w_j). As said previously, this method has the particularity of measure the inconsistency from the calculations performed on the pairwise judgment. The judgment matrix is considered of acceptable consistency, when the consistency ratio (CR) is smaller than 0.1.

The consistency ratio is evaluated as the ratio CI/RI. The consistency index (CI) is calculated as Equation 10.1 shows:

$$CI = \frac{\lambda_{max} - n}{n - 1} \qquad \textbf{Equation 10.1}$$

where λ_{max} is the maximum eigenvalue of the judgment matrix and n is the order of the matrix. RI is 0.525 for a matrix of order 3.

AHP-VIKOR under uncertainty proposes triangular distributions to represent AHP values. The uncertainty range depends on the sureness of the expert first assessment. Thus, the triangular function is based on two different types of assessments. Figure 10.1 shows the triangular distribution. The top of the triangle (P) is obtained by a conventional AHP assessment using a pairwise. These values are obtained from table 10.1. The bottom length of the triangle (b) is determined by a second assessment, which depends in turn on the first assessment. Table 10.2 provides the uncertainty values (UV) that correspond to each verbal scale of uncertainty. Five verbal scales define the grade of certainty in the first assessment. The uncertainty value depends on P value. This is explained by the fact that judgments that affirm that one element is much important than the other have less uncertainty than others that state same importance.

Table 10.1. Saaty's fundamental scale

Numerical scale (P)	Verbal scale	Explanation
1	Same importance	The two elements make a similar contribution to the criterion.
3	One item moderately more important than another	Judgment and earlier experience favor one element over another.
5	One item significantly more important than another	Judgment and earlier experience strongly favor one element over another
7	One item much more important than another	One element dominates strongly. Its domination is proven in practice.
9	One item very much more important than another.	One element dominates the other with the greatest order or magnitude possible

For example, if experts say that they are certain that one criterion is significantly more important than other criterion, P value is equal to 5 and the UV is 5/3. As the triangle is equilateral, A and B take, respectively, the values 3.33 and 6.66. Note that even the equilateral triangle has the same probability in both sides of the triangle; the matrix values cannot have negative values. Therefore, A and B values take the following points (1/10, 1/9, 1/8, 1/7, 1/6, 1/5, 1/4, 1/3, 1/2, 1, 2, 3, 4, 5, 6, 7, 8, 9, 10). It is considered that there is one unit value between each value. Therefore, the furthest values that can take A and B are 1/10 and 10. This case corresponds to an expert very uncertain that both criteria have the same importance.

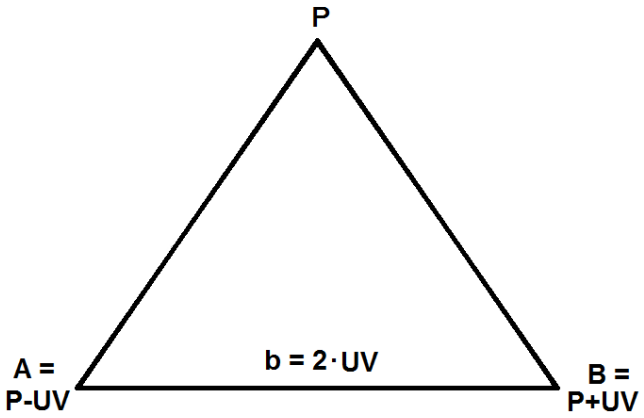

Figure 10.1. Triangle AHP

Table 10.2. Uncertainty value

Numerical scale (UV)	Verbal scale	Explanation
$\frac{0}{3}(10-P)$	Very certain	The expert is very certain that AHP assessment is correct.
$\frac{1}{3}(10-P)$	Certain	The expert is certain that AHP assessment is correct.
$\frac{1}{2}(10-P)$	Fairly certain	The expert is fairly certain that AHP assessment is correct.
$\frac{2}{3}(10-P)$	Uncertain	The expert is uncertain that AHP assessment is correct.
$\frac{3}{3}(10-P)$	Very uncertain	The expert is very uncertain that AHP assessment is correct.

Monte Carlo simulations have been used to get AHP matrices. The weights that correspond to consistent matrices are saved and applied to each criteria. Then, the following step obtains the closest solution to the ideal point according to VIKOR method (Opricovic, 1998). The ideal solution contains the best values of each criterion from the set of solutions. Contrarily, the negative-ideal solution is obtained as the worst values of each criterion. The values Q_j for each solution j are obtained from the Manhattan (L_1) and Tchebycheff (L_∞) metrics, also called S and R metric. The distance L_p from any point to the ideal vector (z*) is evaluated in the p norm as:

$$Q_j = v\frac{S_j - S^*}{S^- - S^*} + (1-v)\frac{R_j - R^*}{R^- - R^*} \qquad \textbf{Equation 10.2}$$

$$L_p = [\sum_{j=1}^{q} \lambda_j^p \left| z_j^* - z_j(x) \right|^p]^{1/p}$$ **Equation 10.3**

$$L_\infty = \lim_{p\to\infty} L_p = \max_{j=1,\ldots,q} \lambda_j \left| z_j^* - z_j(x) \right|$$ **Equation 10.4**

$$\lambda_j = w_j / \delta_j = \frac{w_j}{(z_j^* - z_j^-)}$$ **Equation 10.5**

where S^* and R^* are the best values and S^- and R^- are the worst values of the Manhattan (L_1) and Tchebycheff (L_∞) metrics, $z_j(x)$, j = 1, …, q are the criteria considered in the problem, $z^* = (z_1^*,\ldots,z_q^*)$ is the ideal solution, $z^- = (z_1^-,\ldots,z_q^-)$ is the negative-ideal solution and λ_j (j = 1, …, q) are the normalized weights associated with the criteria. Therefore, the weights obtained from the previous step (w_j) are normalized. The parameter v is introduced as weight of the strategy of the maximum group utility. This study considers v =0.5.

10.3. Results

AHP-VIKOR under uncertainty is applied to the set of optimal solutions obtained in the case study of Chapter 8. Cost, corrosion initiation time, and overall safety criteria are compared through the pairwise comparison. Note that an overall safety factor of one implies a strict compliance with the code. As all of the solutions have an overall safety factor greater than one, the minimum safety level required by the code is guaranteed. On this basis, the pairwise comparison between overall safety and the other criteria are carried out.

A set of experts can be consulted using Delphi (Dalkey & Helmer, 1963) process to get a consensus for each pairwise comparison. The following case is exposed:

- Experts are certain that cost is very much more important than overall safety factor. This leads to P=9, UV=1/3, A=8.66, B=9.33.
- Experts are certain that initiation of corrosion is much more important than overall safety factor. This leads to P=7, UV=3/3, A=6, B=8.
- Experts are fairly certain that cost is moderately more importance than initiation of corrosion. This leads to P=3, UV=7/2, A=1/2.5, B=6.5.

These comparisons lead to the following matrix. The points [A,P,B] of the triangular distributions are shown. Random values are obtained based on each distribution. The histograms of weights that correspond to consistent matrices are represented in Figures 10.2-4. It is important to mention that 10,000 different consistent AHP matrices are calculated to generate a histogram of each criterion.

	Cost	Overall safety	Corrosion initiation
Cost	1	[8.66,9,9.33]	[1/2.5,3,6.5]
Overall safety	[1/9.33,1/9,1/8.66]	1	[1/8,1/7,1/6]
Corrosion initiation	[1/6.5,1/3,2.5]	[6,7,8]	1

The histogram of cost weights (Figure 10.2) takes values between 0.4674 and 0.5987. The median value is 0.5486. Regarding the corrosion initiation (Figure 10.3), weights acquire values between 0.3421 and 0.4773. In this case, the median value is 0.3934. Experts considered that overall safety factor would be of less importance than the other criteria. For this reason, weights of overall safety criterion take smaller values compared to cost and corrosion initiation time (see Figure 10.4). Weights adopt values between 0.0541 and 0.0636, where the median is 0.0579.

Analyzing Figure 10.2 and 10.3, the difference between the median values of cost and corrosion initiation time weights is 0.15. The weight of corrosion initiation time is higher than that of cost in few cases. Note that some ranges of values for one criteria may lead to inconsistent matrices. Therefore, it may happen that increasing the uncertainty range the results do not change. The histograms provide decision makers with a range of weights that can be assigned to the criteria and ensure consistency between them.

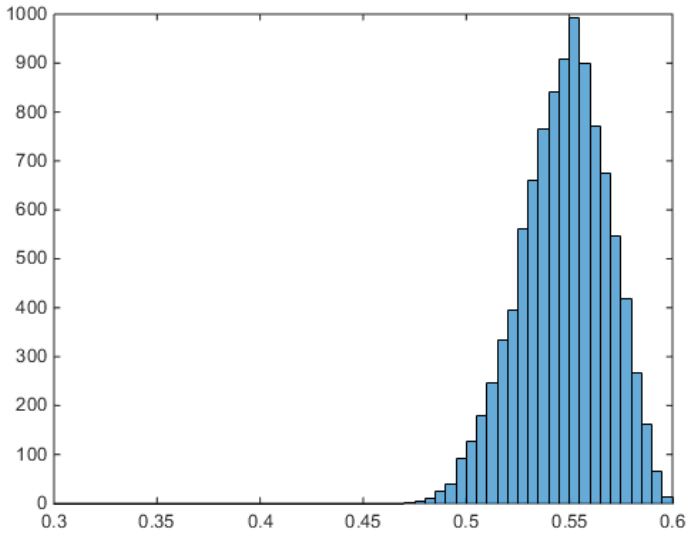

Figure 10.2. Histogram of cost weight

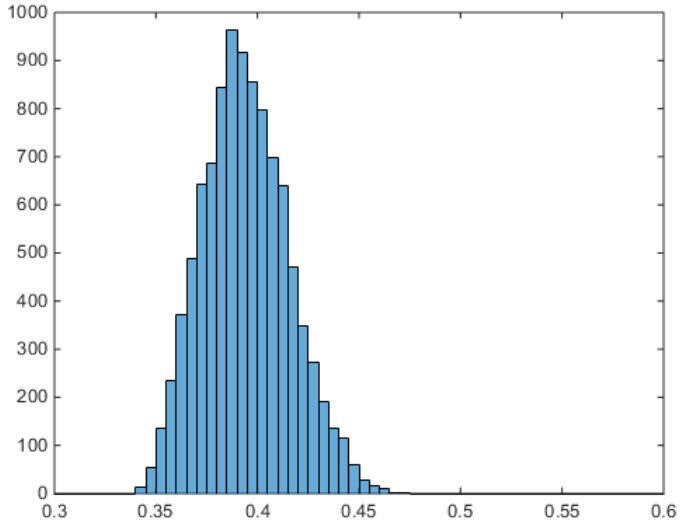

Figure 10.3. Histogram of corrosion initiation time weight

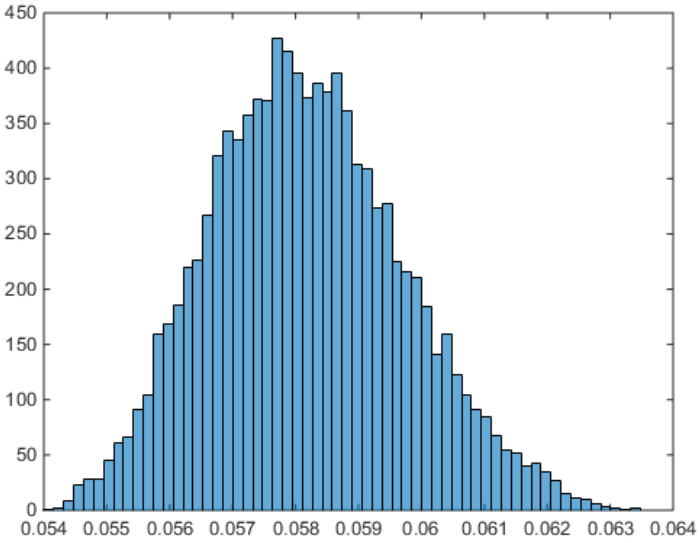

Figure 10.4. Histogram of overall safety factor weight

The next step obtains the best solutions by VIKOR method. These results depend on the weights. Each iteration leads to one set of weights. These weights, in turn, give rise to different distances from each solution to the ideal one. VIKOR method ranks these solutions based on Equation 10.2. Finally, one solution is selected as the

preferred one. After 10000 iterations, the set of Pareto front is reduced to a set of preferred solutions. The final solutions are those that can be selected within the stated uncertainty of the criteria comparison.

In this case, three bridge designs are the preferred solutions (P1-P3). Table 10.3 summarizes the percentages, the objective values and the concrete strength. The preferred solution P1 has been selected in 77.84% cases. This solution takes the highest value of corrosion initiation time. P2 and P3 also acquire 500 years of corrosion initiation time. The results suggest that the increment in durability, evaluated as initiation of corrosion, does not entail big cost differences. Therefore, the solutions with higher durability are preferred. Comparing P1 and the cheapest solution, this solution is 8% more expensive but increases the safety and the corrosion time in 14% and 4684%. The other solutions (P2 and P3) are 6% more expensive and improve the safety in 6%. Figure 10.5 shows the Pareto set, the ideal solution and the preferred solutions P1-P3. It is worth noting that P2 is the second cheapest solution with 500 years of service life. P3 and P1 are the following solutions in this order.

Table 10.3. Preferred solutions of AHP-VIKOR under uncertainty

	Percentage (%)	Cost (€)	Initiation of corrosion (years)	Overall safety factor	fck (MPa)
P1	77.84	432716	500	1.22	55
P2	12.34	425233	500	1.14	60
P3	9.82	425549	500	1.14	60

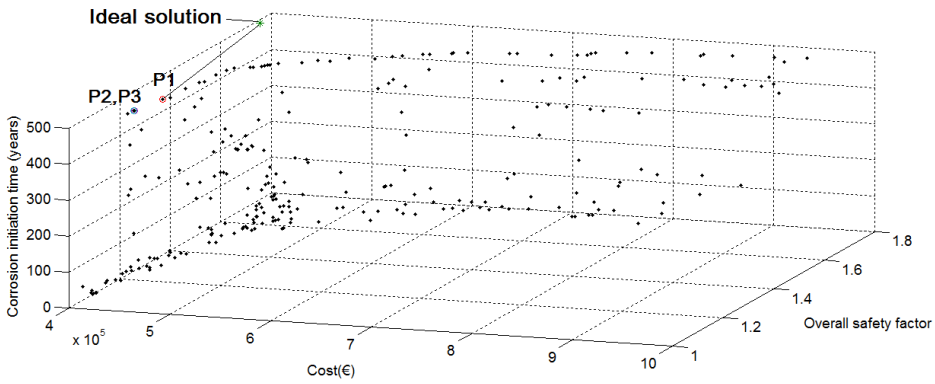

Figure 10.5. Preferred solutions of AHP-VIKOR under uncertainty

In addition, limit values for the criteria can be set. For example, if cost is limited to 500000 € the Pareto set is reduced to one preferred solution shown in Figure 10.6. In this case, preferred solution is P4, regardless of the weight selected. Table 10.4

shows the information about the solution. P4 is the cheapest solution that has an initiation of corrosion of 500 years. Note that the limitation reduces the cost range, and consequently, solutions acquire more normalized cost. Thus, there is an incentive to take smaller cost values. The same approach can be applied to other criteria. The method is open to any limitation that the decision-maker considers.

Table 10.4. Preferred solutions of AHP-VIKOR under uncertainty when limiting cost

	Percentage (%)	Cost (€)	Initiation of corrosion (years)	Overall safety factor	fck (MPa)
P4	100	424641	500	1.12	60

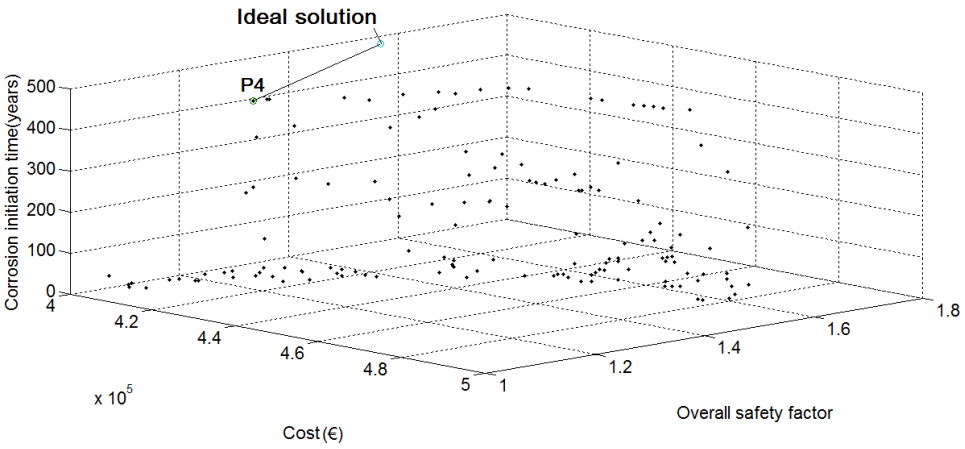

Figure 10.6. Preferred solutions of AHP-VIKOR under uncertainty when limiting cost

10.4. Conclusions

Decision support systems can help engineers and decision-makers to evaluate and select the most appropriate solution by rational techniques. This study proposes a method called AHP-VIKOR under uncertainty to reduce the set of optimum solutions of a multi-objective optimization to preferred solutions. Ex-pert preferences are introduced by a modified AHP that takes into account the decision-maker uncertainty. AHP allows the decision-maker to perform consist judgments regarding the relative importance among the criteria. A triangular distribution represents the pairwise comparison values. AHP under uncertainty provides the weights that are later used in VIKOR method to select the closest solution to the ideal point. Preferred solutions are obtained by Monte Carlo simulations.

The triangular distribution is defined by the top of the triangle and bottom length. The top point coincides with the conventional AHP assessment, in which a numerical scale define the relative importance of the compared elements. The

bottom length is determined by a second assessment that takes into account the uncertainty of the first assessment. The numerical scale of the uncertainty depends on the P value. Theoretically, the reason behind this is that judgments that affirm that one element dominates the other have less uncertainty than others that state same importance. The triangular distributions lead to different weights for each criterion. It is worth noting that some values may lead to inconsistent matrices and therefore, the corresponding weights are not allowed. For this reason, the triangular distributions help decision-maker's to assign weights to criteria according to their preferences and ensuring consistency.

This methodology has been applied to the set of optimal solutions regarding cost, corrosion initiation time, and overall safety factor. The preferred solutions are obtained with a percentage of being selected. For this case study, solutions with the highest corrosion initiation time are preferred, since the durability improvement does not entail big cost differences. Regarding cost, the case considers that cost is much more important than overall safety factor. This results in cheap preferred solutions. Besides, the method is open to any limitation that the decision-maker considers. If a cost threshold is taken into account, solutions acquire more normalized cost. Thus, there is an incentive to take the cheapest solution with the longest life-span.

Chapter 11
Conclusions and future work

11.1. Conclusions

This dissertation has investigated the efficient design of post-tensioned concrete box-girder road bridges through a multi-objective optimization based on sustainable criteria. Several previous studies were conducted to examine the use of blended cements, the importance of carbonation as a CO_2 capture and durability, the concrete reuse, the use of self-compacting concrete, the sustainable designs of precast-prestressed concrete U-beam road bridges, the relationship between cost and CO_2, as well as the embodied energy, the sustainable designs of post-tensioned concrete box-girder pedestrian bridges, the heuristic algorithms, and the decision-making techniques to analyze and reduce the Pareto optimal set. The outcomes were the basis for the following main statements. The multi-objective optimization was formulated based on economic, environmental, durability and safety criteria. A computer support tool that uses a commercial software for finite-element analysis carried out the automatic design process.

The design of post-tensioned concrete box-girder road bridges was firstly studied regarding cost, CO_2 emissions, and overall safety factor. A case study of a three-span continuous box-girder road bridge located in a coastal region was proposed. Results showed that both cost and CO_2 emission objective lead to a reduction in material consumption and therefore, the cost optimization is a good approach to achieve an environmentally friendly design. The analysis of the Pareto front provided valuable knowledge about the most efficient variables to improve safety with the minimum cost and CO_2 emissions. Given that cost and emissions were closely related, the challenge was translated to converting the structural safety and durability constraints to objectives. This approach allowed us to find multiple trade-

off solutions that hardly increased the cost and achieved improved safety and durability. Besides, the efficiency of increasing concrete strength and concrete cover to lengthen service life were highlighted. The optimum set was later compared according to the life-cycle perspective. The optimum maintenance plans were obtained based on its initial level of safety and durability. This is consistent with the argument that the deterioration process may cause a reduction in structural safety. This study allowed us to analyze the benefits of designing for longevity and safety. A sustainable maintenance lifetime optimization was conducted using a probabilistic-based approach. The maintenance plan aimed at minimizing the economic, environmental and societal impacts while satisfying the reliability target during a life-span. Finally, the life-cycle costs and emissions between alternatives were compared.

In parallel, a meta-model for the constraints prediction was developed for reducing the computational cost. Artificial neural networks were integrated in a multi-objective optimization. ANNs were trained to predict the structural response in terms of the limit states based on the design variables, without the need to analyze the bridge response. The multi-objective harmony search was improved by several intensification-diversification strategies. Diversification arranged better in the design space exploration without trapping in local optima, and intensification improved the convergence. Finally, a decision-making technique called AHP-VIKOR under uncertainty was proposed to reduce the set of solutions to preferred solutions. This method allows the decision-maker to introduce easily the preferences to a specific criterion subject to uncertainty while guaranteeing the consistency of the judgments.

11.1.1. *General conclusions*

The general conclusions obtained from this thesis are:

- Cost and CO_2 emission minimization lead to a bridge design that favors the structural efficiency by minimizing the amount of materials. The inclusion of the safety objective highlights the robustness of each variable to the efficient design. Results indicate that a bridge designer can improve the safety with a little cost increment by choosing the correct design variables. Regarding the initiation of corrosion, a good combination of both concrete strength and concrete cover can achieve the durability and cost goals.
- The depth, thickness of the bottom slab, post-tensioned steel, and longitudinal reinforcement are the main variables providing the flexure capacity. However, the increment in thickness of the top slab and external flange is not advisable to improve structural safety, since it results in an additional weight. To provide better transverse flexure performance, the thickness of the internal flange section is increased and the flange length is decreased. The slope of the web inclination can be constant, since both the depth and the web inclination width increase in parallel to improve safety. The thickness of the web is not the most economic variable to increase

shear resistance. Instead, the reinforcing steel is increased.

- The use of high-strength concrete may lead to a reduction in depth or amount of reinforcement. Nevertheless, the constraints regarding serviceability limit states and minimum amount of reinforcement restrict these variables. Thus, high-strength concrete grade is not the best solution to improve safety. However, this outcome changes when the life-cycle is taken into account. An increment in concrete strength favors strategies of higher service life targets. On one hand, it results in a higher corrosion initiation time. On the other hand, the increment in concrete strength has better life-cycle results for designs with similar corrosion initiation time, compared to concrete cover increment.
- A durability-conscious initial design is especially beneficial for life-cycle performance. Designs with longer corrosion initiation time result in lower life-cycle cost even it entails higher initial cost. However, a higher initial safety level does not always lead to a better life-cycle performance.

11.1.2. *Specific conclusions*

The specific conclusions drawn from the studies are:

- The use of blended cements entails a reduction in carbon capture and service life due to carbonation. In spite of this, blended cements decrease the emissions per year. Self-compacting concrete is not advisable for an environmental point of view. In terms of cost, few differences are obtained between conventional vibrated and self-compacting concrete.
- It is crucial to reuse concrete as concrete gravel-filling material to achieve a complete carbonation and reduce the CO_2 emissions.
- The relationship between criteria is studied for the post-tensioned concrete box-girder road bridges. The relation between cost and CO_2 emissions shows that decreasing the cost by one Euro reduces the CO_2 emissions by 2.34 kg. As for the overall safety factor, three linear relations between cost and this objective are obtained. To increase the overall safety factor from 1 to 1.4, costs increase in 12.5%. After this point, the safety improvement results are more expensive. Regarding the corrosion initiation time, small cost increments are needed to lengthen it.
- The decompression limit state is a restricting limit state and conditions variables such as depth and number of strands. As these variables also influence flexure, this limit state is not restrictive until the overall safety factor reaches 1.4.
- The relationship between cost and CO_2 is maintained regardless of the safety level. Therefore, cost optimization is a good approach for emission minimization.
- In structures with narrow feasible space, cost and emission are particularly likely to present good relationship. However, reinforced concrete

structures with wider feasible space, usually prefer larger sections, greater amount of concrete, less steel and concrete with lower strength from an environmental point of view.

- An increment in concrete strength favors strategies of longer service life targets, while an increment in concrete cover favors strategies of shorter service life targets.
- Optimal maintenance plan is that with fewer maintenance actions that repair all deteriorating surfaces simultaneously. Despite the distinctive deterioration of individual members, due to their different deterioration conditions, results recommend not to adjust the optimum maintenance over each surface separately. Maintenance actions should be scheduled at the same time to reduce the impact of traffic disruptions.
- Generally, maintenance cost optimization also results in CO_2 emission minimization. This is attributed to the fact that both emission and cost objective seek to reduce the total number of maintenance applications. However, cost optimization has an additional incentive to delay the first application date. Thus, fixing the number of maintenance applications and delaying the first maintenance date, the cost is also minimized.
- ANN is a good tool to predict the structure response, provide a good search direction and reduce the computational cost. However, finer models to converge closer to the true Pareto front are needed at the end.
- The transition from diversification to intensification, which progressively eliminates the combination of solutions and the random selection, improves the algorithm performance.
- AHP-VIKOR under uncertainty method reduced the Pareto set to few preferred solutions. For this case study, the cheapest solutions with the longest life-spans are preferred, since the durability improvement does not entail big cost differences.

11.2. Future work

The pursuit of a sustainable bridge design is very extensive and cannot be covered by a single dissertation. Other different scenarios should be explored. Under this premise, some recommendations on future work can be given.

Regarding the design, the case study can be extended to longer and wider bridges. In this context, other designs that include varying depth, different phases of prestressing, multiple-cell box-girder and transverse prestressing, can be studied. As for the construction methods, the following cases can also be considered: precast segmental balanced cantilever bridge, cast-in-place segmental balanced cantilever bridges, precast segmental span-by-span bridges, precast segmental progressive cantilever bridges, and incremental launching, among others. The use of other materials for both the initial design and maintenance could also be studied and

included in the optimization problem.

In case the scope is extended, the number of criteria should also be increased. Esthetics, constructability, job creation and construction risk could be considered to make a better comparison between alternatives. In addition, other interesting line of research is the analysis of the bridge capacity to absorb the demand in bridge network management. Considering this principle, traffic disruption would be avoided, and therefore, its economic and environmental consequences. To deal with multiple conflicting criteria, a decision-making tool that considers the consequences of each criterion to the sustainable goal would be helpful.

References

Abu Dabous, S., & Alkass, S. (2010). A multi-attribute ranking method for bridge management. *Engineering, Construction and Architectural Management*, *17*(3), 282–291. http://doi.org/10.1108/09699981011038079

Aghdaie, M. H., Zolfani, S. H., & Zavadskas, E. K. (2012). Prioritizing constructing projects of municipalities based on AHP and COPRAS-G: A case study about footbridges in Iran. *The Baltic Journal of Road and Bridge Engineering*, *7*(2), 145–153. http://doi.org/10.3846/bjrbe.2012.20

Aguilar, R. J., Movassaghi, K., Brewer, J. A., & Porter, J. C. (1973). Computerized optimization of bridge structures. *Computers & Structures*, *3*(3), 429–442. http://doi.org/10.1016/0045-7949(73)90089-8

Aïtcin, P. C. (2000). Cements of yesterday and today. *Cement and Concrete Research*, *30*(9), 1349–1359. http://doi.org/10.1016/S0008-8846(00)00365-3

Akin, A., & Saka, M. P. (2015). Harmony search algorithm based optimum detailed design of reinforced concrete plane frames subject to ACI 318-05 provisions. *Computers & Structures*, *147*, 79–95. http://doi.org/10.1016/j.compstruc.2014.10.003

Alberdi, R., & Khandelwal, K. (2015). Comparison of robustness of metaheuristic algorithms for steel frame optimization. *Engineering Structures*, *102*, 40–60. http://doi.org/10.1016/j.engstruct.2015.08.012

Alberdi, R., Murren, P., & Khandelwal, K. (2015). Connection topology optimization of steel moment frames using metaheuristic algorithms. *Engineering Structures*, *100*, 276–292. http://doi.org/10.1016/j.engstruct.2015.06.014

Alcalá González, J. (2009). *Optimización heurística económica de tableros de puentes losa pretensados*. Universitat Politècnica de València.

Alia, O. M., & Mandava, R. (2011). The variants of the harmony search algorithm: an overview. *Artificial Intelligence Review*, *36*(1), 49–68. http://doi.org/10.1007/s10462-010-9201-y

Angst, U., Elsener, B., Larsen, C. K., & Vennesland, Ø. (2009). Critical chloride content in reinforced concrete — A review. *Cement and Concrete Research*, *39*(12), 1122–1138. http://doi.org/10.1016/j.cemconres.2009.08.006

Ardeshir, A., Mohseni, N., Behzadian, K., & Errington, M. (2014). Selection of a bridge construction site using Fuzzy Analytical Hierarchy Process in Geographic Information System. *Arabian Journal for Science and Engineering*, *39*(6), 4405–4420. http://doi.org/10.1007/s13369-014-1070-2

Ates, S. (2011). Numerical modelling of continuous concrete box girder bridges considering construction stages. *Applied Mathematical Modelling*, *35*(8), 3809–3820. http://doi.org/10.1016/j.apm.2011.02.016

Balali, V., Mottaghi, A., Shoghli, O., & Golabchi, M. (2014). Selection of appropriate material, construction technique, and structural system of bridges by use of multicriteria decision-making method. *Transportation Research Record: Journal of the Transportation Research Board*, *2431*, 79–87. http://doi.org/10.3141/2431-11

Barandica, J. M., Fernández-Sánchez, G., Berzosa, Á., Delgado, J. A., & Acosta, F. J. (2013). Applying life cycle thinking to reduce greenhouse gas emissions from road projects. *Journal of Cleaner Production*, *57*, 79–91. http://doi.org/10.1016/j.jclepro.2013.05.036

Barr, A. S., Sarin, S. C., & Bishara, A. G. (1989). Procedure for structural optimization. *ACI Structural Journal*, *86*(5), 524–531.

BEDEC. Institute of Construction Technology of Catalonia. Barcelona, Spain. Available at www.itec.cat (August 10, 2014).

Behnamian, J., Zandieh, M., & Fatemi Ghomi, S. M. T. (2009). Parallel-machine scheduling problems with sequence-dependent setup times using an ACO, SA and VNS hybrid algorithm. *Expert Systems with Applications*, *36*(6), 9637–9644. http://doi.org/10.1016/j.eswa.2008.10.007

Bertolini, L., Elsener, B., Pedeferri, P., & Polder, R. B. (2004). *Corrosion of Steel in Concrete: Prevention, Diagnosis, Repair*. Weinheim: Wiley-VCH.

Beume, N., Naujoks, B., & Emmerich, M. (2007). SMS-EMOA: Multiobjective selection based on dominated hypervolume. *European Journal of Operational Research*, *181*(3), 1653–1669. http://doi.org/10.1016/j.ejor.2006.08.008

Blum, C., Puchinger, J., Raidl, G. R., & Roli, A. (2011). Hybrid metaheuristics in combinatorial optimization: A survey. *Applied Soft Computing*, *11*(6), 4135–4151. http://doi.org/10.1016/j.asoc.2011.02.032

Bond, D. (1975). An examination of the automated design of prestressed concrete bridge decks by computer. *Proceedings of the Institution of Civil Engineers*, *59*(4), 669–697. http://doi.org/10.1680/iicep.1975.3634

Bonet, J. L., Romero, M. L., Miguel, P. F., & Fernandez, M. A. (2004). A fast stress integration algorithm for reinforced concrete sections with axial loads and biaxial bending. *Computers & Structures*, *82*(2), 213–225.

http://doi.org/10.1016/j.compstruc.2003.10.009

Börjesson, P., & Gustavsson, L. (2000). Greenhouse gas balances in building construction: wood versus concrete from life-cycle and forest land-use perspectives. *Energy Policy*, *28*(9), 575–588. http://doi.org/10.1016/S0301-4215(00)00049-5

Bouassida, Y., Bouchon, E., Crespo, P., Croce, P., Davaine, L., Denton, S., … G., T. (2010). Bridge design to Eurocodes- Worked examples. In A. Athanasopoulou, M. Poljansek, A. Pinto, G. Tsionis, & S. Denton (Eds.), *Workshop "Bridge design to Eurocodes."* Vienna, 4 - 6 Octobe 2010: Luxe mbourg: Publications Office of the European Union.

Butlin, J. (1989). Our common future. By World commission on environment and development. (London, Oxford University Press, 1987, pp.383). *Journal of International Development*, *1*(2), 284–287. http://doi.org/10.1002/jid.3380010208

Caglar, N., Elmas, M., Yaman, Z. D., & Saribiyik, M. (2008). Neural networks in 3-dimensional dynamic analysis of reinforced concrete buildings. *Construction and Building Materials*, *22*(5), 788–800. http://doi.org/10.1016/j.conbuildmat.2007.01.029

Cai, H., & Aref, A. J. (2015). A genetic algorithm-based multi-objective optimization for hybrid fiber reinforced polymeric deck and cable system of cable-stayed bridges. *Structural and Multidisciplinary Optimization*, *52*(3), 583–594. http://doi.org/10.1007/s00158-015-1266-4

Camp, C. V., & Assadollahi, A. (2013). CO2 and cost optimization of reinforced concrete footings using a hybrid big bang-big crunch algorithm. *Structural and Multidisciplinary Optimization*, *48*(2), 411–426. http://doi.org/10.1007/s00158-013-0897-6

Camp, C. V., & Assadollahi, A. (2015). CO2 and cost optimization of reinforced concrete footings subjected to uniaxial uplift. *Journal of Building Engineering*, *3*, 171–183. http://doi.org/10.1016/j.jobe.2015.07.008

Camp, C. V., & Huq, F. (2013). CO2 and cost optimization of reinforced concrete frames using a big bang-big crunch algorithm. *Engineering Structures*, *48*, 363–372. http://doi.org/10.1016/j.engstruct.2012.09.004

Cao, M. S., Pan, L. X., Gao, Y. F., Novák, D., Ding, Z. C., Lehký, D., & Li, X. L. (2015). Neural network ensemble-based parameter sensitivity analysis in civil engineering systems. *Neural Computing and Applications*, 1–8. http://doi.org/10.1007/s00521-015-2132-4

Carbonell, A., González-Vidosa, F., & Yepes, V. (2011, April). Design of reinforced concrete road vaults by heuristic optimization. http://doi.org/10.1016/j.advengsoft.2011.01.002

Castañón, A. M., García-Granda, S., Guerrero, A., Lorenzo, M. P., & Angulo, S. (2015). Energy and environmental savings via optimisation of the production process at a Spanish cement factory. *Journal of Cleaner Production*, *98*, 47–52. http://doi.org/10.1016/j.jclepro.2014.03.028

Chang, S. T., & Gang, J. Z. (1990). Analysis of cantilever decks of thin-walled box girder bridges. *Journal of Structural Engineering*, *116*(9), 2410–2418. http://doi.org/10.1061/(ASCE)0733-9445(1990)116:9(2410)

Chatterjee, S., Sarkar, S., Hore, S., Dey, N., Ashour, A. S., & Balas, V. E. (2016). Particle swarm optimization trained neural network for structural failure prediction of multistoried RC buildings. *Neural Computing and Applications*. http://doi.org/10.1007/s00521-016-2190-2

Chen, S. M., Sarosh, A., & Dong, Y. F. (2012). Simulated annealing based artificial bee colony algorithm for global numerical optimization. *Applied Mathematics and Computation*, *219*(8), 3575–3589. http://doi.org/10.1016/j.amc.2012.09.052

Cheung, M. M., Zhao, J., & Chan, Y. B. (2009). Service life prediction of RC bridge structures exposed to chloride environments. *Journal of Bridge Engineering*, *14*(3), 164–178. http://doi.org/10.1061/(ASCE)1084-0702(2009)14:3(164)

Chiu, C. K., & Lin, Y. F. (2014). Multi-objective decision-making supporting system of maintenance strategies for deteriorating reinforced concrete buildings. *Automation in Construction*, *39*, 15–31. http://doi.org/10.1016/j.autcon.2013.11.005

Coello, C. (1994). Uso de Algoritmos Genéticos para el Diseño Optimo de Armaduras. In *Congreso Nacional de Informática "Herramientas Estratégicas para los Mercados Globales"* (pp. 290–305). Fundación Arturo Rosenblueth, México, D.F.

Coello, C. A. C. (2002). Theoretical and numerical constraint-handling techniques used with evolutionary algorithms: a survey of the state of the art. *Computer Methods in Applied Mechanics and Engineering*, *191*(11-12), 1245–1287. http://doi.org/10.1016/S0045-7825(01)00323-1

Coello, C. A. C., Lamont, G. B., & Veldhuizen, D. A. Van. (2006). *Evolutionary algorithms for solving multi-objective problems*. Springer-Verlag New York, Inc.

Cohn, M. Z., & Dinovitzer, A. S. (1994). Application of Structural Optimization. *Journal of Structural Engineering*, *120*(2), 617–650. http://doi.org/10.1061/(ASCE)0733-9445(1994)120:2(617)

Collins, F. (2010). Inclusion of carbonation during the life cycle of built and recycled concrete: influence on their carbon footprint. *The International Journal of Life Cycle Assessment*, *15*(6), 549–556. http://doi.org/10.1007/s11367-010-0191-4

Colorni, A., Dorigo, M., & Maniezzo, V. (1991). Distributed optimization by ant colonies. In *Proceeding of ECALEuropean Conference on Artificial Life* (pp. 134–142). Paris: Elsevier.

Crespo-Minguillón, C., & Casas, J. R. (1998). Fatigue reliability analysis of prestressed concrete bridges. *Journal of Structural Engineering*, *124*(12), 1458–1466. http://doi.org/10.1061/(ASCE)0733-9445(1998)124:12(1458)

Dalkey, N., & Helmer, O. (1963). An experimental application of the Delphi method to the use of experts. *Managment Science*, *9*(3), 458–467.

de Albuquerque, A. T., El Debs, M. K., & Melo, A. M. C. (2012). A cost optimization-

based design of precast concrete floors using genetic algorithms. *Automation in Construction*, *22*, 348–356. http://doi.org/10.1016/j.autcon.2011.09.013

de Medeiros, G. F., & Kripka, M. (2014). Optimization of reinforced concrete columns according to different environmental impact assessment parameters. *Engineering Structures*, *59*, 185–194. http://doi.org/10.1016/j.engstruct.2013.10.045

Deb, K. (2011). Multi-objective optimisation using evolutionary algorithms: An introduction. In L. Wang, A. H. C. Ng, & K. Deb (Eds.), *Multi-objective Evolutionary Optimisation for Product Design and Manufacturing* (pp. 3–34). London: Springer London. http://doi.org/10.1007/978-0-85729-652-8

Deb, K., & Nain, P. K. S. (2007). An evolutionary multi-objective adaptive meta-modeling procedure using artificial neural networks. In S. Yang, Y.-S. Ong, & Y. Jin (Eds.), *Evolutionary Computation in Dynamic and Uncertain Environments* (Vol. 51, pp. 297–322). Berlin, Heidelberg: Springer Berlin Heidelberg. http://doi.org/10.1007/978-3-540-49774-5

Degertekin, S. O., Saka, M. P., & Hayalioglu, M. S. (2008). Optimal load and resistance factor design of geometrically nonlinear steel space frames via tabu search and genetic algorithm. *Engineering Structures*, *30*(1), 197–205. http://doi.org/10.1016/j.engstruct.2007.03.014

Dodoo, A., Gustavsson, L., & Sathre, R. (2009). Carbon implications of end-of-life management of building materials. *Resources, Conservation and Recycling*, *53*(5), 276–286. http://doi.org/10.1016/j.resconrec.2008.12.007

Dong, Y., Frangopol, D. M., & Saydam, D. (2013). Time-variant sustainability assessment of seismically vulnerable bridges subjected to multiple hazards. *Earthquake Engineering & Structural Dynamics*, *42*(10), 1451–1467. http://doi.org/10.1002/eqe.2281

DRIZORO S.A.U. Productos para la Construcción. Available at http://www.drizoro.com/ (December 21, 2015)

Dueck, G., & Scheuer, T. (1990). Threshold accepting: A general purpose optimization algorithm appearing superior to simulated annealing. *Journal of Computational Physics*, *90*(1), 161–175. http://doi.org/10.1016/0021-9991(90)90201-B

Dutta, R., Ganguli, R., & Mani, V. (2011). Swarm intelligence algorithms for integrated optimization of piezoelectric actuator and sensor placement and feedback gains. *Smart Materials and Structures*, *20*(10), 105018.

ECO-SERVE. (2004). *Baseline report on sustainable aggregate and concrete industries in Europe*. European Commission, Hellerup.

Elkington, J. (1998). *Cannibals with forks: the triple bottom line of 21st century business*. New Society Publishers.

Ellingwood, B., Galambos, T. V, MacGregor, J. G., & Cornell, C. A. (1980). *Development of a probability based load criterion for American National Standard A58: building code requirements for minimum design loads in buildings and other structures, volume 13*. U.S. Department of Commerce, National Bureau

of Standards.

Emmerich, M., & Naujoks, B. (2004). Metamodel assisted multiobjective optimisation strategies and their application in airfoil design. In I. C. Parmee (Ed.), *Adaptive Computing in Design and Manufacture VI* (pp. 249–260). London: Springer London. http://doi.org/10.1007/978-0-85729-338-1

Erdem, H. (2010). Prediction of the moment capacity of reinforced concrete slabs in fire using artificial neural networks. *Advances in Engineering Software*, *41*(2), 270–276. http://doi.org/10.1016/j.advengsoft.2009.07.006

European Commission.Climate Action. The EU Emissions Trading System (EU ETS).

European Committee for Standardisation. (2003a). *EN 1991-1-5:2003. Eurocode 1: Actions on structures - Part 1-5: General actions - Thermal actions*.

European Committee for Standardisation. (2003b). *EN 1991-2:2003. Eurocode 1: Actions on structures-Part 2: Traffic loads bridges*.

European Committee for Standardisation. (2005). *EN1992-2:2005. Eurocode 2: Design of concrete structures- Part 2: Concrete Bridge-Design and detailing rules.* Brussels.

European Federation of Concrete Admixtures Associations. (2006). Environmental Product Declaration (EPD) for Normal Plasticising admixtures. Available at www.efca.info/downloads/324 ETG Plasticiser EPD.pdf

Felkner, J., Chatzi, E., & Kotnik, T. (2013). Interactive particle swarm optimization for the architectural design of truss structures. In *2013 IEEE Symposium on Computational Intelligence for Engineering Solutions (CIES)* (pp. 15–22). IEEE. http://doi.org/10.1109/CIES.2013.6611723

Fernandes, B., Titus, M., Nims, D. K., Ghorbanpoor, A., & Devabhaktuni, V. (2012). Field test of magnetic methods for corrosion detection in prestressing strands in adjacent box-beam bridges. *Journal of Bridge Engineering*, *17*(6), 984–988.

Fernandez-Ceniceros, J., Fernandez-Martinez, R., Fraile-Garcia, E., & Martinez-de-Pison, F. J. (2013). Decision support model for one-way floor slab design: A sustainable approach. *Automation in Construction*, *35*, 460–470. http://doi.org/10.1016/j.autcon.2013.06.002

fib. International Federation for Structural Concrete. Task Group 3.8, T. for green concrete structures. (2012). *Guidelines for green concrete structures*. International Federation for Structural Concrete. Task Group 3.8, Technologies for green concrete structures.

Flower, D. J. M., & Sanjayan, J. G. (2007). Green house gas emissions due to concrete manufacture. *The International Journal of Life Cycle Assessment*, *12*(5), 282–288. http://doi.org/10.1065/lca2007.05.327

Fomento M. (2000). *New overpasses: general concepts*. Madrid, Spain: Ministerio de Fomento.

Fomento, M. (2008). *EHE-08: Code on structural concrete*. Madrid, Spain: Ministerio

de Fomento.

Fomento, M. (2011). *IAP-11: Code on the actions for the design of road bridges*. Madrid, Spain: Ministerio de Fomento.

Fonseca, C. M., & Fleming, P. J. (1993). Genetic algorithms for multiobjective optimization: Formulation, discussion and generalization, 416–423.

Fraile-Garcia, E., Ferreiro-Cabello, J., Martinez-Camara, E., & Jimenez-Macias, E. (2016). Optimization based on life cycle analysis for reinforced concrete structures with one-way slabs. *Engineering Structures*, *109*, 126–138. http://doi.org/10.1016/j.engstruct.2015.12.001

Frangopol, D. M. (2011). Life-cycle performance, management, and optimisation of structural systems under uncertainty: accomplishments and challenges. *Structure and Infrastructure Engineering*, *7*(6), 389–413. http://doi.org/10.1080/15732471003594427

Frangopol, D. M., & Kim, S. (2011). Service life, reliability and maintenance of civil structures. In L. S. Lee & V. Karbari (Eds.), *Service Life Estimation and Extension of Civil Engineering Structures* (pp. 145–178). Elsevier. http://doi.org/10.1533/9780857090928.2.145

Frangopol, D. M., & Soliman, M. (2016). Life-cycle of structural systems: recent achievements and future directions. *Structure and Infrastructure Engineering*, *12*(1), 1–20. http://doi.org/10.1080/15732479.2014.999794

Galán, I. (2011). *Carbonatación del hormigón: combinación de CO2. Dissertation*. Universidad Complutense de Madrid.

Galan, I., Andrade, C., Mora, P., & Sanjuan, M. A. (2010). Sequestration of CO2 by concrete carbonation. *Environmental Science & Technology*, *44*(8), 3181–6. http://doi.org/10.1021/es903581d

Gandomi, A. H., Kashani, A. R., Roke, D. A., & Mousavi, M. (2015). Optimization of retaining wall design using recent swarm intelligence techniques. *Engineering Structures*, *103*, 72–84. http://doi.org/10.1016/j.engstruct.2015.08.034

García-Segura, T., & Yepes, V. (2016). Multiobjective optimization of post-tensioned concrete box-girder road bridges considering cost, CO2 emissions, and safety. *Engineering Structures*, *125*, 325–336. http://doi.org/10.1016/j.engstruct.2016.07.012

García-Segura, T., Yepes, V., & Alcalá, J. (2014a). Life cycle greenhouse gas emissions of blended cement concrete including carbonation and durability. *The International Journal of Life Cycle Assessment*, *19*(1), 3–12. http://doi.org/10.1007/s11367-013-0614-0

García-Segura, T., Yepes, V., & Alcalá, J. (2014b). Sustainable design using multiobjective optimization of high-strength concrete I-beams. In *The 2014 International Conference on High Performance and Optimum Design of Structures and Materials HPSM/OPTI* (Vol. 137, pp. 347–358). Ostend, Belgium. http://doi.org/10.2495/HPSM140331

García-Segura, T., Yepes, V., Alcalá, J., & Pérez-López, E. (2015). Hybrid harmony search for sustainable design of post-tensioned concrete box-girder pedestrian bridges. *Engineering Structures*, *92*, 112–122. http://doi.org/10.1016/j.engstruct.2015.03.015

García-Segura, T., Yepes, V., & Frangopol, D. M. Multi-objective design of post-tensioned concrete road bridges using artificial neural networks. [submitted(a)].

García-Segura, T., Yepes, V., Frangopol, D. M., & Yang, D. Y. Lifetime reliability-based optimization of post-tensioned box-girder bridges. [submitted(b)].

García-Segura, T., Yepes, V., Martí, J. V., & Alcalá, J. (2014). Optimization of concrete I-beams using a new hybrid glowworm swarm algorithm. *Latin American Journal of Solids and Structures*, *11*(7), 1190–1205. http://doi.org/10.1590/S1679-78252014000700007

Gartner, E. (2004). Industrially interesting approaches to "low-CO2" cements. *Cement and Concrete Research*, *34*(9), 1489–1498. http://doi.org/10.1016/j.cemconres.2004.01.021

Geem, Z. W., Kim, J. H., & Loganathan, G. V. (2001). A new heuristic optimization algorithm: Harmony search. *Simulation*, *76*(2), 60–68.

Giannakoglou, K. C. (2002). Design of optimal aerodynamic shapes using stochastic optimization methods and computational intelligence. *Progress in Aerospace Sciences*, *38*(1), 43–76. http://doi.org/10.1016/S0376-0421(01)00019-7

Glover, F. (1989). Tabu Search—Part I. *ORSA Journal on Computing*, *1*(3), 190–206. http://doi.org/10.1287/ijoc.1.3.190

Glover, F. (1990). Tabu Search—Part II. *ORSA Journal on Computing*, *2*(1), 4–32. http://doi.org/10.1287/ijoc.2.1.4

González, M. J., & García Navarro, J. (2006). Assessment of the decrease of CO2 emissions in the construction field through the selection of materials: Practical case study of three houses of low environmental impact. *Building and Environment*, *41*(7), 902–909. http://doi.org/10.1016/j.buildenv.2005.04.006

Gulvanessian, H. (2003). SAKO Report. Appendix B – Investigation by BRE (using reliability analysis) of the alternative combination rules provided in EN 1990 "Basis of Structural Design."

Gulvanessian, H., & Holický, M. (2002). Reliability based calibration of Eurocodes considering a steel member. In *JCSS Workshop on reliability based code calibration*. Zurich.

Guo, T., Sause, R., Frangopol, D. M., & Li, A. (2010). Time-Dependent Reliability of PSC Box-Girder Bridge Considering Creep, Shrinkage, and Corrosion. *http://dx.doi.org/10.1061/(ASCE)BE.1943-5592.0000135*.

Guzmán, S., Gálvez, J. C., & Sancho, J. M. (2011). Cover cracking of reinforced concrete due to rebar corrosion induced by chloride penetration. *Cement and Concrete Research*, *41*(8), 893–902.

http://doi.org/10.1016/j.cemconres.2011.04.008

Hadzima-Nyarko, M., Nyarko, E. K., & Morić, D. (2011). A neural network based modelling and sensitivity analysis of damage ratio coefficient. *Expert Systems with Applications*, *38*(10), 13405–13413. http://doi.org/10.1016/j.eswa.2011.04.169

Hajipour, V., Rahmati, S. H. A., Pasandideh, S. H. R., & Niaki, S. T. A. (2014). A multi-objective harmony search algorithm to optimize multi-server location–allocation problem in congested systems. *Computers & Industrial Engineering*, *72*, 187–197. http://doi.org/10.1016/j.cie.2014.03.018

Hambly; E.C. (1991). Bridge Deck Behaviour, Second Edition. CRC Press.

Hancock, B. J., & Mattson, C. A. (2013). The smart normal constraint method for directly generating a smart Pareto set. *Structural and Multidisciplinary Optimization*, *48*(4), 763–775. http://doi.org/10.1007/s00158-013-0925-6

Hare, W., Nutini, J., & Tesfamariam, S. (2013). A survey of non-gradient optimization methods in structural engineering. *Advances in Engineering Software*, *59*, 19–28. http://doi.org/10.1016/j.advengsoft.2013.03.001

Hidrodemolición. Available at http://www.hidrodemolicion.com/ (December 21, 2015)

Holland, J. (1975). *Adaptation in Natural and Artificial Systems*. *University of Michigan Press, Ann Arbor, USA,*.

Houst, Y. F., & Wittmann, F. H. (2002). Depth profiles of carbonates formed during natural carbonation. *Cement and Concrete Research*, *32*(12), 1923–1930. http://doi.org/10.1016/S0008-8846(02)00908-0

Hwang, C. L., & Yoon, K. (1981). Multiple Attributes Decision Making Methods and Applications. *Springer, Berlin Heidelberg*.

International Organization for Standardization; (2006). *ISO 14040:2006 - Environmental management -- Life cycle assessment -- Principles and framework*. Geneva, Switzerland.

Ishac, I. I., & Smith, T. R. G. (1985). Approximations for Moments in Box Girders. *Journal of Structural Engineering*, *111*(11), 2333–2342. http://doi.org/10.1061/(ASCE)0733-9445(1985)111:11(2333)

Izquierdo López, D. (2002). *Bases de diseño para un tratamiento probabilista de los procesos de corrosión de la armadura en el hormigón*. Universidad Poltécnica de Madrid.

Jakiel, P., & Fabianowski, D. (2015). FAHP model used for assessment of highway RC bridge structural and technological arrangements. *Expert Systems with Applications*, *42*(8), 4054–4061. http://doi.org/10.1016/j.eswa.2014.12.039

Jato-Espino, D., Castillo-Lopez, E., Rodriguez-Hernandez, J., & Canteras-Jordana, J. C. (2014). A review of application of multi-criteria decision making methods in construction. *Automation in Construction*, *45*, 151–162. http://doi.org/10.1016/j.autcon.2014.05.013

Jefatura del Estado. (2005). *Ley 1/2005, de 9 de marzo, por la que se regula el régimen del comercio de derechos de emisión de gases de efecto invernadero.BOE-A-2005-3941*.

Jiang, L., Lin, B., & Cai, Y. (2000). A model for predicting carbonation of high-volume fly ash concrete. *Cement and Concrete Research*, *30*(5), 699–702. http://doi.org/10.1016/S0008-8846(00)00227-1

Joshi, P. K., Sharma, P. C., Upadhyay, S., & Sharma, S. (2004). Multi objective fuzzy decision making approach for selection of type of caisson for bridge foundation. *Indian Journal Pure Application Mathematics*.

Karaboga, D., & Basturk, B. (2008). On the performance of artificial bee colony (ABC) algorithm. *Applied Soft Computing*, *8*(1), 687–697. http://doi.org/10.1016/j.asoc.2007.05.007

Kaveh, A., & Shakouri Mahmud Abadi, A. (2010). Cost optimization of a composite floor system using an improved harmony search algorithm. *Journal of Constructional Steel Research*, *66*(5), 664–669. http://doi.org/10.1016/j.jcsr.2010.01.009

Kendall, A., Keoleian, G. A., & Helfand, G. E. (2008). Integrated life-cycle assessment and life-cycle cost analysis model for concrete bridge deck applications. *Journal of Infrastructure Systems*, *14*(3), 214–222. http://doi.org/10.1061/(ASCE)1076-0342(2008)14:3(214)

Kennedy, J., & Eberhart, R. (1995). Particle swarm optimization. In *Proceedings of ICNN'95 - International Conference on Neural Networks* (Vol. 4, pp. 1942–1948). IEEE. http://doi.org/10.1109/ICNN.1995.488968

Kim, S., Frangopol, D. M., & Soliman, M. (2013). Generalized probabilistic framework for optimum inspection and maintenance planning. *Journal of Structural Engineering*, *139*(3), 435–447. http://doi.org/10.1061/(ASCE)ST.1943-541X.0000676

Kirkpatrick, S., Gelatt, C. D., & Vecchi, M. P. (1983). Optimization by simulated annealing. *Science*, *220*(4598), 671–680.

Koumousis, V. K., & Arsenis, S. J. (1998). Genetic Algorithms in Optimal Detailed Design of Reinforced Concrete Members. *Computer-Aided Civil and Infrastructure Engineering*, *13*(1), 43–52. http://doi.org/10.1111/0885-9507.00084

Kripka, M., & Chamberlain Pravia, Z. M. (2013). Cold-formed steel channel columns optimization with simulated annealing method. *Structural Engineering and Mechanics*, *48*(3), 383–394. http://doi.org/10.12989/sem.2013.48.3.383

Krishnanand, K. N., & Ghose, D. (2009). Glowworm swarm optimisation: a new method for optimising multi-modal functions. *International Journal of Computational Intelligence Studies*, *1*(1), 93–119.

Lagaros, N. D., Fragiadakis, M., Papadrakakis, M., & Tsompanakis, Y. (2006). Structural optimization: A tool for evaluating seismic design procedures.

Engineering Structures, *28*(12), 1623–1633. http://doi.org/10.1016/j.engstruct.2006.02.014

Lagerblad, B. (2005). *Carbon dioxide uptake during concrete life cycle – State of the art*. Swedish Cement and Concrete Research Institute.

Leber, I., & Blakely, F. A. (1956). Some effects of carbon dioxide on mortars and concrete. *Journal of American Concrete Institute*, *53*(9), 295–308.

Lee, K. M., Lee, Y. B., Shim, C. S., & Park, K. L. (2010). Bridge information models for construction of a concrete box-girder bridge. *http://dx.doi.org/10.1080/15732471003727977*.

Lee, K. M., Cho, H. N., & Cha, C. J. (2006). Life-cycle cost-effective optimum design of steel bridges considering environmental stressors. *Engineering Structures*, *28*(9), 1252–1265. http://doi.org/10.1016/j.engstruct.2005.12.008

Li, L. J., Huang, Z. B., & Liu, F. (2009). A heuristic particle swarm optimization method for truss structures with discrete variables. *Computers & Structures*, *87*(7-8), 435–443. http://doi.org/10.1016/j.compstruc.2009.01.004

Liao, T. W., Egbelu, P. J., Sarker, B. R., & Leu, S. S. (2011). Metaheuristics for project and construction management – A state-of-the-art review. *Automation in Construction*, *20*(5), 491–505. http://doi.org/10.1016/j.autcon.2010.12.006

Lippiatt, B. C. (1999). Selecting Cost-Effective Green Building Products: BEES Approach. *Journal of Construction Engineering and Management*, *125*(6), 448–455.

Liu, C., DeWolf, J. T., & Kim, J. H. (2009). Development of a baseline for structural health monitoring for a curved post-tensioned concrete box–girder bridge. *Engineering Structures*, *31*(12), 3107–3115. http://doi.org/10.1016/j.engstruct.2009.08.022

Liu, M., & Frangopol, D. M. (2005). Multiobjective maintenance planning optimization for deteriorating bridges considering condition, safety, and life-cycle cost. *Journal of Structural Engineering*, *131*(5), 833–842. http://doi.org/10.1061/(ASCE)0733-9445(2005)131:5(833)

Liu, S., Tao, R., & Tam, C. M. (2013). Optimizing cost and CO2 emission for construction projects using particle swarm optimization. *Habitat International*, *37*, 155–162. http://doi.org/10.1016/j.habitatint.2011.12.012

Lounis, Z., & Cohn, M. Z. (1993). Optimization of precast prestressed concrete bridge girder systems. *PCI Journal*, *38*(4), 60–78.

Luo, Q. F., & Zhang, J. L. (2011). Hybrid Artificial Glowworm Swarm Optimization Algorithm for Solving Constrained Engineering Problem. *Advanced Materials Research*, *204-210*, 823–827. http://doi.org/10.4028/www.scientific.net/AMR.204-210.823

Luo, Q. Z., Li, Q. S., & Tang, J. (2002). Shear lag in box girder bridges. *http://dx.doi.org/10.1061/(ASCE)1084-0702(2002)7:5(308)*.

Madhkhan, M., Kianpour, A., & Torki Harchegani, M. E. (2013). Life-cycle cost optimization of prestressed simple-span concrete bridges with simple and spliced girders. *IJST, Transactions of Civil Engineering*, *37*, 53–66.

Martí, J. V., Gonzalez-Vidosa, F., Yepes, V., & Alcalá, J. (2013). Design of prestressed concrete precast road bridges with hybrid simulated annealing. *Engineering Structures*, *48*, 342–352. http://doi.org/10.1016/j.engstruct.2012.09.014

Martí, J. V., Yepes, V., & González-Vidosa, F. (2015). Memetic algorithm approach to designing precast-prestressed concrete road bridges with steel fiber reinforcement. *Journal of Structural Engineering*, *141*(2), 04014114. http://doi.org/10.1061/(ASCE)ST.1943-541X.0001058

Martí, J. V., García-Segura, T., & Yepes, V. (2016). Structural design of precast-prestressed concrete U-beam road bridges based on embodied energy. *Journal of Cleaner Production*, *120*, 231–240. http://doi.org/10.1016/j.jclepro.2016.02.024

Martínez, F. J., González-Vidosa, F., & Hospitaler, a. (2011). A parametric study of piers for motorway bridge viaducts. *Revista Internacional de Metodos Numericos Para Calculo Y Diseno En Ingenieria*, *27*(6), 236–250. http://doi.org/10.1016/j.rimni.2011.07.004

Martinez-Martin, F. J., Gonzalez-Vidosa, F., Hospitaler, A., & Yepes, V. (2012). Multi-objective optimization design of bridge piers with hybrid heuristic algorithms. *Journal of Zhejiang University: Science A*, *13*(6), 420–432. http://doi.org/10.1631/jzus.A1100304

Martínez-Martín, F. J., González-Vidosa, F., Hospitaler, A., & Yepes, V. (2013). A parametric study of optimum tall piers for railway bridge viaducts. *Structural Engineering and Mechanics*, *45*(6), 723–740.

Marti-Vargas, J. R., Ferri, F. J., & Yepes, V. (2013). Prediction of the transfer length of prestressing strands with neural networks. *Computers and Concrete*, *12*(2), 187–209. http://doi.org/10.12989/cac.2013.12.2.187

Mattson, C. A., Mullur, A. A., & Messac, A. (2004). Smart Pareto filter: obtaining a minimal representation of multiobjective design space. *Engineering Optimization*, *36*(6), 721–740. http://doi.org/10.1080/0305215042000274942

McGee, R. (1999). Modeling of durability performance of Tasmanian bridges. In R. Melchers & S. M.G (Eds.), *Applications of statistics and probability: civil engineering, reliability and risk analysis* (pp. 297–306). Rotterdam: A.A. Balkema.

Mentrasti, L. (1991). Torsion of box girders with deformable cross sections. *Journal of Engineering Mechanics*, *117*(10), 2179–2200. http://doi.org/10.1061/(ASCE)0733-9399(1991)117:10(2179)

Miller, D., Doh, J. H., & Mulvey, M. (2015). Concrete slab comparison and embodied energy optimisation for alternate design and construction techniques. *Construction and Building Materials*, *80*, 329–338. http://doi.org/10.1016/j.conbuildmat.2015.01.071

Moon, D. Y., Sim, J., & Oh, H. (2005). Practical crack control during the construction of precast segmental box girder bridges. *Computers & Structures*, *83*(31-32), 2584–2593. http://doi.org/10.1016/j.compstruc.2005.05.001

Moscato, P. (1989). *On evolution, search, optimization, genetic algorithms and martial arts: Towards memetic algorithms,. Caltech Concurrent Computation Program (report 826)*. Caltech, Pasadena, California, USA.

Murren, P., & Khandelwal, K. (2014). Design-driven harmony search (DDHS) in steel frame optimization. *Engineering Structures*, *59*, 798–808. http://doi.org/10.1016/j.engstruct.2013.12.003

Neves, L. A. C., Frangopol, D. M., & Petcherdchoo, A. (2006). Probabilistic lifetime-oriented multiobjective optimization of bridge maintenance: combination of maintenance types. *Journal of Structural Engineering*, *132*(11), 1821–1834. http://doi.org/10.1061/(ASCE)0733-9445(2006)132:11(1821)

Neves, L. C., & Frangopol, D. M. (2005). Condition, safety and cost profiles for deteriorating structures with emphasis on bridges. *Reliability Engineering & System Safety*, *89*(2), 185–198. http://doi.org/10.1016/j.ress.2004.08.018

Nigdeli, S. M., Bekdas, G., Kim, S., & Geem, Z. W. (2015). A novel harmony search based optimization of reinforced concrete biaxially loaded columns. *Structural Engineering and Mechanics*, *54*(6), 1097–1109. http://doi.org/10.12989/sem.2015.54.6.1097

Nowak, A. S. (1993). Live load model for highway bridges. *Structural Safety*, *13*(1-2), 53–66. http://doi.org/10.1016/0167-4730(93)90048-6

Oficemen. (2012). *Annual report of Spanish cement sector 2012*. *Annual report of Spanish cement sector 2012*. Available at www.oficemen.com/Uploads/docs/Anuario 2012(1).pdf (September 1, 2014)

Opricovic, S. (1998). Multicriteria Optimization of Civil Engineering Systems. *Faculty of Civil Engineering, Belgrade*.

Opricovic, S., & Tzeng, G. H. (2004). Compromise solution by MCDM methods: A comparative analysis of VIKOR and TOPSIS. *European Journal of Operational Research*, *156*(2), 445–455. http://doi.org/10.1016/S0377-2217(03)00020-1

Ortiz-Rodriguez, O., Castells, F., & Sonnemann, G. (2009). Sustainability in the construction industry: A review of recent developments based on LCA. *Construction and Building Materials*, *23*(1), 28–39. http://doi.org/10.1016/j.conbuildmat.2007.11.012

Pade, C., & Guimaraes, M. (2007). The CO2 uptake of concrete in a 100 year perspective. *Cement and Concrete Research*, *37*(9), 1348–1356. http://doi.org/10.1016/j.cemconres.2007.06.009

Papadakis, V. G., Roumeliotis, A. P., Fardis, M. N., & Vagenas, C. G. (1996). Mathematical modelling of chloride effect on concrete du-rability and protection measures. In R. K. Dhir & M. R. Jones (Eds.), *Concrete repair, rehabilitation and protection* (pp. 165–174). London: E&FN Spon.

Papadakis, V. G., Vayenas, C. G., & Fardis, M. N. (1991). Fundamental Modeling and Experimental Investigation of Concrete Carbonation. *ACI Materials Journal*, *88*(4), 363–373.

Park, H., Kwon, B., Shin, Y., Kim, Y., Hong, T., & Choi, S. (2013). Cost and CO2 emission optimization of steel reinforced concrete columns in high-rise buildings. *Energies*, *6*(11), 5609–5624. http://doi.org/10.3390/en6115609

Pavelski, L. M., Almeida, C. P., & Goncalves, R. A. (2012). Harmony search for multi-objective optimization. In *2012 Brazilian Symposium on Neural Networks* (pp. 220–225). IEEE. http://doi.org/10.1109/SBRN.2012.19

Paya, I., Yepes, V., González-Vidosa, F., & Hospitaler, A. (2008). Multiobjective optimization of reinforced concrete building frames by simulated annealing. *Computer-Aided Civil and Infrastructure Engineering*, *23*(8), 596–610. http://doi.org/10.1111/j.1467-8667.2008.00561.x

Paya-Zaforteza, I., Yepes, V., González-Vidosa, F., & Hospitaler, A. (2010). On the Weibull cost estimation of building frames designed by simulated annealing. *Meccanica*, *45*(5), 693–704. http://doi.org/10.1007/s11012-010-9285-0

Paya-Zaforteza, I., Yepes, V., Hospitaler, A., & González-Vidosa, F. (2009). CO2-optimization of reinforced concrete frames by simulated annealing. *Engineering Structures*, *31*(7), 1501–1508. http://doi.org/10.1016/j.engstruct.2009.02.034

Pei, Y., & Xia, Y. (2012). Design of Reinforced Cantilever Retaining Walls using Heuristic Optimization Algorithms. *Procedia Earth and Planetary Science*, *5*, 32–36. http://doi.org/10.1016/j.proeps.2012.01.006

Perea, C., Alcala, J., Yepes, V., Gonzalez-Vidosa, F., & Hospitaler, A. (2008). Design of reinforced concrete bridge frames by heuristic optimization. *Advances in Engineering Software*, *39*(8), 676–688. http://doi.org/10.1016/j.advengsoft.2007.07.007

Protopapadakis, E., Schauer, M., Pierri, E., Doulamis, A. D., Stavroulakis, G. E., Böhrnsen, J.-U., & Langer, S. (2016). A genetically optimized neural classifier applied to numerical pile integrity tests considering concrete piles. *Computers and Structures*, *162*, 68–79. http://doi.org/10.1016/j.compstruc.2015.08.005

Qu, L., He, D., & Wu, J. (2011). Hybrid Coevolutionary Glowworm Swarm Optimization Algorithm with Simplex Search Method for System of Nonlinear Equations. *Journal of Information & Computational Science*, *8*(13), 2693– 2701.

Quaglia, C. P., Yu, N., Thrall, A. P., & Paolucci, S. (2014). Balancing energy efficiency and structural performance through multi-objective shape optimization: Case study of a rapidly deployable origami-inspired shelter. *Energy and Buildings*, *82*, 733–745. http://doi.org/10.1016/j.enbuild.2014.07.063

Rabbat, B. G., & Russell, H. G. (1982). Optimized sections for precast prestressed bridge girders. *PCI Journal*, *27*(4), 88–108.

Rachmawati, L., & Srinivasan, D. (2009). Multiobjective evolutionary algorithm with controllable focus on the knees of the Pareto front. *IEEE Transactions on*

Evolutionary Computation, *13*(4), 810–824. http://doi.org/10.1109/TEVC.2009.2017515

Rana, S., Islam, N., Ahsan, R., & Ghani, S. N. (2013). Application of evolutionary operation to the minimum cost design of continuous prestressed concrete bridge structure. *Engineering Structures*, *46*, 38–48. http://doi.org/10.1016/j.engstruct.2012.07.017

Razaqpur, A. G., & Li, H. (1991). Thin-walled multicell box-girder finite element. *http://dx.doi.org/10.1061/(ASCE)0733-9445(1991)117:10(2953)*.

Ricart, J., Hüttemann, G., Lima, J., & Barán, B. (2011). Multiobjective harmony search algorithm proposals. *Electronic Notes in Theoretical Computer Science*, *281*, 51–67. http://doi.org/10.1016/j.entcs.2011.11.025

Saad-Eldeen, S., Garbatov, Y., & Guedes Soares, C. (2013). Effect of corrosion severity on the ultimate strength of a steel box girder. *Engineering Structures*, *49*, 560–571. http://doi.org/10.1016/j.engstruct.2012.11.017

Saaty, R. W. (1987). The analytic hierarchy process—what it is and how it is used. *Mathematical Modelling*, *9*(3-5), 161–176. http://doi.org/10.1016/0270-0255(87)90473-8

Sabatino, S., Frangopol, D. M., & Dong, Y. (2015). Sustainability-informed maintenance optimization of highway bridges considering multi-attribute utility and risk attitude. *Engineering Structures*, *102*, 310–321. http://doi.org/10.1016/j.engstruct.2015.07.030

Saha, S., & Bandyopadhyay, S. (2009). A new multiobjective clustering technique based on the concepts of stability and symmetry. *Knowledge and Information Systems*, *23*(1), 1–27. http://doi.org/10.1007/s10115-009-0204-4

Sanad, A., & Saka, M. P. (2001). Prediction of ultimate shear strength of reinforced-concrete deep beams using neural networks. *Journal of Structural Engineering*, *127*(7), 818–828. http://doi.org/10.1061/(ASCE)0733-9445(2001)127:7(818)

Sanpaolesi, L., & Croce, P. (2005). handbook 4: design of bridges-guide to basis of bridge design related to Eurocodes supplement by practical examples,. In *Bridges – Actions and load combinations*. Pisa.

Sarma, K. C., & Adeli, H. (1998). Cost optimization of concrete structures. *Journal of Structural Engineering*, *124*(5), 570–578. http://doi.org/10.1061/(ASCE)0733-9445(1998)124:5(570)

Sattary, S., & Thorpe, D. (2012). Optimizing embodied energy of building construction through bioclimatic principles. *Proceedings of the 28th Annual Conference on Association of Researchers in Construction Management (ARCOM 2012)*. Association of Researchers in Construction Management (ARCOM).

Schlaich, J., & Scheff, H. (1982). *Concrete Box-girder Bridges. International Association for Bridge and Structural Engineering*. Zürich, Switzerland.

SendeCO2. Sistema electrónico de negociación de derechos de emisión de dióxido de

carbono. Available at www.sendeco2.com (August 12, 2014)

Sennah, K. M., & Kennedy, J. B. (2002). Literature review in analysis of box-girder bridges. *Journal of Bridge Engineering*, *7*(2), 134–143. http://doi.org/10.1061/(ASCE)1084-0702(2002)7:2(134)

Shi, X. (2016). Experimental and modeling studies on installation of arc sprayed Zn anodes for protection of reinforced concrete structures. *Frontiers of Structural and Civil Engineering*, *10*(1), 1–11. http://doi.org/10.1007/s11709-016-0312-7

Shieh, H. L., Kuo, C. C., & Chiang, C. M. (2011). Modified particle swarm optimization algorithm with simulated annealing behavior and its numerical verification. *Applied Mathematics and Computation*, *218*(8), 4365–4383. http://doi.org/10.1016/j.amc.2011.10.012

Shushkewich, K. W. (1988). Approximate analysis of concrete box girder bridges. *Journal of Structural Engineering*, *114*(7), 1644–1657. http://doi.org/10.1061/(ASCE)0733-9445(1988)114:7(1644)

Sivasubramani, S., & Swarup, K. S. (2011). Multi-objective harmony search algorithm for optimal power flow problem. *International Journal of Electrical Power & Energy Systems*, *33*(3), 745–752. http://doi.org/10.1016/j.ijepes.2010.12.031

Srinivas, V., & Ramanjaneyulu, K. (2007). An integrated approach for optimum design of bridge decks using genetic algorithms and artificial neural networks. *Advances in Engineering Software*, *38*(7), 475–487. http://doi.org/10.1016/j.advengsoft.2006.09.016

Stewart, M. G. (2001). Reliability-based assessment of ageing bridges using risk ranking and life cycle cost decision analyses. *Reliability Engineering & System Safety*, *74*(3), 263–273. http://doi.org/10.1016/S0951-8320(01)00079-5

Stewart, M. G., & Suo, Q. (2009). Extent of spatially variable corrosion damage as an indicator of strength and time-dependent reliability of RC beams. *Engineering Structures*, *31*(1), 198–207. http://doi.org/10.1016/j.engstruct.2008.08.011

Tae, S., Baek, C., & Shin, S. (2011). Life cycle CO2 evaluation on reinforced concrete structures with high-strength concrete. *Environmental Impact Assessment Review*, *31*(3), 253–260. http://doi.org/10.1016/j.eiar.2010.07.002

Torres-Machi, C., Chamorro, A., Pellicer, E., Yepes, V., & Videla, C. (2015). Sustainable pavement management: Integrating economic, technical, and environmental aspects in decision making. *Transportation Research Record: Journal of the Transportation Research Board*, *2523*, 56–63. http://doi.org/10.3141/2523-07

Valdez, F., Melin, P., & Castillo, O. (2011). An improved evolutionary method with fuzzy logic for combining Particle Swarm Optimization and Genetic Algorithms. *Applied Soft Computing*, *11*(2), 2625–2632. http://doi.org/10.1016/j.asoc.2010.10.010

Vu, K. A. T., & Stewart, M. G. (2000). Structural reliability of concrete bridges including improved chloride-induced corrosion models. *Structural Safety*, *22*(4),

313–333. http://doi.org/10.1016/S0167-4730(00)00018-7

Wang, E., & Shen, Z. (2013). A hybrid Data Quality Indicator and statistical method for improving uncertainty analysis in LCA of complex system – application to the whole-building embodied energy analysis. *Journal of Cleaner Production*, *43*, 166–173. http://doi.org/10.1016/j.jclepro.2012.12.010

Wang, H., Sun, H., Li, C., Rahnamayan, S., & Pan, J. (2013). Diversity enhanced particle swarm optimization with neighborhood search. *Information Sciences*, *223*, 119–135. http://doi.org/10.1016/j.ins.2012.10.012

Wang, H. L., Zhang, Z., Qin, S. F., & Huang, C. L. (2001). Fuzzy optimum model of semi-structural decision for lectotype. *China Ocean Engineering*, *15*(4), 453–466.

Wang, T., Lee, I. S., Kendall, A., Harvey, J., Lee, E. B., & Kim, C. (2012). Life cycle energy consumption and GHG emission from pavement rehabilitation with different rolling resistance. *Journal of Cleaner Production*, *33*, 86–96. http://doi.org/10.1016/j.jclepro.2012.05.001

Wills, J. (1973). *A mathematical optimization procedure and its application to the design of bridge structures*. Wokingham, Berkshire, United Kingdom.

Wisniewski, D. F., Casas, J. R., & Ghosn, M. (2009). Simplified probabilistic non-linear assessment of existing railway bridges. *Structure and Infrastructure Engineering*, *5*(6), 439–453. http://doi.org/10.1080/15732470701639906

Wong, J. K. W., Li, H., Wang, H., Huang, T., Luo, E., & Li, V. (2013). Toward low-carbon construction processes: the visualisation of predicted emission via virtual prototyping technology. *Automation in Construction*, *33*, 72–78. http://doi.org/10.1016/j.autcon.2012.09.014

World Commission on Environment and Development (WCED). (1987). *Our Common Future, Brundtland GH*.

Worrell, E., Price, L., Martin, N., Hendriks, C., & Meida, L. O. (2001). Carbon dioxide emissions from the global cement industry. *Annual Review of Energy and the Environment*, *26*, 303–329.

Xu, H., Gao, X. Z., Wang, T., & Xue, K. (2010). Harmony search optimization algorithm: application to a reconfigurable mobile robot prototype. In Z. W. Geem (Ed.), *Recent advances in harmony search algorithm* (pp. 11–22). Berlin, Heidelberg: Springer Berlin Heidelberg. http://doi.org/10.1007/978-3-642-04317-8_2

Yang, S. I., Frangopol, D. M., Kawakami, Y., & Neves, L. C. (2006). The use of lifetime functions in the optimization of interventions on existing bridges considering maintenance and failure costs. *Reliability Engineering & System Safety*, *91*(6), 698–705. http://doi.org/10.1016/j.ress.2005.06.001

Yellishetty, M., Mudd, G. M., Ranjith, P. G., & Tharumarajah, A. (2011). Environmental life-cycle comparisons of steel production and recycling: sustainability issues, problems and prospects. *Environmental Science & Policy*, *14*(6), 650–663. http://doi.org/10.1016/j.envsci.2011.04.008

Yeo, D., & Gabbai, R. D. (2011). Sustainable design of reinforced concrete structures through embodied energy optimization. *Energy and Buildings*, *43*(8), 2028–2033. http://doi.org/10.1016/j.enbuild.2011.04.014

Yeo, D., & Potra, F. A. (2015). Sustainable design of reinforced concrete structures through CO2 emission optimization. *Journal of Structural Engineering*, *141*(3), B4014002. http://doi.org/10.1061/(ASCE)ST.1943-541X.0000888

Yepes, V., Alcala, J., Perea, C., & González-Vidosa, F. (2008). A parametric study of optimum earth-retaining walls by simulated annealing. *Engineering Structures*, *30*(3), 821–830. http://doi.org/10.1016/j.engstruct.2007.05.023

Yepes, V., García-Segura, T., & Moreno-Jiménez, J. M. (2015). A cognitive approach for the multi-objective optimization of RC structural problems. *Archives of Civil and Mechanical Engineering*, *15*(4), 1024–1036. http://doi.org/10.1016/j.acme.2015.05.001

Yepes, V., Gonzalez-Vidosa, F., Alcala, J., & Villalba, P. (2012). CO2-optimization design of reinforced concrete retaining walls based on a VNS-threshold acceptance strategy. *Journal of Computing in Civil Engineering*, *26*(3), 378–386. http://doi.org/10.1061/(ASCE)CP.1943-5487.0000140

Yepes, V., Martí, J. V., & García-Segura, T. (2015). Cost and CO2 emission optimization of precast–prestressed concrete U-beam road bridges by a hybrid glowworm swarm algorithm. *Automation in Construction*, *49*, 123–134. http://doi.org/10.1016/j.autcon.2014.10.013

Yu., C. H., Gupta., N. C. Das, & H. Paul. (1986). Optimization of prestressed concrete bridge girders. *Engineering Optimization*, *10*(1), 13–24. http://doi.org/10.1080/03052158608902524

Zadeh, L. A. (1965). Fuzzy sets. *Information and Control*, *8*(3), 338–353.

Zavala, G. R., Nebro, A. J., Luna, F., & Coello Coello, C. A. (2013). A survey of multi-objective metaheuristics applied to structural optimization. *Structural and Multidisciplinary Optimization*, *49*(4), 537–558. http://doi.org/10.1007/s00158-013-0996-4

Zavrtanik, N., Prosen, J., Tušar, M., & Turk, G. (2016). The use of artificial neural networks for modeling air void content in aggregate mixture. *Automation in Construction*, *63*, 155–161. http://doi.org/10.1016/j.autcon.2015.12.009

Zhang, J., Zhou, G., & Zhou, Y. (2010). A New Artificial Glowworm Swarm Optimization Algorithm Based on Chaos Method. In B. Cao, G. Wang, S. Chen, & S. Guo (Eds.), *Quantitative Logic and Soft Computing 2010* (Vol. 82, pp. 683–693). Berlin, Heidelberg: Springer Berlin Heidelberg. http://doi.org/10.1007/978-3-642-15660-1

Zhong, Y., & Wu, P. (2015). Economic sustainability, environmental sustainability and constructability indicators related to concrete- and steel-projects. *Journal of Cleaner Production*, *108*, 748–756. http://doi.org/10.1016/j.jclepro.2015.05.095

Zitzler, E., & Thiele, L. (1998). Multiobjective optimization using evolutionary

algorithms - a comparative case study. In A. E. Eiben, T. Bäck, M. Schoenauer, & H.-P. Schwefel (Eds.), *Conference on parallel problem solving from nature-PPSN V* (pp. 292–301). Amsterdam, The Netherlands: Springer Berlin Heidelberg. http://doi.org/10.1007/BFb0056872

Zornoza, E., Payá, J., Monzó, J., Borrachero, M. V., & Garcés, P. (2009). The carbonation of OPC mortars partially substituted with spent fluid catalytic catalyst (FC3R) and its influence on their mechanical properties. *Construction and Building Materials*, *23*(3), 1323–1328. http://doi.org/10.1016/j.conbuildmat.2008.07.024

ANNEX I.
Author publications

JCR Journal articles

- **García-Segura, T**., Yepes, V., & Alcalá, J. (2014a). Life cycle greenhouse gas emissions of blended cement concrete including carbonation and durability. *The International Journal of Life Cycle Assessment*, *19*(1), 3–12. http://doi.org/10.1007/s11367-013-0614-0
- **García-Segura, T**., Yepes, V., Martí, J. V., & Alcalá, J. (2014c). Optimization of concrete I-beams using a new hybrid glowworm swarm algorithm. *Latin American Journal of Solids and Structures*, *11*(7), 1190–1205. http://doi.org/10.1590/S1679-78252014000700007
- **García-Segura, T.**, Yepes, V., Alcalá, J., & Pérez-López, E. (2015). Hybrid harmony search for sustainable design of post-tensioned concrete box-girder pedestrian bridges. *Engineering Structures*, *92*, 112–122. http://doi.org/10.1016/j.engstruct.2015.03.015
- **García-Segura, T**., & Yepes, V. (2016). Multiobjective optimization of post-tensioned concrete box-girder road bridges considering cost, CO2 emissions, and safety. *Engineering Structures*, *125*, 325–336. http://doi.org/10.1016/j.engstruct.2016.07.012
- **García-Segura, T.**, Yepes, V., & Frangopol, D.M. Multi-objective design of post-tensioned concrete road bridges using artificial neural networks. *[submitted(a)]*
- **García-Segura, T.**, Yepes, V., Frangopol, D.M. & Yang, D.Y. Lifetime Reliability-Based Optimization of Post-Tensioned Box-Girder Bridges. *[submitted(b)]*
- **García-Segura, T.**, Penadés-Plà, V. & Yepes, V. AHP-VIKOR under uncertainty for the selection of post-tensioned concrete road bridges. *[submitted(c)]*
- Martí, J. V., **García-Segura, T**. & Yepes, V. (2016). Structural design of precast-prestressed concrete U-beam road bridges based on embodied energy. *Journal of Cleaner Production*, *120*, 231–240. http://doi.org/10.1016/j.jclepro.2016.02.024

- Molina-Moreno, F., **García-Segura, T.**, Martí, J.V. & Yepes, V. Hybrid Harmony Search Algorithm for Economic Optimization of Buttressed Earth-Retaining Walls: A Parametric Study *[submitted]*
- Penadés-Plà, V., **García-Segura, T.**, Martí, J. V. & Yepes, V., A review of multi-criteria decision-making methods applied to the sustainable design of bridges. *[submitted]*
- Penadés-Plà, V., **García-Segura, T.** & Yepes, V., Aplicación de la metodología de respuesta para la optimización de tableros de puente pretensados para carreteras. *[submitted]*
- Sierra, L.A., Yepes, V., **García-Segura, T.** & Pellicer, E. Bayesian network method for making decisions about socially sustainable infrastructure projects. *[submitted]*
- Yepes, V., **García-Segura, T**. & Moreno-Jiménez, J. M. (2015a). A cognitive approach for the multi-objective optimization of RC structural problems. *Archives of Civil and Mechanical Engineering*, *15*(4), 1024–1036. http://doi.org/10.1016/j.acme.2015.05.001
- Yepes, V., Martí, J. V. & **García-Segura, T.** (2015b). Cost and CO2 emission optimization of precast–prestressed concrete U-beam road bridges by a hybrid glowworm swarm algorithm. *Automation in Construction*, *49*, 123–134. http://doi.org/10.1016/j.autcon.2014.10.013
- Yepes, V., Martí, J. V. & **García-Segura, T.** Heuristics in optimal detailed design of precast road bridges. *[submitted]*
- Yepes, V., Pérez-López, E., **García-Segura, T.** & Alcalá, J. Optimization of high-performance concrete post-tensioned box-girder pedestrian bridges. *[submitted]*
- Zastrow, P., Molina-Moreno, F., **García-Segura, T.**, Martí, J.V. & Yepes, V. Life cycle assessment of cost-optimized buttress earth-retaining walls: a parametric study. *[submitted]*

Congress contributions

- **García-Segura, T.**; Yepes, V.; Alcalá, J. & Martí, J.V. (2013). Optimización multiobjetivo de viga en I de hormigón armado con criterios sostenibles. *2º Congreso Nacional de la Enseñanza de las Matemáticas en la Ingeniería de Edificación, EIMIE*, 18-19 de julio, Valencia, pp. 135-148. ISBN: 978-84-8363-992-4.
- **García-Segura, T.**; Yepes, V.; Alcalá, J. & Martí, J.V. (2014). Influencia de la carbonatación y durabilidad en el ciclo de vida del hormigón fabricado con cementos con adiciones. *VI Congreso de ACHE*, Madrid.
- **García-Segura, T.**; Yepes, V.; Alcalá, J. & Martí, J.V. (2014). Optimización multiobjetivo para el estudio de la sostenibilidad del hormigón autocompactante. *VI Congreso de ACHE*, Madrid.
- **García-Segura, T.**, Yepes, V., & Alcalá, J. (2014b). Sustainable design using multiobjective optimization of high-strength concrete I-beams. In *The 2014 International Conference on High Performance and Optimum Design of Structures and Materials HPSM/OPTI* (Vol. 137, pp. 347–358). Ostend, Belgium. http://doi.org/10.2495/HPSM140331
- **García-Segura, T.**; Yepes, V. & Alcalá, J. (2014). Life-cycle emissions of

reinforced concrete made with blended cements. *The 8th International Congress on Project Management and Engineering*, Alcañiz, Spain.

- **García-Segura, T.;** Yepes, V.; Martí, J.V. & Alcalá, J. (2015). Algoritmo híbrido de enjambre de luciérnagas y aceptación por umbrales para diseño de vigas. X *Congreso Español de Metaheurísticas, Algoritmos Evolutivos y Bioinspirados – MAEB 2015*, 4-6 de febrero, Mérida, pp. 699-705. ISBN: 978-84-697-2150-6
- **García-Segura, T**.; Yepes, V. & Alcalá, J. (2016). Computer-support tool for automatically optimize bridges. *HPSM/OPTI 2016 [accepted]*
- **García-Segura, T.**; Frangopol, D.; Yang, D. & Yepes, V. (2016). Lifetime-reliability-based approach for comparing the life-cycle cost of optimal bridge designs. *Fifth International Symposium on Life-Cycle Civil Engineering IALCCE* '16, 16-19 October 2016, Delft, The Netherlands *[accepted]*
- Martí, J.V.; Yepes, V. & **García-Segura, T.** (2013). Aplicación de algoritmos meméticos híbridos de doble fase en la optimización de tableros de puentes de vigas artesa de hormigones no convencionales. *IX Congreso Español de Metaheurísticas, Algoritmos Evolutivos y Bioinspirados, MAEB 2013*, Madrid.
- Martí, J.V.; Yepes, V.; Alcalá, J. & **García-Segura, T.** (2013). Diseño de vigas en "U" de hormigón con fibras mediante la heurística SA con criterios económicos. *2º Congreso Nacional de la Enseñanza de las Matemáticas en la Ingeniería de Edificación, EIMIE*, 18-19 de julio, Valencia, pp. 299-309. ISBN: 978-84-8363-992-4.
- Martí, J.V.; Yepes, V.; Alcalá, J. & **García-Segura, T.** (2013). Optimización memética de vigas artesa prefabricadas con criterios sostenibles de hormigón con fibras. *2º Congreso Nacional de la Enseñanza de las Matemáticas en la Ingeniería de Edificación, EIMIE*, 18-19 de julio, Valencia, pp. 91-104. ISBN: 978-84-8363-992-4.
- Martí, J.V.; Yepes, V. & **García-Segura, T.** (2015). Aplicación de metaheurísticas en la optimización de pasos superiores de carreteras. *X Congreso Español de Metaheurísticas, Algoritmos Evolutivos y Bioinspirados – MAEB 2015*, 4-6 de febrero, Mérida, pp. 241-247. ISBN: 978-84-697-2150-6.
- Martí, J.V.; Alcalá, J.; **García-Segura, T**. & Yepes, V. (2016). Heuristic design of precast-prestressed concrete U-beam and post-tensioned cast-in-place concrete slab road bridges. *HPSM/OPTI 2016 [accepted]*
- Yepes, V.; Martí, J.V.; Alcalá, J. & **García-Segura, T.** (2013). Métodos empleados en el proyecto HORSOST sobre diseño sostenible con hormigón no convencional. *2º Congreso Nacional de la Enseñanza de las Matemáticas en la Ingeniería de Edificación, EIMIE*, 18-19 de julio, Valencia, pp. 259-272. ISBN: 978-84-8363-992-4.
- Yepes, V.; Alcalá, J. & **García-Segura, T.** (2013). Multiobjective optimization of high-performance reinforced concrete I-beams by simulated annealing. *22nd International Conference on Multiple Criteria Decision Making*, 17-21 June, Málaga, (Spain).
- Yepes, V.; Martí, J.V.; Alcalá, J. & **García-Segura, T.** (2013). Métodos empleados en el proyecto HORSOST sobre diseño sostenible con hormigón no convencional. *2º Congreso Nacional de la Enseñanza de las Matemáticas en la*

Ingeniería de Edificación, *EIMIE*, 18-19 de julio, Valencia, pp. 135-148. ISBN: 978-84-8363-992-4.

- Yepes, V.; Martí, J.V.; Alcalá, J. & **García-Segura, T.** (2014). Diseño eficiente de estructuras con hormigones no convencionales basados en criterios sostenibles multiobjetivo: HORSOST. *VI Congreso de ACHE*, Madrid.
- Yepes, V.; Martí, J.V. & **García-Segura, T.** (2016). Design optimization of precast-prestressed concrete road bridges with steel fiber-reinforcement by a hybrid evolutionary algorithm. *HPSM/OPTI 2016 [accepted]*